Small-Signal Frequency Response Theory

for

Ideal Dc-to-Dc Converter Systems

Thesis by

Billy Ying Bui Lau

In Partial fulfillment of the Requirements

for the Degree of

Doctor of Philosophy

California Institute of Technology

Pasadena, California

1987

(Submitted September 11, 1986)

to my parents

Acknowledgements

I am deeply indebted to my advisor Professor R. D. Middlebrook for his invaluable encouragement, guidance, and support during my stay at Caltech. He has given me the freedom to select the research direction. I would like to thank Professor Ćuk for introducing me to the field of Power Electronics. Both of them have offered me the opportunity to conduct my research in the Power Electronics Group.

I would also like to thank Professor T. Caughey for introducing me to Advanced System Theory, Professor J. Knowles for introducing me to Advanced Mathematical Methods, and Professor A. Šabanović of Energoinvest, Yugoslavia, for introducing me to Variable Structure System Theory and Sliding Mode Control during his stay as Visiting Professor of Electrical Engineering at Caltech 1983–85. The bulk of this thesis is based on what I learned from them.

I would like to acknowledge the financial support provided by Caltech in the form of Graduate Teaching Assistantships, and by Garrett AiResearch, IBM, GTE, and Emerson in the form of Graduate Research Assistantships.

I would like to express my gratitude to my colleagues at the Power Electronics Group for the enlightening discussion, the support, and the pleasure of their company. I would like to express my appreciation to my friends at Caltech, who have made my stay at the Institute very enjoyable.

Finally, and most importantly, I would like to express my deepest thanks to my family, especially my parents, for their encouragement, support, and understanding.

Abstract

The *frequency response problem* of switching dc-to-dc converter systems is the problem of computing the small-signal frequency response of the system with respect to its inputs. It arises in the study of the small-signal behavior and in the design of a feedback controller for the dc-to-dc converter system. There are two approaches in tackling the problem: the numerical approach and the analytical approach. This thesis is limited to the analytical approach. There are previous efforts in developing approximate analytical methods for solving the problem; however, these methods are unsatisfactory in one way or another because they are applicable only to few special cases, and valid only in limited range of frequency — less than half the switching frequency in many cases.

The *Small-Signal Frequency Response Theory* presented in this thesis is developed to overcome the problems encountered in the application of the approximate analytical methods. Instead of finding an approximate model for a dc-to-dc converter system and postulating that the response of the model is the same as that of the converter system, as in the approximate analytical methods, the new theory computes the frequency response of the perturbed output with respect to perturbations at the control-inputs by the direct application of Fourier Analysis. Hence, the theory is exact in the *small-signal limit.* Unlike the approximate analytical methods, the results given by the theory are valid at all frequencies provided that the system model used in the calculation of frequency response is valid at all frequencies. In short, the *Small-Signal Frequency Response Theory* is a mathematical theory for the linearization of an ideal dc-to-dc converter

system in the vicinity of its periodic steady state solution.

In the derivation of the results of the *Small-Signal Frequency Response Theory*, two steps are taken: First, find a difference equation that describes the small-signal motion of the system in the vicinity of the given steady state solution. Second, find the *equivalent hold* that relates the samples of the perturbed state of the system, given by the difference equation, to the analog output signal. The z-transform of the difference equation with $z = e^{sT_s}$ is used to relate the spectrum of the sampled perturbed control-input to the spectrum of the sampled perturbed output. The frequency response of the converter system given by the theory resembles the frequency response of a classical single-rate sampled-data system.

The prediction given by the theory and the experimental results for three converter circuits are compared. These three converter circuit have the same basic circuit topology, but different control strategies. The control strategies in these three examples are: constant-switching-frequency PWM, constant-switching-frequency programmed, and bang-bang controlled. It is found that the theory consistently gives good predictions, even up to many times of the switching frequency, while, in many cases, the approximate analytical methods break down.

The theory has the best of both the time domain approach and the frequency domain approach for the analysis of switching dc-to-dc converter systems. It has the exactness of the time domain approach, which uses a difference equation to describe the system, and the measurability of the of frequency domain approach. The exactness and the uniformity of the theory, which has not been achieved before, results in significant impact in the fields of *computer-aided design* and *modelling and analysis* in power electronics.

Contents

Introduction

For any control system design, one of the most important objectives is to achieve high performance. The criteria for high performance are defined by a set of performance specifications. For both high performance plant and high performance feedback controller design, it is necessary to find the response of the plant to excitations at its control-inputs. Depending on the problem, the response required may be in the time domain, or the frequency domain, or both. When the control system is a dc-to-dc converter system, the performance specifications are usually in both the time domain and the frequency domain. Time domain response requirements usually influence the choice of the converter circuit topology, the control strategy, the switching frequency, and the technology used in building the converter system. Frequency domain response requirements usually influence the design of the controller. Time domain response requirements are usually handled by heuristic methods. Frequency domain response requirements are usually handled by frequency domain controller design methods.

For both the frequency domain performance specification and the frequency domain controller design of a dc-to-dc converter system, it is necessary to compute the small-signal frequency domain response of the system. The computation of the small-signal frequency response of dc-to-dc converter systems is the *frequency response problem* of dc-to-dc converter systems.

The *frequency response problem* of a physical dc-to-dc converter system is not a simple problem. Nevertheless, this problem may be simplified by modelling the physical

dc-to-dc converter system under study with an ideal dc-to-dc converter system. An ideal dc-to-dc converter system is a linear time varying system that may be describe by a system of first-order differential equations in which the coefficients are piecewise constant functions of time. The control of an ideal dc-to-dc converter system is achieved by varying the time at which the system differential equation switches from a set of coefficients to another set of coefficients.

There are two directions in which the *frequency response problem* of ideal dc-to-dc converter systems can be tackled:

1. Numerical Simulation — Computation-intensive and expensive.

2. Analytical Solution — Many approximate analytical methods.

In this thesis, only the analytical methods for calculating the frequency response of ideal dc-to-dc converter systems will be studied.

There are previous efforts to develop approximate analytical methods for computing the frequency response of ideal dc-to-dc converter systems. Common to all the analytical methods are two essential steps:

1. Find a first-order difference equation that describes the small-signal motion of the system, with the sampled control-input as the input sequence of the difference equation and the sampled perturbed state of the converter system as the state sequence of the difference equation.

2. Relate the sequences in the difference equation to the physical analog input and output quantities of the converter system.

Different approximate analytical methods handle these two steps differently. The following is a summary of the manner in which these two steps are handled by three representative approximate analytical methods:

1. The *State Space Averaging Method* of Middlebrook and Ćuk[6]:

   (a) Goal: To find a simple linear time-invariant approximate model for ideal dc-to-dc converter systems, and to find a linear time-invariant circuit model, the canonical circuit model, for dc-to-dc converter circuits.

   (b) The difference equation: Approximate, uses the ***small-ripple assumption*** and the ***straight line approximation*** to simplify the expressions.

   (c) The relation between the sequences and the I/O quantities: Assumes that the switching frequency goes to infinity; the difference equation becomes a differential equation. The input to this differential equation is a continuous signal.

   (d) Remarks: The method is developed primarily for predicting the low-frequency small-signal behavior of constant switching frequency open-loop pulse-width-modulated converter systems. The frequency response problem of converter systems is tackled as a circuit problem. The method allows semi-analytical pole-zero placement on the s-plane in converter system design by choosing the values of the components used in the converter circuit. A modulator model is added in the frequency domain in an attempt to extend this method to other classes of converter systems[4,5], such as constant-switching-frequency current-programmed converter systems. Nevertheless, it fails to predict the high-frequency behavior (of the order of the switching frequency) of current-programmed converter systems because the linear time-invariant model breaks down when there is a feedback loop with crossover frequencies close to or higher than the switching frequency in the system[1].

2. The *Sampled-Data Modelling Method* of Brown[1]:

(a) Goal: To find an approximate linear sample-data system model for ideal dc-to-dc converter systems that can predict the high-frequency behavior of constant-switching-frequency programmed converter systems.

(b) The difference equation: Approximate, uses the *small-ripple assumption* and the *straight line approximation* as in the *State Space Averaging Method.* The additional sampling processes, however, allows the addition of the modulator model in the difference equation accurately in the frequency domain (the z-domain with $z = e^{sT_s}$, where T_s is the switching period).

(c) The relation between the sequences and the I/O quantities: Assumes that the switching frequency goes to infinity so that the difference equation becomes a differential equation. The input to this differential equation is a train of narrow pulses in time.

(d) Remarks: The method is developed to overcome the difficulties of the *State Space Averaging Method* in predicting the high-frequency behavior of constant-switching-frequency current-programmed converter system. The frequency response problem of converter systems is tackled as a system problem. The method can take into account the finite switching frequency in converter systems. In comparison to the *State Space Averaging Method*, this method provides much better accuracy in the modulator model at high frequencies and works for a larger class of dc-to-dc converter systems. Nevertheless, the results of this method are more complex. Pole-zero placement in the z-plane for converter system design is possible.

3. The *Small-Signal Analysis of Resonant Converters* of Vorpérian[9]:

(a) Goal: To predict the low-frequency response of resonant converter systems.

(b) Difference equation: Exact in the *small-signal limit* .

(c) Relation between the sequences and the I/O quantities: The method uses the time-average of the waveform between the consecutive samples of the perturbed state of the system given by the difference equation to form another sequence. A difference equation that relates the control-input sequence and this sequence is constructed. The z-transform, with $z = e^{sT_s}$, is then used to relate this difference equation to the analog I/O quantities.

(d) Remarks: This method is developed primarily for resonant converters, in which the switching period T_s is of the same order magnitude as the circuit time constants. The frequency response problem of converter systems is tackled as a system problem. The method gives good low-frequency predictions for resonant converters. Nevertheless, in taking the time average, the high-frequency information in the output signal is destroyed. The result is essentially a low-frequency approximation. Very simple converter systems can be easily found for which this method fails to predict their high-frequency behavior.

Since all the approximate analytical methods for computing the frequency response of ideal dc-to-dc converter systems work for limited classes of dc-to-dc converter systems and break down under many conditions, it is natural to ask whether the frequency response of a dc-to-dc converter can be computed without any approximation; in other words, whether any *exact analytical method* exists at all!

The *Small-Signal Frequency Response Theory* for dc-to-dc converter systems is developed to answer this question affirmatively. The control-input-to-output frequency domain response corresponding to a stable steady state solution of any linearizable dc-to-dc converter system can be computed by using the *Small-Signal Frequency Response Theory* without any approximation in the *small-signal limit*. The steady state solution of a dc-to-dc converter system is the periodic solution of the system. In other words, the

Small-Signal Frequency Response Theory is the *exact analytical solution* to the *frequency response problem* of ideal dc-to-dc converter systems.

The (line) input-to-output frequency response is not treated in this thesis because the exact solution in the *small-signal limit* contains convolution integrals in the frequency domain and does not give much insight. Nevertheless, useful analytical approximations may be obtained by modelling the input signal appropriately.

In the *Small-Signal Frequency Response Theory* for dc-to-dc converter systems, the steady state solution of the converter system under study is assumed to be given. If the converter system under study has multiple stable steady state solutions under a given operating condition, then there is a frequency response corresponding to each of the stable steady state solutions. In general, different stable steady state solutions have different frequency responses, even though the stable steady state solutions may correspond to a single operating condition. In order to obtain a closed-form result, the dc-to-dc converter system under study is assumed to be ideal. An ideal dc-to-dc converter system is a linear time varying system that may be describe by a system of first-order differential equations in which the coefficients are piecewise constant functions of time. In the language of *Variable Structure System Theory*[8], an ideal dc-to-dc converter system is a variable structure system, in which each of the structures is linear and time-invariant. The use of an ideal dc-to-dc converter system model of the physical dc-to-dc converter system under study in the frequency domain analysis of dc-to-dc converter performance gives satisfactory results in most practical cases.

The following is a summary of the manner in which the *Small-Signal Frequency Response Theory* handles the two steps in computing the frequency response:

1. Goal: To find the exact solution to the frequency response problem of dc-to-dc converter systems in the *small-signal limit.*

2. The difference equation: Exact in the *small-signal limit.*

3. The relation between the sequences and the I/O quantities: The exact perturbed output waveform between the sample points given by the difference equation is computed. From the exact perturbed output waveform, an *equivalent hold* is computed to relate the samples of the perturbed state, which is given by the state sequence of the difference equation, to the analog output signal. The continuous control-input and the sampled control-input are related by Shannon's Sampling Theorem[7].

4. Remarks: The frequency response of an ideal dc-to-dc converter system given by the theory in the vicinity of its stable steady state solution is exact in the *small-signal limit.* The frequency response problem of a converter system is tackled as a system problem. This is the only *exact analytical method.*

In the *Small-Signal Frequency Response Theory* for an ideal dc-to-dc converter system, the first step in finding the frequency response of the system in the vicinity of a given steady state solution is to construct a linear difference equation that describes the small-signal motion of the system in the vicinity of the given steady state solution. Since the theory is developed to be applicable to any linearizable ideal dc-to-dc converter system, it is necessary to define an ideal dc-to-dc converter system so that the term *linearizable* may be defined, and ideal dc-to-dc converter systems may be classified systematically. This classification is essential to the construction of the difference equation. The classification method adopted in the theory is very different from what is commonly used in the power electronics community. The theory classifies converter systems according to their control strategy. The control strategy of a converter system is the sequence of modulation methods that determines the instants at which the switching from one switched-state or structure to another occurs in the system. With this classification method, the matrices in the difference equation and the frequency response can

be mechanically associated with the control strategy.

Although the *Small-Signal Frequency Response Theory* is the only analytical method that provides a systematic procedure for constructing the difference equation that describes the small-signal motion of all linearizable ideal dc-to-dc converter systems, the major difference between the theory and the approximate analytical methods discussed above is not in this procedure for constructing the difference equation. The major difference is in the relation between the sequences in the difference equation and the analog input and output quantities. In all the existing approximate analytical methods, these relations are postulated intuitively rather than derived mathematically. This is the reason that all these approximate analytical methods break down at some point. In the *Small-Signal Frequency Response Theory*, the contribution of each of the samples of the perturbed state, which is given by the state sequence of the difference equation, to the analog perturbed output waveform before the arrival of the next sample, is computed first in the time domain by using the converter system description in the state space representation. Then, the contribution is computed in the frequency domain by applying Fourier Analysis to the contribution in the time domain. The overall result is that the contribution of the samples of the perturbed state, given by the state sequence of the difference equation, to the perturbed output in the frequency domain, may be treated as the *hold* in a classical sampled-data system. This hold, which is called *equivalent hold* in the theory, is different for each of the steady state solutions of each different converter system. As a result of the direct application of Fourier Analysis, the theory is valid at any frequency. At very high frequencies, however, the predictions given by the theory and experimental results are expected not to agree with each other owing to the breakdown of the ideal dc-to-dc converter system model used in the calculation. The breakdown of the system model comes from unmodelled delay in the physical converter circuit, unmodelled

high-frequency dynamics, and the breakdown of the circuit model used in obtaining the state space description of the system.

From the perspective of the *Small-Signal Frequency Response Theory*, an ideal dc-to-dc converter system operating in the vicinity of a particular steady state solution is a sampled-data system in the *small-signal limit*. The *difference equation* that describes the small-signal motion of the converter system in the vicinity of its steady state solution corresponds to the discrete time system in the classical sampled-data system. The *equivalent hold* corresponds to the hold in the classical sampled-data system.

This thesis is divided into five chapters and two appendices. In Chapter 1, ideal dc-to-dc converter systems are defined and the modulation methods used in ideal dc-to-dc converter systems are discussed. The linearizability of ideal dc-to-dc converter system is also discussed in Chapter 1. In Chapter 2, the basic concepts of the *Small-Signal Frequency Response Theory* are introduced through a very simple example converter system — a constant-switching-frequency current-programmed buck converter system with a very large output capacitor. This simple example converter is chosen because the system can be analyzed with simple geometry. The properties of the steady state solutions and the concept of the stability of ideal dc-to-dc converter systems are also introduced in this chapter.

With the foundation of the theory laid down in Chapter 2, the *Small-Signal Frequency Response Theory* in the state space formulation for an important class of ideal dc-to-dc converter systems, the class of two-switched-states converter systems with continuous output signals, is formally introduced in Chapter 3. This class of converter systems includes most of the commonly used converter systems. The theoretical predictions and the experimental results of converter circuits with the same circuit topology but different control strategies are compared. These control strategies are: constant-

switching-frequency time modulation (PWM), constant-switching-frequency constraint modulation (programming), and bang-bang control.

In Chapter 4, the mathematics used in Chapter 3 to derive the results of the *Small-Signal Frequency Response Theory* is discussed in detail. In Chapter 5, the results from Chapter 3 are generalized to all the ideal multiple-switched-network dc-to-dc converter systems defined in Chapter 1, which includes converter system that have discontinuous output signals. The procedure introduced in this chapter, for finding the frequency response of an ideal dc-to-dc converter system given its steady state solution in the *small-signal limit*, is uniform with respect to the control strategy of the system.

The exactness and the uniformity of the *Small-Signal Frequency Response Theory* make it ideal for a lot of applications. One of the most important applications of the theory is in the computer-aided design of dc-to-dc converter systems. Some of these applications and the impact of the theory in the field of *Modelling and Analysis* in Power Electronics are discussed in the Conclusion of this thesis.

At the end of this thesis, there are two appendices. In Appendix A, two concepts of stability are discussed. The concept of the stability of an operating point, which is widely used in electronic circuits, is first introduced. Unfortunately, this concept is found to be neither satisfactory nor sufficient for nonlinear systems in general, and ideal dc-to-dc converter systems in particular. The concept of the stability of a solution is then introduced to overcome these difficulties.

In Appendix B the different concepts of average are discussed and compared. The concept of average is used in most of the approximate analytical methods to relate the samples of the perturbed state, given by the state sequence in the difference equation that describes the small-signal motion of the system, to the physical analog output signal. Different concepts of average are used in the different methods. The concepts of average

used in the *State Space Averaging Method*[6], the *Sampled-Data Modelling Method*[1], the *Small-Signal Analysis of Resonant Converters*[9], and the *Sliding-Mode Control* in *Variable Structure System Theory*[8] are examined. The inadequacy of the concept of average for computing the frequency response of ideal dc-to-dc converter systems is also discussed.

Chapter 1

Ideal Dc-to-Dc Converter Systems

Physical systems are never ideal. Nevertheless, in many cases, for the behavior under study, an ideal system model that approximates the physical system can be found. A physical dc-to-dc converter circuit is nonlinear. None of the switching devices in the circuit behaves like an ideal switch, and the magnetic components have nonlinearities with memory. Fortunately, for the study of its frequency domain behavior, a physical dc-to-dc converter system may be modelled as an ideal converter system. Even in the worst case, the addition of parasitic elements to the model usually gives satisfactory results. Nevertheless, an ideal converter system model is usually not sufficient to model the detailed time domain behavior of physical converter systems.

The *Small-Signal Frequency Response Theory* is a mathematical theory for the linearization of ideal dc-to-dc converter systems for a given steady state solution of the system. For a full understanding of the *Small-Signal Frequency Response Theory*, it is necessary to define ideal dc-to-dc converter systems mathematically and to study their properties and the implications of their properties. Furthermore, formally defining ideal dc-to-dc converter systems allows the definition of the *linearizability* of converter systems and the easy classification of converter systems. This classification is necessary for the construction of the equations that describe the small-signal motion and the frequency response of the converter systems in the vicinity of their stable steady state solutions.

In Section 1.1, ideal dc-to-dc converter systems are defined. The methods for

controlling ideal dc-to-dc converter systems are introduced in Section 1.2. The linearizability of ideal dc-to-dc converter systems is discussed in Section 1.3. The properties of ideal dc-to-dc converter systems and their implications which are relevant to the *Small-Signal Frequency Response Theory* are discussed in Section 1.4.

1.1 The Definition of Ideal Dc-to-Dc Converter Systems

An ideal dc-to-dc converter system is a linear time varying system that has state space realization in which the **A**, **B**, **C**, and **D** matrices are piecewise constant functions of time. An ideal dc-to-dc converter system have many mathematical properties. These properties, in turn, have implications on how the system should be handled mathematically. Before discussing the properties of an ideal dc-to-dc converter system, it is necessary to define the system.

An ideal dc-to-dc converter system is described by Eq. (1.1):

$$\begin{aligned} \dot{\mathbf{x}}(t) &= \mathbf{A}(t)\,\mathbf{x}(t) + \mathbf{B}(t)\,\mathbf{u} \\ \mathbf{y}(t) &= \mathbf{C}(t)\,\mathbf{x}(t) + \mathbf{D}(t)\,\mathbf{u} \end{aligned} \tag{1.1}$$

where $\mathbf{x}(t)$ is the *state vector*, $\mathbf{u}$ is the *input vector*, $\mathbf{y}(t)$ is the *output vector*, $\mathbf{A}(t)$ is the *system matrix*, $\mathbf{B}(t)$ is the *input matrix*, $\mathbf{C}(t)$ is the *output matrix*, and $\mathbf{D}(t)$ is the *transmission matrix*. The matrices $\mathbf{A}(t)$, $\mathbf{B}(t)$, $\mathbf{C}(t)$, and $\mathbf{D}(t)$ have the following properties:

1. $\mathbf{A}(t)$, $\mathbf{B}(t)$, $\mathbf{C}(t)$ and $\mathbf{D}(t)$ are piecewise constant functions in time t; i.e.,

$$(\mathbf{A}(t),\mathbf{B}(t),\mathbf{C}(t),\mathbf{D}(t)) = (\mathcal{A}_j,\mathcal{B}_j,\mathcal{C}_j,\mathcal{D}_j), \qquad \mathcal{T}_j < t < \mathcal{T}_{j+i}$$

2. The ordered quadruple $(\mathbf{A}(t),\mathbf{B}(t),\mathbf{C}(t),\mathbf{D}(t))$ assumes only a finite set of values; i.e.,

$$(\mathcal{A}_j,\mathcal{B}_j,\mathcal{C}_j,\mathcal{D}_j) \in \{(\mathbf{A}_i^*,\mathbf{B}_i^*,\mathbf{C}_i^*,\mathbf{D}_i^*) \mid 1 \le i \le N_n\}$$

where N_n is the *number of switched-networks.*

3. An ideal dc-to-dc converter system is not controlled by its input vector $\mathbf{u}$, but by varying its $\mathcal{T}_j$'s (See Section 1.2). If $\mathbf{u}$ can be controlled, the converter system is unnecessary. The scheme that determines the $\mathcal{T}_j$'s is the control strategy of the converter system. The control strategy consists of a sequence of methods that determine the $\mathcal{T}_j$'s, i.e., the modulation methods. The modulation method that determines $\mathcal{T}_j$ is $\mathcal{M}_j$.

An ideal dc-to-dc converter system and its solution can be fully characterized by the sequences: $\{(\mathcal{A}_j, \mathcal{B}_j, \mathcal{C}_j, \mathcal{D}_j)\}$, $\{\mathcal{T}_j\}$, and $\{\mathcal{M}_j\}$.

In the language of *Variable structure System Theory*[8], an ideal dc-to-dc converter system is a variable structure system, in which each of its structures is linear time-invariant with state space realization.

When an ideal dc-to-dc converter system is operating in steady state, its solution is periodic and may be characterized by the sequences $\{(\mathbf{A}_j, \mathbf{B}_j, \mathbf{C}_j, \mathbf{D}_j)\}$, $\{\mathbf{T}_j\}$ and $\{M_j\}$. These are the sequences $\{(\mathcal{A}_j, \mathcal{B}_j, \mathcal{C}_j, \mathcal{D}_j)\}$, $\{\mathcal{T}_j\}$ and $\{\mathcal{M}_j\}$, respectively, corresponding to the steady state solution. The following are the properties of these sequences:

1. In steady state, the sequence $\{(\mathbf{A}_j, \mathbf{B}_j, \mathbf{C}_j, \mathbf{D}_j)\}$ is periodic with period N_q; i.e.,

$$(\mathbf{A}_j, \mathbf{B}_j, \mathbf{C}_j, \mathbf{D}_j) = (\mathbf{A}_{j+N_q}, \mathbf{B}_{j+N_q}, \mathbf{C}_{j+N_q}, \mathbf{D}_{j+N_q}), \qquad \forall j \in \mathbf{Z}$$

For a system to operate as a converter system, $N_q \geq 2$.

2. In steady state, the sequence $\{M_j\}$ is periodic with period N_M; i.e.,

$$M_j = M_{j+N_M}, \qquad \forall j \in \mathbf{Z}$$

3. Define: $T_j \equiv \mathbf{T}_{j+1} - \mathbf{T}_j$. The sequence $\{T_j\}$ is periodic with period N_T; i.e.,

$$T_{j+N_T} = T_j, \qquad \forall j \in \mathbf{Z}$$

4. The *number of switched-states* N_s is defined as the least common multiplier of N_q, N_T, and N_M; i.e.,

$$N_s \equiv \text{lcm}(N_q, N_T, N_M)$$

For most common converter systems in their steady state, the *number of switched-states* is the same as the number of switched-networks.

The steady state switching period T_s is defined as:

$$T_s \equiv \sum_{i=0}^{N_s-1} T_i$$

The steady state switching frequency f_s is the reciprocal of the steady state switching period T_s.

1.2 The Control of Ideal Dc-to-Dc Converter Systems

Dc-to-dc converter systems, as discussed in Section 1.1, are not controlled by the input vector $\mathbf{u}$. The input vector usually represents the power sources. If the power source can be varied to control the dc-to-dc converter system, the converter system is unnecessary. In most cases, the variations in the input vector $\mathbf{u}$ are regarded as disturbances. Dc-to-dc converter systems are controlled by changing the $\mathcal{T}_j$'s defined in Section 1.1. There are four major modulation methods that determine the $\mathcal{T}_j$'s. In the following discussion: define $\Delta t_j \equiv \mathcal{T}_j - \mathbf{T}_j$, and in the *small-signal limit*, terms of $O(\Delta^2)$ or higher are dropped and $\Delta \rightarrow \delta$; e.g., $\Delta t_j \rightarrow \delta t_j$.

The four major modulation methods may be described as follows:

1. *Unmodulated* — The modulation method is denoted by M^u. The Δt_j's corresponding to this method are zeros; i.e. $\Delta t_j \equiv 0$, $\forall j \in \{j \mid \mathcal{M}_j = M^u\}$. Quantities corresponding to the *unmodulated* case are denoted with the superscript u.

2. *Time-Modulated* — The modulation method is denoted by M^t. The Δt_{i+nN_s}'s, fixed i, corresponding to this modulation method are determined by a sequence in the following manner:

$$\Delta t_{i+nN_s} = (m_i^t)^{-1}\,\Delta r_i[n], \qquad \forall\, i \in \{i \mid 0 \le i < N_s,\ \mathcal{M}_{i+nN_s} = M^t,\ n \in \mathbf{Z}\}$$

where N_s is the number of switched-states, $\Delta r_i[n]$ is the sampled control-input sequence formed from sampling the perturbed control-input signal $\Delta r_i(t)$, and m_i^t is the slope of the PWM ramp used in $\mathcal{M}_{i+nN_s}$. Quantities corresponding to the *time-modulated* case are denoted with the superscript t. If $\Delta r_i[n] = \Delta r_i(\mathcal{T}_{i+nN_s})$ for some signal $\Delta r(t)$, then Δr is naturally sampled. If $\Delta r_i[n] = \Delta r_i(\mathbf{T}_{i+nN_s} + c)$ for some signal $\Delta r(t)$ and constant c, then Δr is uniformly sampled. In this thesis, c is assumed to be zero. It turns out that these two sampling processes do not make a difference in the result given by the *Small-signal Frequency Response Theory* for $c = 0$; see Section 4.3.

3. *Constraint-Modulated* — Better known as programming. The modulation method is denoted by M^c. Suppose that the transition from switched-state $i + nN_s - 1$ to switched-state $i + nN_s$ is controlled by this modulation method, then the time at which this transition occurs $\mathcal{T}_{i+nN_s}$ satisfies the following *constraint equation*:

$$\mathbf{f}_i^T\,\mathbf{x}(\mathcal{T}_{i+nN_s}) + m_i^c\,\Delta t_{i+nN_s} + c_i - r_i[n] = 0 \tag{1.2}$$

where N_s is the number of switched-networks, $\mathbf{f}_i$ is a vector, $r_i[n]$ is the sampled control-input sequence formed from sampling the control-input signal $r_i(t)$, c_i is a constant, and m_i^c is the slope of a sawtooth wave. The *constraint equation* is the condition under which the converter system switches from switched-state $i + nN_s - 1$ to switched-state $i + nN_s$. In a converter circuit, the *constraint equation* is the mathematical model of the switching action of the comparator circuit that

determines when this change of the switched-state occurs. This comparator circuit has the control-input $r_i(t)$ at one of its inputs, and the sum of a sawtooth ramp with slope m_i^c and the weighted sum of the system states $\mathbf{f}_i^T \mathbf{x}(t)$ at its other input. This sawtooth ramp is the ramp of the sawtooth wave in the case of a closed-loop PWM converter system, and the stabilizing ramp in the case of the programmed converter system. Quantities corresponding to the *constraint-modulated* case are denoted with the superscript c. The derivation of the time of transition from its steady state value δt_{i+nN_s} may be obtained by linearizing the constraint equation, Eq. (1.2), and expressing δt_{i+nN_s} in terms of other quantities in the linearized constraint equation.

4. *Modified-Constraint-Modulated* — The modulation method is denoted by M^m. It is used in the control strategies of constant on/off time converters and frequency modulated converters. Suppose that the transition from switched-state $i+nN_s-1$ to switched-state $i+nN_s$ is controlled by this modulation method, then the time at which this transition occurs τ_{i+nN_s} satisfies the following *modified-constraint equation*:

$$\mathbf{f}_i^T \mathbf{x}(\tau_{i+nN_s}) - r_i[n] + m_i^m \left(\Delta t_{i+nN_s} - h_i^m \, \Delta t_{i-1+nN_s}\right) + c_i = 0 \qquad (1.3)$$

where N_s is the number of switched-networks, $\mathbf{f}_i$ is a vector, $r_i[n]$ is the sampled control-input sequence formed from sampling the control-input signal $r_i(t)$, c_i is a constant, and m_i^m is the slope of the added ramp. The *modified-constraint equation* is the condition under which the converter system switches from switched-state $i+nN_s-1$ to switched-state $i+nN_s$. In a converter circuit, the *modified-constraint equation* is the mathematical model of the switching action of the comparator circuit that determines when this change of the switched-state occurs. This comparator circuit has the control-input $r_i(t)$ at one of its inputs, and the sum of a sawtooth

ramp with slope m_i^m which is delayed by $h_i^m \Delta t_{i-1+nN_s}$ and the weighted sum of the system states $\mathbf{f}_i^T \mathbf{x}(t)$ at its other input. The quantity h_i^m is a constant, which is unity in most converter systems. Quantities corresponding to the *modified-constraint-modulated* case are denoted with the superscript m. The derivation of the time of transition from its steady state value δt_{i+nN_s} may be obtained by linearizing the modified-constraint equation, Eq. (1.3), and expressing δt_{i+nN_s} in terms of other quantities in the linearized modified-constraint equation.

As an example, consider the bang-bang controlled converter system. This converter system is not a constant-switching-frequency converter system. In general, for any converter system to operate with constant switching frequency, it is necessary that $M^u \in \{M_i\}$. For a two switched-state bang-bang controlled converter system, $N_M = 1$, and all the transitions from one switched-state to the next one are constraint-modulated; i.e., $M_i = M^c$, $N_T = 2$ and $N_q = 2$, $N_s = \text{lcm}(1,2,2) = 2$. From the perspective of *Variable Structure System Theory*[8], a bang-bang controlled converter is a simple *sliding mode controlled* variable structure system.

1.3 The Linearizability of Ideal Dc-to-Dc Converter Systems

Although an ideal dc-to-dc converter system may be linear with respect to its input vector $\mathbf{u}$, it is nonlinear with respect to the its control-input r_i. For an ideal dc-to-dc converter system to be linearizable in the vicinity of its steady state solution, it is necessary that there exists a $\delta > 0$, such that for any perturbation with magnitude smaller than δ, the sequences $\{(\mathcal{A}_j, \mathcal{B}_j, \mathcal{C}_j, \mathcal{D}_j)\} = \{(\mathbf{A}_j, \mathbf{B}_j, \mathbf{C}_j, \mathbf{D}_j)\}$ and $\{\mathcal{M}_j\} = \{\mathbf{M}_j\}$. Another way of stating the condition is that, for an ideal dc-to-dc converter system to be linearizable in the vicinity of its steady state solution, it is necessary that the order of the appearance of the switched-states and the control strategy used to control the

converter system do not change in the presence of *small* perturbations, especially, in the *small-signal limit.* Furthermore, it is necessary that the sequence indexed by j formed from the modulation parameters used in the modulation methods M_j's is periodic with period N_s. All the ideal dc-to-dc converter systems discussed in this thesis are assumed to be linearizable.

1.4 The Properties of Ideal Dc-to-Dc Converter Systems

In order to understand the ideal dc-to-dc converter system problem, the properties of ideal dc-to-dc converter systems must be studied. Many of the properties of ideal dc-to-dc converter systems are stated in Section 1.1. The most interesting properties are the following:

- The system is described by a linear differential equation at any instant of time except at τ_i's, the instants of switching.
- The differential equation has *piecewise constant coefficients* in time.
- The switching time is zero.
- The system is nonlinear with respect ot its control-inputs.
- The switching frequency is finite.
- The system state vector is continuous in time.
- The system output vector is discontinuous in time if the output matrix $\mathbf{C}$ or the transmission matrix $\mathbf{D}$ is discontinuous in time.

These properties imply that a solution to the ideal dc-to-dc converter system exists at all times, and given the control $r(t)$ and the initial condition, the output waveform is unique and can be computed. In fact, the output waveform between two consecutive switching

instants can be computed analytically. The *Small-Signal Frequency Response Theory* makes use to its full advantage of the fact that the output waveform can be computed.

An interesting fact about ideal dc-to-dc converter systems which has always been overlooked is that these systems, like any nonlinear system, may have multiple stable steady state solutions for a given operating condition. Therefore, contrary to what most power electronics engineers think, the small-signal behavior of a converter system corresponds to a periodic steady state solution of the system, instead of to the operating condition of the system. It is observed in experiments, that for a given operating condition, there may be multiple stable steady state solutions in a dc-to-dc converter circuit (see Section 2.1 and Section 3.4). In addition, the frequency responses of the converter circuit corresponding to different stable steady state solutions of the circuit are different in spite of the fact that the operating condition that gives rise to the different solutions is the same.

Chapter 2

An Example Ideal Dc-to-Dc Converter System

In this chapter, a very simple example ideal dc-to-dc converter system is used to demonstrate the basic ideas behind the *Small-Signal Frequency Response Theory*. The aim is to provide an understanding as well as a geometrical interpretation of the theory before introducing it formally in Chapter 3.

Consider the circuit shown in Fig. 2.1, a current-programmed buck converter circuit. If a sufficiently large output capacitor with very low ESR (equivalent series resistance) is used, and if the inductor current is the only concern, the circuit shown in Fig. 2.2 can be used to model this converter circuit. In this chapter, the steady state operation and the motion of this converter circuit will be studied in detail. Since the interest of this discussion is limited to the inductor current only, the circuit shown in Fig. 2.2 will be used in this discussion instead of that shown in Fig. 2.1.

The steady state solutions of the inductor current of the converter circuit shown in Fig. 2.2 are discussed in Section 2.1. This converter circuit may have infinitely many solutions for a given operating condition; nevertheless, not all of the solutions are stable. In Section 2.2, the motion of the converter system for a steady state solution is studied by using a difference equation. The concept of the stability of the solution of the converter system is introduced. In Section 2.3, the relation between the difference equation and the frequency response of the converter are established. The basic concepts of *Small-Signal Frequency Response Theory* are those introduced in Sections 2.2 and 2.3.

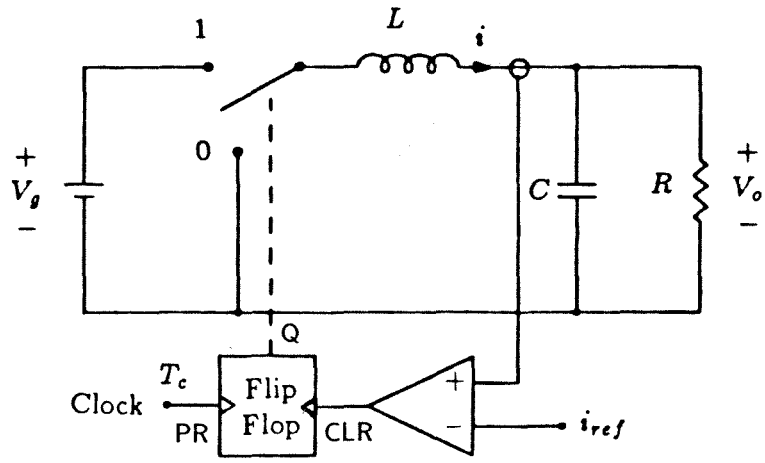

Figure 2.1: A current-programmed buck converter circuit.

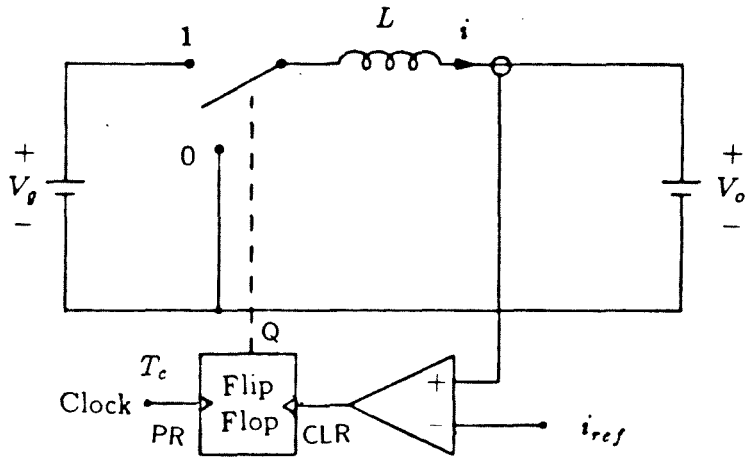

Figure 2.2: The circuit model for inductor current calculation of the converter circuit shown in Fig. 2.1.

2.1 The Steady State Solutions of the Converter Circuit

The steady state solutions of the converter circuit shown in Fig. 2.2 can easily be calculated. The quantity of interest in this study is the inductor current i. The state equation of the circuit for the switch in position 0 is:

$$\frac{di}{dt} = -\frac{V_o}{L} \tag{2.1}$$

and for the switch in position 1 is:

$$\frac{di}{dt} = \frac{V_g - V_o}{L} \tag{2.2}$$

In the framework laid out in Chapter 1, the converter may be described as follows:

$$\mathbf{x}(t) = i(t) \qquad \mathbf{u} = \begin{pmatrix} V_g \\ V_o \end{pmatrix}$$

$$\mathbf{A}_{2n} = 0 \qquad \mathbf{A}_{2n+1} = 0$$

$$\mathbf{B}_{2n} = \left(0, -\frac{1}{L}\right) \qquad \mathbf{B}_{2n+1} = \left(\frac{1}{L}, -\frac{1}{L}\right)$$

$$N_q = 2$$

$\forall\ n \in \mathbf{Z}$. In this example, the order of the system is one; as a result, the system matrices and the state vector degenerate to scalars. In order to simplify the example, the state of the system $\mathbf{x}(t)$ will be used as the output; therefore the output equation will be ignored.

The control strategy of this converter is: the transition from switched-state $2n-1$ to switched-state $2n$ is a *constraint-modulated* transition, and the transition from switched-state $2n$ to switched-state $2n+1$ is an *unmodulated* transition, $n \in \mathbf{Z}$. In the framework for describing the control strategy of a converter system laid out in Chapter 1, the control strategy of this converter system may be described as follows:

$$N_M = 2$$

$$\mathcal{M}_{2n+1} = M^u$$

$$\mathcal{M}_{2n} = M^c$$

where $n \in \mathbf{Z}$. Denote the steady state solution of the converter system by $\mathbf{X}(t)$. The steady state solution must satisfy the boundary condition:

$$\mathbf{X}(t) = \mathbf{X}(t + \sum_{j=1}^{N_s} T_j) \tag{2.3}$$

where N_s is the number of switched-states and T_j is the duration that the system is in the switched-state j.

From the description of the switched-networks of the converter circuit, its control strategy, and the boundary condition of its steady state solution, the steady state solution of the converter cannot be uniquely determined. Valid steady state solutions of the system can be found easily by the application of the framework for describing a converter system and its steady state solution in Chapter 1. For example, a valid steady state solution with $N_T = k\,N_M$, where k is a positive integer, can be found, and the number of switched-states $N_s = \text{lcm}(N_M, N_T, N_q) = k\,N_M = 2\,k$. For each of the different choices of k, a unique valid steady state solution of the converter system can be found.

For the case $k = 1$, $N_s = 2$, and $T_0 + T_1 = T_s = T_c$, where T_c is the clock period. The waveform of the inductor current is Solution (a) shown in Fig. 2.3. The slope of the waveform of the current ramping up is:

$$m_1 = \frac{V_g - V_o}{L} \tag{2.4}$$

The slope of the current ramping down is:

$$m_0 = \frac{-V_o}{L} \tag{2.5}$$

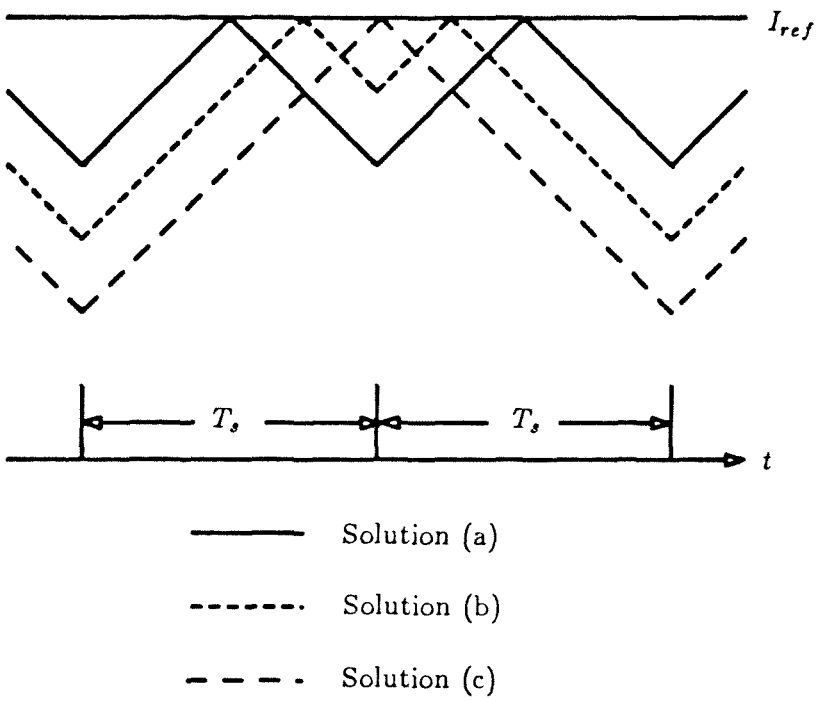

Figure 2.3: Three steady state solutions of the inductor current for a given operating condition of the converter circuit shown in Fig. 2.2.
Solution (a): $n = 1$, $T_s = T_c$, $N_T = 2$, $N_s = 2$.
Solution (b): $n = 2$, $T_s = 2\,T_c$, $N_T = 4$, $N_s = 4$.
Solution (c): $n = 1$, $T_s = 2\,T_c$, $N_T = 2$, $N_s = 2$.

The boundary condition for the steady state solution is:

$$m_0 T_0 + m_1 T_1 = 0$$

$$\frac{T_0}{T_1} = \frac{V_g - V_o}{V_o}$$

The steady state duty ratio $D \equiv T_1/(T_0 + T_1) = V_o/V_g$.

For the case $k = 2$, $N_s = N_T = kN_M = 4$, $T_s = T_0 + T_1 + T_2 + T_3$, and $T_1 + T_2 = T_c$, $T_3 + T_0 = T_c$. The waveform of the inductor current is Solution (b) shown in Fig. 2.3. The slope of the waveform is the same as the case for $k = 1$. Nevertheless, the boundary conditions for the steady state solution become:

$$m_0 T_0 = m_1 T_1 \tag{2.6}$$

$$m_1 T_2 = m_1 T_3 \tag{2.7}$$

Equation (2.6) and Eq. (2.7) together with $T_1 + T_2 = T_c$ and $T_3 + T_0 = T_s$ form a system of four linear equations with four unknowns T_0, T_1, T_2, T_3, which can be solved.

In general, for the case $k = k^*$, there is a system of k^* linear equations with k^* unknowns. Therefore, for each $k^* \in \mathbf{Z}^+$, a steady state solution of this converter system can be found for each given operating condition — V_g and V_o. Nevertheless, not all of the steady state solutions are stable solutions. Therefore, it does not make any sense to use an operating condition (or an operating point), a term that is commonly used in electronic circuits, to characterize the steady state solution for this class of converter circuits. Any constant-switching-frequency converter circuit which uses the *constraint* modulation in its control strategy has this problem. This phenomenon is a manifestation of the nonlinearity of the ideal dc-to-dc converter circuit, which comes from the switching action in the circuit.

Furthermore, it is obvious that it is possible to have $T_1 + T_0 = kT_c$, $k \in \mathbf{Z}^+$, in this converter circuit, provided $T_1 > (k-1)T_c$. For the case of $T_1 + T_0 = 2T_c$, the

phenomenon is also referred to as period doubling, which is quite commonly observed experimentally (See Fig. 2.3). Nevertheless, not all operating conditions can result in this type of phenomenon. It is also possible to have a hybrid of the phenomena discussed above.

From the steady state solutions of this simple example converter circuit, the following conclusions can be drawn:

1. It is not sufficient to characterize the steady state solution of converter circuits with circuit operation parameters, such as the supplied voltages, the supplied currents, the reference voltages, and reference currents.

2. A possible way to specify the steady state solution is to use the circuit operation parameters and the T_j's.

3. As a result, it is not appropriate to speak of the frequency response of a converter circuit under a certain operating condition. Instead, the frequency response of a converter circuit corresponds to a particular steady state solution of the converter circuit.

For an example physical converter circuit that has multiple stable steady state solutions for a given operating condition, see Section 3.4.

2.2 The Small-Signal Motion of the System

Before discussing the frequency response of an ideal dc-to-dc converter system, the motion of the system in the time domain must be studied. The motion of an ideal dc-to-dc converter system is complicated. In general, the detailed large-signal motion of the system can only be studied by numerical simulation. Fortunately, if an ideal dc-to-dc converter system is linearizable, the small-signal motion of the system can be

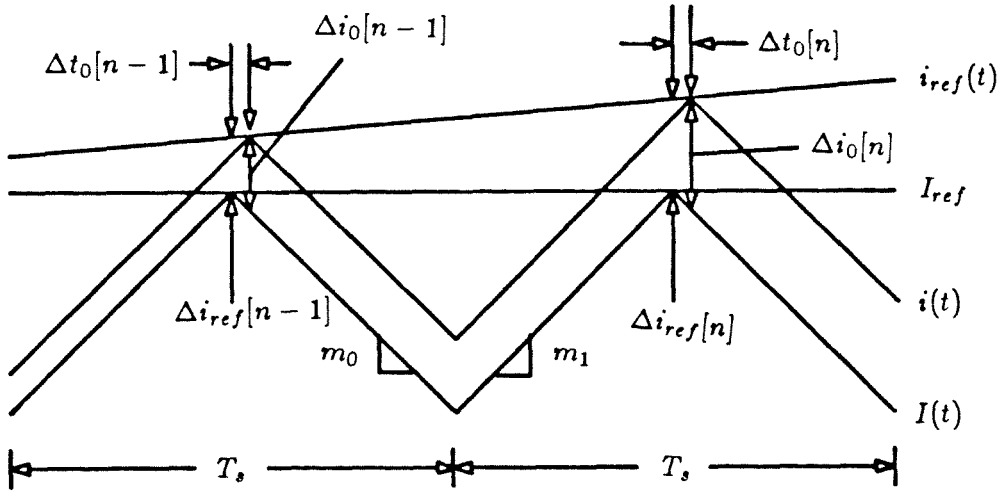

Figure 2.4: Steady state inductor current — $I(t)$, perturbed inductor current — $i(t)$, and related definitions.

characterized by a difference equation. The sequences in the difference equation represent the sampled control-input signals and the sampled system states. The trajectory of the system between the sample points can always be found (See Section 1.4). This is a fortunate property of ideal dc-to-dc converter systems.

In this section, the small-signal motion of only one particular steady state solution of the circuit shown in Fig. 2.2 is discussed. This particular steady state solution is the two-switched-state solution in which $T_0 + T_1 = T_c$ (Solution (a) shown in Fig. 2.3). The steady state solution waveform, that is, the steady state inductor current waveform, and the perturbed waveform are shown in Fig. 2.4.

The difference equation that describes the small motion of a N_s-switched-state converter system, i.e., a converter system with a N_s-switched-state solution, in the vicinity

of its steady state solution has the function of relating a sample of the perturbed system state at a sample point to the sample of the perturbed system state at a similar sample point N_s switched-states earlier, and to the sample of the perturbed control-input. From the geometry shown in Fig. 2.4, an expression for $\Delta t_0[n]$ can be obtained easily:

$$\Delta t_0[n] = \frac{1}{m_1} \{\Delta i_{ref}[n] - \Delta i_0[n-1]\} + O(\Delta^2) \tag{2.8}$$

With $\Delta t_0[n]$ known, $\Delta i_0[n]$ may be expressed in terms of $\Delta t_0[n]$, and then in terms of $\Delta i_{ref}[n]$ and $\Delta i_0[n-1]$ as follows:

$$\begin{aligned} \Delta i_0[n] &= \Delta i_0[n-1] + (m_1 - m_0)\, \Delta t_0[n] \\ &= \left(1 - \frac{m_1 - m_0}{m_1}\right) \Delta i_0[n-1] + \frac{m_1 - m_0}{m_1} \Delta i_{ref}[n] + O(\Delta^2) \\ &= k\, \Delta i_0[n-1] + (1-k)\, \Delta i_{ref}[n] + O(\Delta^2) \end{aligned} \tag{2.9}$$

where $k \equiv \frac{m_0}{m_1}$. In the *small-signal limit*, terms of $O(\Delta^2)$ or higher are dropped, $\Delta \rightarrow \delta$, and the difference equation becomes:

$$\delta i_0[n] = k\, \delta i_0[n-1] + (1-k)\, \delta i_{ref}[n] \tag{2.10}$$

It is obvious that the small-signal motion of the system is unstable when $k > 1$. Though not discussed here, the difference equation that describes the small-signal motion in the vicinity of other stable steady solutions of this simple example converter system can be found easily by using a geometrical approach similar to that discussed above.

2.3 The Frequency Response of the System

In this section, the frequency response of the output, inductor current i, with respect to the control-input, reference current i_{ref}, is studied, where $i(t) = I(t) + \delta i(t)$, $i_{ref}(t) = I_{ref} + \delta i_{ref}(t)$, in which $I(t)$ is the steady state solution of $i(t)$ and I_{ref} is the

controlling reference signal i_{ref} in the steady state. Since $I(t)$ is periodic with period T_s, the switching period, it does not contribute to the frequency response. The steady state reference current I_{ref} is a dc quantity; therefore, it does not contribute to the frequency response either. As a result, the frequency response of i with respect to i_{ref} is the same as the frequency response of δi with respect to δi_{ref}.

In Section 2.2, the difference equation that describes the relation between $\delta i_0[n]$ and $\delta i_0[n-1]$, Eq. (2.10), is derived. In order to find the small-signal frequency domain relation between i and i_{ref}, the following three *missing links* must be established in addition to the difference equation:

1. The relation between $\delta i_{ref}(s)$ — the Laplace transform of the perturbed control-input $\delta i_{ref}(t)$, and $\delta i^*_{ref}(s)$ — the Laplace transform of the sampled $\delta i_{ref}(t)$; $\delta i^*_{ref}(s)$ is defined below:

$$\delta i^*_{ref}(s) \equiv \mathcal{L}\left\{\sum_n \delta i_{ref}(nT_s)\,\delta(t-nT_s)\right\}$$

2. The relation between $\delta i^*_{ref}(s)$, and $\delta i^*_0(s)$ — the Laplace transform of the sampled $\delta i(t)$; $\delta i^*_0(s)$ is defined below:

$$\delta i^*_0(s) \equiv \mathcal{L}\left\{\sum_n \delta i_0[n]\,\delta(t-nT_s)\right\}$$

   where $i_0[n]$ is defined in Fig. 2.4.

3. The contribution of a sample of the perturbed state $\delta i_0[n]$ to the perturbed state $\delta i(t)$ over one switching period T_s and to the spectrum of the perturbed state $\delta i(s)$; see Fig. 2.5.

The first link is established by Shannon's *Sampling Theorem*[7]:

$$\delta i^*_{ref}(s) = \frac{1}{T_s}\sum_n \delta i_{ref}(s+in\omega_s) \tag{2.11}$$

where $i = \sqrt{-1}$, $\omega_s = \frac{2\pi}{T_s}$. Nevertheless, there is a complication that i_{ref} may be naturally sampled. In other words, i_{ref} is not uniformly sampled. Fortunately, it may be shown that the effect of this *almost periodic sampling* process is merely the introduction of additional noise into the system in the *small-signal limit* when compared to the uniform sampling process (See Section 4.3).

The second link is obtained by the application of the z-transform to the difference equation that describes the small-signal motion of the system with $z = e^{sT_s}$ [3]. If the z-transform is applied to the difference equation Eq. (2.10), it becomes:

$$\delta i(z) = z^{-1}\, k\, \delta i(z) + (1 - k)\, \delta i_{ref}(z) \tag{2.12}$$

Substituting e^{sT_s} for z, then, $i(z) \rightarrow i^*(s)$, $i_{ref}(z) \rightarrow i^*_{ref}(s)$, and Eq. (2.12) becomes:

$$\delta i^*(s) = \frac{1 - k}{1 - ke^{-sT_s}}\, i^*_{ref}(s) \tag{2.13}$$

The third link is one of the major features of the *Small-Signal Frequency Response Theory*, which makes it different from other approximate analytical methods. While most other methods use a concept called *averaging* to relate the sequence of the sampled perturbed state $\{\delta i_0[n]\}$ to the spectrum of the analog perturbed state $\delta i(s)$, the *Small Signal Frequency Response Theory* computes, first, the time domain contribution of $\delta i_0[n]$ to the $\delta i(t)$ over one switching period T_s, and then, from the time domain contribution, computes the frequency domain contribution to $\delta i(s)$.

Figure 2.5 shows the time domain contribution of $\Delta i_0[n]$ on the $\Delta i(t)$. The shaded area under the waveform of $\Delta i(t)$ is the contribution of $\Delta i_0[n]$ to $\Delta i(t)$ over one switching period T_s. In the *small-signal limit*, $\Delta i_{ref} \rightarrow \delta i_{ref}$, $\delta i_{ref} \rightarrow 0$, $\Delta i_0[n] \rightarrow \delta i_0[n]$ and $\Delta i(t) \rightarrow \delta i(t)$. The trapezoidal areas under the waveform approach zero much faster than the rectangular areas in the *small-signal limit*; therefore, they can be neglected for small-signal calculations. Consequently, the contribution of $\delta i_0[n]$ to $\delta i(t)$ may be

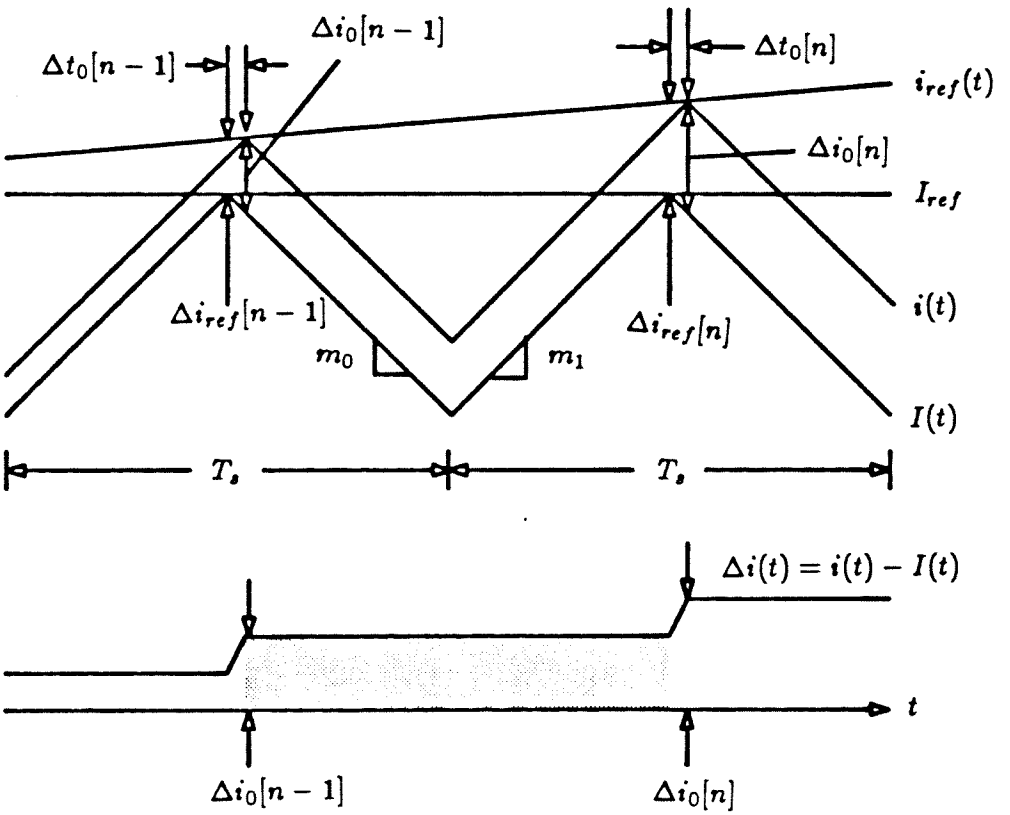

Figure 2.5: The contribution of $\Delta i_0[n]$ to $\Delta i(t)$ — shaded area.

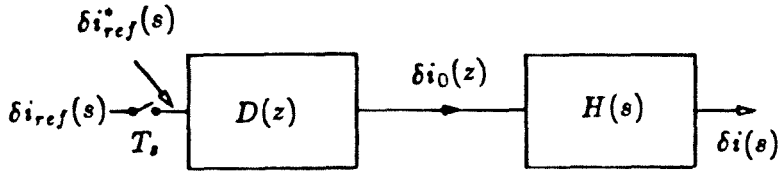

$$k = \frac{m_0}{m_1} \qquad D(z) = \frac{1-k}{1-k\,z^{-1}} \qquad H(s) = \frac{1-e^{-sT_s}}{s}$$

Figure 2.6: The equivalent linear system for the converter circuit shown in Fig. 2.2.

treated as a rectangular piece of the waveform of *"length"* in time T_s, and of *"height"* $\delta i_0[n]$. This shaded part in the *small-signal limit* is exactly the same as the output of the *zero-order-hold*[3] with a δ-function with magnitude $\delta i_0[n]$ at the input of the hold. Hence, the third link is a *zero-order-hold.* This link may be described by:

$$\delta i(s) = \frac{1-e^{-sT_s}}{s}\,\delta i_0^*(s) \tag{2.14}$$

The relation between the spectrum of the output δi and the spectrum of the control-input δi_{ref} can therefore be described by a sampled-data system shown in Fig. 2.6. The overall result is:

$$\delta i(s) = G(s)\,\delta i^*_{ref}(s) \tag{2.15}$$

where

$$\delta i^*_{ref}(s) = \frac{1}{T_s}\sum_n \delta i_{ref}\left(s + \frac{2n\pi i}{T_s}\right)$$

$$G(s) = \frac{1-e^{-sT_s}}{s}\,\frac{1-k}{1-k\,e^{-sT_s}}$$

Equation (2.15) describes the frequency response of δi with respect to δi_{ref}. The ratio $\delta i(s)/\delta i_{ref}(s)$ may be loosely referred to as the *"transfer function"* from i_{ref} to i, and $G(s)$ is the *pulse transfer function.*

The small-signal frequency response of δi with respect to δi_{ref} of the converter circuit shown in Fig. 2.2 for the steady state solution with $T_0 + T_1 = T_c$, Eq. (2.15), may have little practical application for the converter circuit. For the converter circuit shown in Fig. 2.1, however, Eq. (2.15) is a good approximation of the frequency response of the inductor current to the reference current (using the circuit shown in Fig. 2.2 as the model). The frequency response of δi with respect to δi_{ref} is extremely useful for designing a controller for regulating its average inductor current and its output voltage with analog controller design techniques.

Chapter 3

Simple Two-Switched-State Converter Systems

Most of the converter circuits in common use have two switched-networks. In the example converter circuit in Chapter 2, it is found that even though the converter circuit has only two switched-networks, the number of switched-states in its steady state solution may be infinite. Nevertheless, in most cases, one would like to operate a converter circuit so that the number of switched-states of the steady state solution is the same as the number of switched-networks of the converter circuit. Therefore, the discussion of this chapter will concentrate on two switched-state converters systems, in which the number of switched-states is the same as the number of switched-networks. Furthermore, in this chapter, the discussion is limited to simple converter systems, those that do not use modified-constraint modulation in their control strategy and do not have the output equation; i.e., the output matrix $\mathbf{C}$ and the transmission matrix $\mathbf{D}$ are ignored. The *non-simple* converter systems will be discussed in Chapter 5.

Given an ideal dc-to-dc converter system and its steady state solution, the *Small-Signal Frequency Response Theory* gives the control-input-to-output frequency response of the system provided that the steady state solution is small-signal stable. The *Small-Signal Frequency Response Theory* does not predict anything about the steady state solution; instead, it assumes that the steady state solution $\mathbf{X}(t)$ is known and given. The steady state solution $\mathbf{X}(t)$ is periodic with period $T_s = T_0 + T_1$, where T_s is the switching period, T_0 is the duration of the switched-state 0, and T_1 is the duration

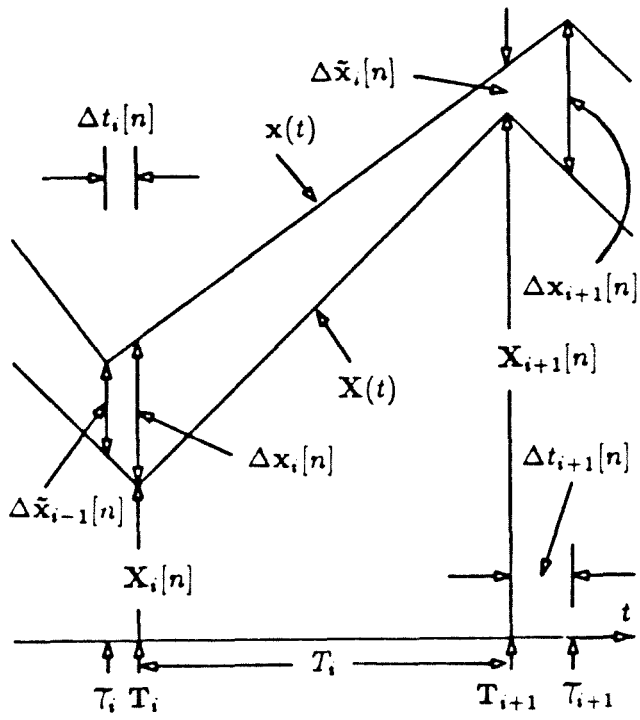

Figure 3.1: Steady state state vector $\mathbf{X}(t)$*, perturbed state vector* $\mathbf{x}(t)$*, and related definitions.*

of the switched-state 1. For the convenience of describing the problem, define:

$$\mathbf{T}_i[n] \equiv \mathbf{T}_{i+nN_s} \tag{3.1}$$

$$\Delta t_j \equiv \mathcal{T}_j - \mathbf{T}_j \tag{3.2}$$

$$\Delta t_i[n] \equiv \Delta t_{i+nN_s} \tag{3.3}$$

$$\mathbf{X}_i \equiv \mathbf{X}(\mathbf{T}_i[n]) \tag{3.4}$$

$$\Delta\mathbf{x}(t) \equiv \mathbf{x}(t) - \mathbf{X}(t) \tag{3.5}$$

$$\Delta\mathbf{x}_j \equiv \Delta\mathbf{x}(\mathbf{T}_j + \max(\delta t_j, 0)) \tag{3.6}$$

$$\Delta\mathbf{x}_i[n] \equiv \Delta\mathbf{x}_{i+nN_s} \tag{3.7}$$

$$\Delta\tilde{\mathbf{x}}_j \equiv \Delta\mathbf{x}(\mathbf{T}_{j+1} + \min(\Delta t_{j+1}, 0)) \tag{3.8}$$

$$\Delta\tilde{\mathbf{x}}_i[n] \equiv \Delta\tilde{\mathbf{x}}_{i+nN_s} \tag{3.9}$$

where $\mathcal{T}_j$ is the time at which the converter system switches from switched-state $j-1$ to switched-state j, $\mathbf{T}_j$ is the $\mathcal{T}_j$ of the steady state solution, Δt_j is the deviation of $\mathcal{T}_j$ from $\mathbf{T}_j$ for the particular solution of the system under study, $\mathbf{x}(t)$ is the particular solution of the state of the system, $\mathbf{X}(t)$ is the periodic steady state solution of the state of the system, $\Delta\mathbf{x}(t)$ is the perturbed state of the system, $\mathbf{X}_i$ is the value of the steady state solution of the state at the transition from switched-state $i-1$ to switched-state i, $\Delta\mathbf{x}_j$ is the value of the perturbed state at the beginning of switched-state j, and $\Delta\tilde{\mathbf{x}}_j$ is the value of the perturbed state at the end of switched-state j. The subscript j is the index for the switched-state j or the transition from switched-state $j-1$ to switched-state j. The subscript i is the index in a switching cycle, and the index for the switching cycle is n. These definitions are depicted in Fig. 3.1.

The procedure for finding the frequency response of an ideal two-switched-state dc-to-dc converter system is essentially the same as that used for the simple example converter circuit in Chapter 2. The first step in the procedure is to find the difference

equation that describes the small-signal system motion in the vicinity of the given steady state solution. Without loss of generality, only the case of modulating $\Delta t_0[n]$ is considered. This step is discussed in Section 3.1. The second step in the procedure is is to find the *equivalent hold* that relates the $\Delta \mathbf{x}_j$'s to $\Delta x(s)$. This step is discussed in Section 3.2.

In the sections following Section 3.2 are three examples of two-switched-state converter systems; each of the examples has a different control strategy. The three control strategies in the examples are:

1. Constant-switching-frequency time modulation (PWM) control.

2. Constant-switching-frequency constraint modulation control (programming).

3. Variable-switching-frequency bang-bang control.

For each example control strategy, the general results are discussed first, followed by the application of these results to predict the frequency response of an example converter circuit. In addition, experimental results are compared to the theoretical predictions. The example converter circuit topology used in all three examples is the simple R-L topology. This topology is chosen for the following reasons: First, its steady state can be calculated analytically. Second, it is a first-order system with only one reactive element; therefore, the result is relatively simple. Third, this converter circuit is so simple that parasitics can be neglected or absorbed into its circuit elements except at relatively high frequencies. As a result, it offers very good control over the experiments on the circuit. Fourth, using the different control strategies with this simple topology can illustrate where the approximate analytical methods fail.

3.1 The Small-Signal Motion of the Systems

The small-signal motion of a simple ideal dc-to-dc converter system in the vicinity of a steady state solution may be described by a difference equation that relates $\delta\mathbf{x}_0[n-1]$ to $\delta\mathbf{x}_0[n]$. This difference equation is sufficient to describe the motion of the system because the differential equation that describes the converter system in steady state has periodic piecewise constant coefficients in time. As a result of the linearity of the switched-networks or structures of the system, the exact trajectory of the system between the sample points given by the difference equation can always be found. Furthermore, if the sequence $\{\delta\mathbf{x}_i[n]\}$ is finite, then $\delta\mathbf{x}(t)$ is finite; i.e., the stability of the difference equation implies the small-signal stability of the system.

Before the derivation of the difference equation that describes the small-signal motion of the system, the converter system and its steady state solution must be put in the framework laid out in Chapter 1. For a two switched-state converter system in steady state, $\forall n \in \mathbf{Z}$:

$$(\mathbf{A}_{2n}, \mathbf{B}_{2n}, \mathbf{C}_{2n}, \mathbf{D}_{2n}) = (\mathbf{A}_0, \mathbf{B}_0, \mathbf{C}_0, \mathbf{D}_0) \tag{3.10}$$

$$(\mathbf{A}_{2n+1}, \mathbf{B}_{2n+1}, \mathbf{C}_{2n+1}, \mathbf{D}_{2n+1}) = (\mathbf{A}_1, \mathbf{B}_1, \mathbf{C}_1, \mathbf{D}_1) \tag{3.11}$$

$$M_{2n} = M_0 \tag{3.12}$$

$$M_{2n+1} = M_1 \tag{3.13}$$

$$T_{2n} = T_0 \tag{3.14}$$

$$T_{2n+1} = T_1 \tag{3.15}$$

For the converter system to be linearizable, it is necessary that when the system is perturbed in the vicinity of the steady state solution in the *small-signal limit*:

$$\{(\mathcal{A}_j, \mathcal{B}_j, \mathcal{C}_j, \mathcal{D}_j)\} = \{(\mathbf{A}_j, \mathbf{B}_j, \mathbf{C}_j, \mathbf{D}_j)\} \tag{3.16}$$

$$\{\mathcal{M}_j\} = \{M_j\} \tag{3.17}$$

$\forall\, j \in \mathbf{Z}$. The modulation method M_j determines τ_j, i.e., the time of the transition from $(\mathbf{A}_{j-1}, \mathbf{B}_{j-1}, \mathbf{C}_{j-1}, \mathbf{D}_{j-1})$ to $(\mathbf{A}_j, \mathbf{B}_j, \mathbf{C}_j, \mathbf{D}_j)$. Furthermore, the modulation parameters used in M_{i+nN_s} $\forall\, n \in \mathbf{Z}$ must not alter with change of n for fixed i. In the following discussion, the converter system under study is assumed to be linearizable.

Without loss of generality, the converter system can be considered to be modulated by the control-input r_0 only. The contribution from modulating M_{2n+1}'s by the control-input r_1 may be taken into account later by superposition. Define $\tilde{\mathbf{\Phi}}_i, \tilde{\mathbf{K}}_i, \tilde{\mathbf{k}}_i$ by the following equations:

$$\delta\tilde{\mathbf{x}}_i[n] = \tilde{\mathbf{\Phi}}_i\, \delta\mathbf{x}_i[n] \tag{3.18}$$

$$\delta\mathbf{x}_i[n] = \tilde{\mathbf{K}}_i\, \delta\tilde{\mathbf{x}}_{i-1}[n] + \tilde{\mathbf{k}}_i\, \delta r_i[n] \tag{3.19}$$

where $\delta r_i[n]$ is the sampled perturbed control-input. The quantity $\tilde{\mathbf{\Phi}}_i$ is the transition matrix that relates value of the perturbed state at the beginning of switched-state $i+nN_s$ to that at the end, and it depends on $\mathbf{A}_i$ and T_i only. The quantity $\tilde{\mathbf{K}}_i$ is the transition matrix that relates value of the perturbed state at the end of switched-state $i-1+nN_s$ to that at the beginning of the switched-state $i+nN_s$. The effect of $\delta r_i[n]$ on $\delta\mathbf{x}_i[n]$ is determined by the vector $\tilde{\mathbf{k}}_i$. There is a different $\tilde{\mathbf{K}}_i$ and a different $\tilde{\mathbf{k}}_i$ corresponding to each modulation method M_{i+nN_s}. The $\tilde{\mathbf{\Phi}}_i$'s, and the $\tilde{\mathbf{K}}_i$ and $\tilde{\mathbf{k}}_i$ for each of the three modulation methods discussed in this chapter, namely, no modulation, time modulation, and constraint modulation, are derived in the following subsections.

3.1.1 Unmodulated Transitions

Consider the case that the transitions from switched-state $i-1+nN_s$ to switched-state $i+nN_s$ are *unmodulated*, i.e., $M_{i+nN_s} = M^u$, $\forall n \in \mathbf{Z}$. Obviously, $\tilde{\mathbf{k}}_i^u = \mathbf{0}$. The state $\mathbf{x}(t)$ is continuous and $\delta t_i[n] \equiv 0$. Therefore, $\mathbf{x}_i[n] = \tilde{\mathbf{x}}_{i-1}[n]$. As a result, $\delta\mathbf{x}_i[n] = \delta\tilde{\mathbf{x}}_{i-1}[n]$, and $\tilde{\mathbf{K}}_i^u \equiv \mathbf{I}$. Quantities related to the *unmodulated* case are denoted

by the superscript u.

3.1.2 Time-Modulated Transitions

Consider the case that the transitions from switched-state $i-1+nN_s$ to switched-state $i+nN_s$ are *time-modulated*, i.e., $M_{i+nN_s} = M^t$, $\forall n \in \mathbf{Z}$. Quantities related to the *time-modulated* case are denoted by the superscript t. If the modulating perturbed control-input sequence is $\delta r_i[n]$, and the slope of the ramp of the sawtooth wave used in the pulse width modulator is m_i^t, then the changes in time of transition may be expressed in terms of $\delta r_i[n]$ as follows:

$$\delta t_i[n] = (m_i^t)^{-1} \delta r_i[n] \tag{3.20}$$

With $\delta t_i[n]$ known, the perturbed state just after the transition $\delta \mathbf{x}_i[n]$ may be expressed in terms of the perturbed state just before the transition $\delta \tilde{\mathbf{x}}_{i-1}[n]$ and the control-input $\delta r_i[n]$. From the geometry shown in Fig. 3.1, it is obvious that:

$$\begin{aligned} \Delta \mathbf{x}_i[n] &= \Delta \tilde{\mathbf{x}}_{i-1}[n] + \{\dot{\mathbf{X}}_i^- + \mathrm{O}(\Delta)\}\, \Delta t_i[n] - \{\dot{\mathbf{X}}_i^+ + \mathrm{O}(\Delta)\}\, \Delta t_i[n] \\ &= \Delta \tilde{\mathbf{x}}_{i-1}[n] + \bar{\mathbf{k}}_i\, \Delta t_i[n] + \mathrm{O}(\Delta^2) \end{aligned} \tag{3.21}$$

where

$$\begin{aligned} \dot{\mathbf{X}}_i^- &= \mathbf{A}_{i-1}\mathbf{X}_i + \mathbf{B}_{i-1}\mathbf{u} \\ \dot{\mathbf{X}}_i^+ &= \mathbf{A}_i\mathbf{X}_i + \mathbf{B}_i\mathbf{u} \\ \bar{\mathbf{k}}_i &\equiv \dot{\mathbf{X}}_i^- - \dot{\mathbf{X}}_i^+ \\ &= (\mathbf{A}_{i-1} - \mathbf{A}_i)\mathbf{X}_i + (\mathbf{B}_{i-1} - \mathbf{B}_i)\mathbf{u} \end{aligned}$$

In the *small-signal limit*:

$$\delta \mathbf{x}_i[n] = \delta \tilde{\mathbf{x}}_{i-1}[n] + \bar{\mathbf{k}}_i\, \delta t_i[n] \tag{3.22}$$

$$\delta \mathbf{x}_i[n] = \delta \tilde{\mathbf{x}}_{i-1}[n] + (m_i^t)^{-1}\, \bar{\mathbf{k}}_i\, \delta r_i[n] \tag{3.23}$$

Hence:

$$\tilde{\mathbf{K}}_i^t = \mathbf{I} \tag{3.24}$$

$$\tilde{\mathbf{k}}_i^t = (m_i^t)^{-1} \{(\mathbf{A}_{i-1} - \mathbf{A}_i)\mathbf{X}_i + (\mathbf{B}_{i-1} - \mathbf{B}_i)\mathbf{u}\} \tag{3.25}$$

3.1.3 Constraint-Modulated Transitions

For the case that the transitions from switched-state $i - 1 + nN_s$ to switched-state $i + nN_s$ are *constraint-modulated*, i.e., $M_{i+nN_s} = M^c$, $\forall n \in \mathbf{Z}$. The first step in finding $\tilde{\mathbf{K}}_i^c$ and $\tilde{\mathbf{k}}_i^c$ is to express $\delta t_i[n]$ in terms of $\delta\tilde{\mathbf{x}}_{i-1}[n]$ and $\delta r_i[n]$. Quantities related to the *constraint-modulated* case are denoted by the superscript c. The constraint equation is:

$$\mathbf{f}_i^T \mathbf{x}(\mathbf{T}_{i+nN_s} + \Delta t_i[n]) + m_i^c \, \Delta t_i[n] + c_i - r_i[n] = 0 \tag{3.26}$$

where $\mathbf{f}_i^T$ is a vector constant and c_i is a scalar constant corresponding to M_i; $r_i[n]$ is the modulating control-input sequence from either the uniform-sampling of the control-input $r_i(t)$, in this case $r_i[n] = r_i(\mathbf{T}_{i+2n})$, or the natural-sampling of the control-input $r_i(t)$, in this case $r_i[n] = r_i(\mathbf{T}_{i+2n} + \Delta t_i[n])$; and m_i^c is a constant which is the slope of the ramp of the sawtooth wave used in the pulse width modulator, in the case of a PWM converter, or the slope of the added stabilization ramp, in the case of a programmed converter. The constraint equation is the condition under which the converter system switches from switched-state $i + nN_s - 1$ to switched-state $i + nN_s$. In a converter circuit, the constraint equation is the mathematical model of the switching action of the comparator circuit that determines when this change of the switched-state occurs. This comparator circuit has the control-input $r_i(t)$ at one of its inputs, and the sum of a sawtooth ramp with slope m_i^c and the weighted sum of the system states $\mathbf{f}_i^T \mathbf{x}(t)$ at its other input. The constraint equation, Eq. (3.26), may be linearized by perturbing it and then subtracting steady

state part from it. In the *small-signal limit* the linearized constraint equation is:

$$\mathbf{f}_i^T\,\delta\tilde{\mathbf{x}}_{i-1}[n] + \mathbf{f}_i^T\,\dot{\mathbf{X}}_i^-\,\delta t_i[n] + m_i^c\,\delta t_i[n] - \delta r_i[n] = 0 \tag{3.27}$$

where $\dot{\mathbf{X}}_i^- = \mathbf{A}_{i-1}\,\mathbf{X}_i + \mathbf{B}_{i-1}\,\mathbf{u}$.

The quantity $\delta t_i[n]$ in the linearized constraint equation may be expressed in terms of the other quantities in the equation as follows,

$$\delta t_i[n] = -\mathbf{p}_i^T\,\delta\tilde{\mathbf{x}}_{i-1}[n] + m_i\,\delta r_i[n] \tag{3.28}$$

where

$$\begin{aligned} m_i &= \left[\mathbf{f}_i^T\,\dot{\mathbf{X}}_i^- + m_i^c\right]^{-1} \\ \mathbf{p}_i &= \left[\mathbf{f}_i^T\,\dot{\mathbf{X}}_i^- + m_i^c\right]^{-1}\mathbf{f}_i \end{aligned}$$

With use of this result and Eq. (3.22), the result of the time-modulated case, then:

$$\begin{aligned} \delta\mathbf{x}_i[n] &= \tilde{\mathbf{K}}_i^t\,\delta\tilde{\mathbf{x}}_{i-1}[n] + \bar{\mathbf{k}}_i\,\left[-\mathbf{p}_i^T\,\delta\tilde{\mathbf{x}}_{i-1}[n] + m_i\,\delta r_i[n]\right] \\ &= \left[\mathbf{I} - \bar{\mathbf{k}}_i\,\mathbf{p}_i^T\right]\delta\tilde{\mathbf{x}}_{i-1}[n] + m_i\,\bar{\mathbf{k}}_i\,\delta r_i[n] \end{aligned} \tag{3.29}$$

Hence:

$$\tilde{\mathbf{K}}_i^c = \mathbf{I} - \bar{\mathbf{k}}_i\,\mathbf{p}_i^T \tag{3.30}$$

$$\tilde{\mathbf{k}}_i^c = m_i\,\bar{\mathbf{k}}_i \tag{3.31}$$

3.1.4 Between the Transitions

The relation between the perturbed state at the end of the switched-state $i + nN_s$, $\delta\tilde{\mathbf{x}}_i[n]$, and the perturbed state at the beginning of the switched-state $i + nN_s$, $\delta\mathbf{x}_i[n]$, is relatively easy to find. Consider the differential equation that describes $\Delta\mathbf{x}(t)$ for $\max(\mathbf{T}_j, \mathcal{T}_j) < t < \min(\mathbf{T}_{j+1}, \mathcal{T}_{j+1})$, $j = i + nN_s$:

$$\Delta\dot{\mathbf{x}}(t) = \dot{\mathbf{x}}(t) - \dot{\mathbf{X}}(t)$$

$$
\begin{aligned}
&= \mathbf{A}_i\,\mathbf{x}(t) - \mathbf{A}_i\,\mathbf{X}(t) \\
&= \mathbf{A}_i\,\{\mathbf{x}(t) - \mathbf{X}(t)\} \\
&= \mathbf{A}_i\,\Delta\mathbf{x}(t) \qquad (3.32)
\end{aligned}
$$

The solution to this equation for $\max(\mathbf{T}_j, \mathcal{T}_j) < t < \min(\mathbf{T}_{j+1}, \mathcal{T}_{j+1})$, $j = i + nN_s$, is:

$$
\Delta\mathbf{x}(t) = e^{\mathbf{A}_i(t-\max(\mathbf{T}_j,\mathcal{T}_j))}\,\Delta\mathbf{x}\left(\max(\mathbf{T}_j, \mathcal{T}_j)\right) \qquad (3.33)
$$

By using the definition of $\Delta\tilde{\mathbf{x}}_i[n]$, then:

$$
\begin{aligned}
\Delta\tilde{\mathbf{x}}_i[n] &= \Delta\mathbf{x}(\min(\mathbf{T}_{j+1}, \mathcal{T}_{j+1})) \\
&= e^{\mathbf{A}_i\left(\min(\mathbf{T}_{j+1},\mathcal{T}_{j+1})-\max(\mathbf{T}_j,\mathcal{T}_j)\right)}\,\Delta\mathbf{x}(\max(\mathbf{T}_j, \mathcal{T}_j)) \\
&= e^{\mathbf{A}_i\left(\min(\mathbf{T}_{j+1},\mathcal{T}_{j+1})-\max(\mathbf{T}_j,\mathcal{T}_j)\right)}\,\Delta\mathbf{x}_j \\
&= e^{\mathbf{A}_i\left(\min(\mathbf{T}_{j+1},\mathcal{T}_{j+1})-\max(\mathbf{T}_j,\mathcal{T}_j)\right)}\,\Delta\mathbf{x}_i[n] \qquad (3.34)
\end{aligned}
$$

In the *small-signal limit*, $\Delta \to \delta$, $\mathcal{T}_j \to \mathbf{T}_j$, $\forall\, j \in \mathbf{Z}$:

$$
\begin{aligned}
\delta\tilde{\mathbf{x}}_i[n] &= e^{\mathbf{A}_i(\mathbf{T}_{j+1}-\mathbf{T}_j)}\,\delta\mathbf{x}_i[n] \\
&= e^{\mathbf{A}_i T_j}\,\delta\mathbf{x}_i[n] \\
&= e^{\mathbf{A}_i T_i}\,\delta\mathbf{x}_i[n] \qquad (3.35) \\
&= \tilde{\mathbf{\Phi}}_i\,\delta\mathbf{x}_i[n] \qquad (3.36)
\end{aligned}
$$

where

$$
\tilde{\mathbf{\Phi}}_i = e^{\mathbf{A}_i T_i} \qquad (3.37)
$$

Note that $j = i + nN_s$, $\mathbf{T}_{j+1} - \mathbf{T}_j = T_j$, and $\mathbf{A}_j$ and T_j are periodic in j with period N_s.

3.1.5 The Difference Equation

With the $\tilde{\mathbf{\Phi}}_i$'s, $\tilde{\mathbf{K}}_i$'s, and $\tilde{\mathbf{k}}_i$'s derived above, the difference equation that describes the small-signal motion of the system in the vicinity of its steady state solution

can be constructed. As mentioned before in this discussion, it is assumed that only M_{2n} is being modulated by the control-input δr_0; $\delta r_1 \equiv 0$. The difference equation is:

$$\begin{aligned}
\delta \mathbf{x}_0[n] &= \tilde{\mathbf{K}}_0\, \delta \tilde{\mathbf{x}}_1[n-1] + \tilde{\mathbf{k}}_0\, \delta r_0[n] \\
&= \tilde{\mathbf{K}}_0\, \tilde{\mathbf{\Phi}}_1\, \delta \mathbf{x}_1[n-1] + \tilde{\mathbf{k}}_0\, \delta r_0[n] \\
&= \tilde{\mathbf{K}}_0\, \tilde{\mathbf{\Phi}}_1\, \tilde{\mathbf{K}}_1\, \delta \tilde{\mathbf{x}}_0[n-1] + \tilde{\mathbf{k}}_0\, \delta r_0[n] \\
&= \tilde{\mathbf{K}}_0\, \tilde{\mathbf{\Phi}}_1\, \tilde{\mathbf{K}}_1\, \tilde{\mathbf{\Phi}}_0\, \delta \mathbf{x}_0[n-1] + \tilde{\mathbf{k}}_0\, \delta r_0[n] \qquad (3.38)
\end{aligned}$$

For convenience, define the following quantities:

$$\tilde{\mathbf{\Phi}} = \tilde{\mathbf{K}}_0\, \tilde{\mathbf{\Phi}}_1\, \tilde{\mathbf{K}}_1\, \tilde{\mathbf{\Phi}}_0 \qquad (3.39)$$

$$\tilde{\mathbf{k}} = \tilde{\mathbf{k}}_0 \qquad (3.40)$$

Then, the difference equation that describes the small-signal motion of the system is:

$$\delta \mathbf{x}_0[n] = \tilde{\mathbf{\Phi}}\, \delta \mathbf{x}_0[n-1] + \tilde{\mathbf{k}}\, \delta r_0[n] \qquad (3.41)$$

3.1.6 The Small-Signal Stability of the Systems

For an ideal dc-to-dc converter system to be *small-signal stable* in the vicinity of a steady state solution, the difference equation that describes its motion in the vicinity of the steady state solution must be stable. For the difference equation to be stable, all the eigenvalues of $\tilde{\mathbf{\Phi}}$ must lie in the unit disk; i.e., $\max \mid \lambda(\tilde{\mathbf{\Phi}}) \mid \leq 1$.

The *small-signal stability* of the difference equation is a necessary condition for the stability of the whole system. If the difference equation is asymptotically stable, i.e., $\max \mid \lambda(\tilde{\mathbf{\Phi}}) \mid < 1$, then there exists a stability region in the vicinity of the steady state solution, such that any perturbation within the stability region will not lead to instability in the system (See Section 4.2). For some classes of converter systems, there are physical constraints in the converter circuit that guarantee that the maximum modulus of the

eigenvalue of the matrix $\tilde{\mathbf{\Phi}}$ is unity regardless of the magnitude of the perturbation to the system and the operating condition of the system.

3.2 The Frequency Response of the Systems

As discussed in Chapter 2, given the difference equation that describes the small-signal motion of a converter system in the vicinity of its steady state solution, Eq. (3.41), three links are required to find the frequency response of the system. The three links are: the relation between $\delta r_0(t)$ and $\delta r_0[n]$ in the frequency domain; the relation between the sequences of δ-functions with magnitude $\{\delta r_0[n]\}$ and $\{\delta \mathbf{x}_0[n]\}$ in the frequency domain; and the contribution of $\delta \mathbf{x}_i[n]$ to $\delta \mathbf{x}(t)$ and therefore $\delta \mathbf{x}(s)$. As in Chapter 2, the first link is given by Shannon's *Sampling Theorem*[7], and the second link is given by the *z-transform* of the difference equation that describes the small-signal motion of the system followed by the substitution of e^{sT_s} for z[3]. The only link that has to be worked on is the contribution of the sampled perturbed state $\delta \mathbf{x}_i[n]$ on the perturbed state $\delta \mathbf{x}(t)$ and therefore on the spectrum of the perturbed state $\delta \mathbf{x}(s)$.

For $\max(\mathbf{T}_j, \mathcal{T}_j) < t < \min(\mathbf{T}_{j+1}, \mathcal{T}_{j+1})$, $j = i + nN_s$, the differential equation that describes $\delta \mathbf{x}(t)$ is given below:

$$\delta \dot{\mathbf{x}}(t) = \mathbf{A}_i \, \delta \mathbf{x}(t) \tag{3.42}$$

There are time intervals in which $\delta \mathbf{x}(t)$ is not described by this equation. Nevertheless, the lengths of these time intervals are of the order of $\delta t_i[n]$; therefore, the perturbed state $\delta \mathbf{x}(t)$ has a negligible contribution to its spectrum $\delta \mathbf{x}(s)$ during these time intervals in the *small-signal limit* (see Section 4.4).

To find out the *equivalent hold* that relates a sample of the perturbed state $\delta \mathbf{x}_i[n]$, which is also an element in the state sequence in the difference equation that describes the small-signal motion of the system in the vicinity of the steady state solu-

tion, to the spectrum of the perturbed state $\delta\mathbf{x}(s)$, the Laplace transform is applied to Eq. (3.42) for time t, $\max(\mathbf{T}_j, \mathcal{T}_j) < t < \min(\mathbf{T}_{j+1}, \mathcal{T}_{j+1})$, $j = i + nN_s$.

$$\int_{\max(\mathbf{T}_j,\mathcal{T}_j)}^{\min(\mathbf{T}_{j+1},\mathcal{T}_{j+1})} \delta\dot{\mathbf{x}}(t)\, e^{-st}\, dt = \mathbf{A}_i \int_{\max(\mathbf{T}_j,\mathcal{T}_j)}^{\min(\mathbf{T}_{j+1},\mathcal{T}_{j+1})} \delta\mathbf{x}(t)\, e^{-st}\, dt \tag{3.43}$$

Define $\delta\mathbf{x}^{\star}_{i,n}(s)$ to be the Laplace transform of the perturbed state $\delta\mathbf{x}(t)$ for time t, such that $\max(\mathbf{T}_j, \mathcal{T}_j) < t < \min(\mathbf{T}_{j+1}, \mathcal{T}_{j+1})$, $j = i + nN_s$,

$$\delta\mathbf{x}^{\star}_{i,n}(s) \equiv \int_{\max(\mathbf{T}_j,\mathcal{T}_j)}^{\min(\mathbf{T}_{j+1},\mathcal{T}_{j+1})} \delta\mathbf{x}(t)\, e^{-st}\, dt$$

Then Eq. (3.43) becomes:

$$\int_{\max(\mathbf{T}_j,\mathcal{T}_j)}^{\min(\mathbf{T}_{j+1},\mathcal{T}_{j+1})} \delta\dot{\mathbf{x}}(t)\, e^{-st}\, dt \;=\; \mathbf{A}_i\, \delta\mathbf{x}^{\star}_{i,n}(s) \tag{3.44}$$

$$\delta\mathbf{x}(t)\, e^{-st}\Big|_{\max(\mathbf{T}_j,\mathcal{T}_j)}^{\min(\mathbf{T}_{j+1},\mathcal{T}_{j+1})} + s\, \delta\mathbf{x}^{\star}_{i,n}(s) \;=\; \mathbf{A}_i\, \delta\mathbf{x}^{\star}_{i,n}(s) \tag{3.45}$$

By using the fact that $\delta\mathbf{x}\left(\min(\mathbf{T}_{j+1}, \mathcal{T}_{j+1})\right) = \delta\tilde{\mathbf{x}}_j$ and $\delta\mathbf{x}\left(\max(\mathbf{T}_j, \mathcal{T}_j)\right) = \delta\mathbf{x}_j$, then,

$$e^{-s\,\min(\mathbf{T}_{j+1},\mathcal{T}_{j+1})}\, \delta\tilde{\mathbf{x}}_j - e^{-s\,\max(\mathbf{T}_j,\mathcal{T}_j)}\, \delta\mathbf{x}_j = [\mathbf{A}_i - s\,\mathbf{I}]\, \delta\mathbf{x}^{\star}_{i,n}(s) \tag{3.46}$$

With use of $j = i + nN_s$; $\delta\mathbf{x}_i[n] = \delta\mathbf{x}_{i+nN_s}$; $\mathbf{T}_{j+1} - \mathbf{T}_j = T_j$; $T_{i+nN_s} = T_i$; in the *small-signal limit*, $\mathcal{T}_{j+1} \to \mathbf{T}_{j+1}$ and $\mathcal{T}_j \to \mathbf{T}_j$; both $\mathbf{A}_j$ and T_j are periodic with period N_s; and Eq. (3.36); then Eq. (3.46) becomes:

$$e^{-s\mathbf{T}_{j+1}}\, \delta\tilde{\mathbf{x}}_i[n] - e^{-s\mathbf{T}_j}\, \delta\mathbf{x}_i[n] \;=\; [\mathbf{A}_i - s\,\mathbf{I}]\, \delta\mathbf{x}^{\star}_{i,n}(s) \tag{3.47}$$

$$e^{-s\mathbf{T}_j} \left\{\delta\mathbf{x}_i[n] - e^{-sT_j}\, e^{\mathbf{A}_j T_j}\, \delta\mathbf{x}_i[n]\right\} \;=\; [s\,\mathbf{I} - \mathbf{A}_i]\, \delta\mathbf{x}^{\star}_{i,n}(s) \tag{3.48}$$

Hence:

$$\delta\mathbf{x}^{\star}_{i,n}(s) = e^{-s\mathbf{T}_j}\, [s\,\mathbf{I} - \mathbf{A}_i]^{-1} \left\{\mathbf{I} - e^{-sT_i}\, e^{\mathbf{A}_i T_i}\right\} \delta\mathbf{x}_i[n] \tag{3.49}$$

The quantity $\delta\mathbf{x}^{\star}_{i,n}(s)$ may be interpreted as the contribution $\delta\mathbf{x}_i[n]$ to $\delta\mathbf{x}(s)$. Equation (3.49) may rewritten as below:

$$\delta\mathbf{x}^{\star}_{i,n}(s) = e^{-s\mathbf{T}_{i+nN_s}}\, \tilde{\mathbf{H}}_i(s)\delta\mathbf{x}_i[n] \tag{3.50}$$

where

$$\tilde{\mathbf{H}}_i(s) = [s\,\mathbf{I} - \mathbf{A}_i]^{-1}\left[\mathbf{I} - e^{-sT_i}\,e^{\mathbf{A}_i T_i}\right] \tag{3.51}$$

The spectrum of the perturbed state $\delta\mathbf{x}(s)$ in the *small-signal limit* is:

$$\begin{aligned}
\delta\mathbf{x}(s) &= \sum_n \delta\mathbf{x}^*_{0,n}(s) + \delta\mathbf{x}^*_{1,n}(s) \\
&= \tilde{\mathbf{H}}_0(s)\,\delta\mathbf{x}^*_0(s) + \tilde{\mathbf{H}}_1(s)\,\delta\mathbf{x}^*_1(s) \\
&= \tilde{\mathbf{H}}_0(s)\,\delta\mathbf{x}^*_0(s) + e^{-sT_0}\,\tilde{\mathbf{H}}_1(s)\,\tilde{\mathbf{K}}_1\,\tilde{\mathbf{\Phi}}_0\,\delta\mathbf{x}^*_0(s) \\
&= \left\{\tilde{\mathbf{H}}_0(s) + e^{-sT_0}\,\tilde{\mathbf{H}}_1(s)\,\tilde{\mathbf{K}}_1\,\tilde{\mathbf{\Phi}}_0\right\}\,\delta\mathbf{x}^*_0(s) \\
&= \tilde{\mathbf{H}}(s)\,\delta\mathbf{x}^*_0(s)
\end{aligned} \tag{3.52}$$

where

$$\begin{aligned}
\tilde{\mathbf{H}}(s) &= \tilde{\mathbf{H}}_0(s) + e^{-sT_0}\,\tilde{\mathbf{H}}_1(s)\,\tilde{\mathbf{K}}_1\,\tilde{\mathbf{\Phi}}_0 \\
\delta\mathbf{x}^*_0(s) &= \sum_n \delta\mathbf{x}_0[n]\,e^{-s\mathbf{T}_0[n]} \\
&= \sum_n \delta\mathbf{x}_0[n]\,e^{-snT_s} \\
\delta\mathbf{x}^*_1(s) &= \sum_n \delta\mathbf{x}_1[n]\,e^{-s\mathbf{T}_1[n]} \\
&= e^{-s\mathbf{T}_1[n]}\sum_n \delta\mathbf{x}_1[n]\,e^{-snT_s} \\
&= e^{-sT_0}\sum_n \tilde{\mathbf{K}}_1\,\tilde{\mathbf{\Phi}}_0\,\delta\mathbf{x}_0[n]\,e^{-snT_s} \\
&= e^{-sT_0}\,\tilde{\mathbf{K}}_1\,\tilde{\mathbf{\Phi}}_0\sum_n \delta\mathbf{x}_0[n]\,e^{-snT_s} \\
&= e^{-sT_0}\,\tilde{\mathbf{K}}_1\,\tilde{\mathbf{\Phi}}_0\,\delta\mathbf{x}^*_0(s)
\end{aligned}$$

and without loss of generality, $\mathbf{T}_0[0]$ is assumed to be zero. The quantity $\tilde{\mathbf{H}}(s)$ is the *equivalent hold* of the system corresponding to the given steady state solution with respect to the perturbed control-input δr_0.

The relation between $\delta r^*_0(s)$, the spectrum of the sampled perturbed control-input δr_0, and $\delta\mathbf{x}^*_0(s)$, the spectrum of the train of δ-functions with magnitude $\{\delta\mathbf{x}_0[n]\}$,

is given by the z-transform of the equation that describes the small-signal motion of the system in the vicinity of its steady state solution, Eq. (3.41), with $z = e^{sT}$:

$$\begin{aligned} \delta \mathbf{x}_0[n] &= \tilde{\mathbf{\Phi}}\, \delta \mathbf{x}_0[n-1] + \tilde{\mathbf{k}}\, \delta r_0[n] \\ Z\{\delta \mathbf{x}_0[n]\} &= \tilde{\mathbf{\Phi}}\, Z\{\delta \mathbf{x}_0[n-1]\} + \tilde{\mathbf{k}}\, Z\{\delta r_0[n]\} \qquad (3.53) \\ \delta \mathbf{x}_0(z) &= z^{-1}\, \tilde{\mathbf{\Phi}}\, \delta \mathbf{x}_0(z) + \tilde{\mathbf{k}}\, \delta r_0(z) \qquad (3.54) \\ \delta \mathbf{x}_0(z) &= [\mathbf{I} - z^{-1}\, \tilde{\mathbf{\Phi}}]^{-1}\, \tilde{\mathbf{k}}\, \delta r_0(z) \qquad (3.55) \end{aligned}$$

where $\delta \mathbf{x}_0(z)$ is the z-transform of the sequence $\{\delta \mathbf{x}_0[n]\}$, and $r_0(z)$ is the z-transform of the sequence $\{\delta r_0[n]\}$. Substitute e^{sT_s} for z in Eq. (3.55), then $\delta \mathbf{x}_0(z)$ becomes $\delta \mathbf{x}_0^*(s)$, and $\delta r_0(z)$ becomes $\delta r_0^*(s)$; and the following equation is obtained:

$$\delta \mathbf{x}_0^*(s) = [\mathbf{I} - e^{-sT_s}\, \tilde{\mathbf{\Phi}}]^{-1}\, \tilde{\mathbf{k}}\, \delta r_0^*(s) \qquad (3.56)$$

where $\delta \mathbf{x}_0^*(s)$ is the spectrum of the train of δ-functions with time T_s between consecutive δ-functions and magnitude $\{\delta \mathbf{x}_0[n]\}$, and $\delta r_0^*(s)$ is the spectrum of the sampled control-input δr_0 with sampling period T_s.

By use of Eq. (3.51), Eq. (3.56), and the Sampling theorem, the spectrum of the output $\delta \mathbf{x}(s)$ is:

$$\delta \mathbf{x}(s) = \tilde{\mathbf{H}}(s)\, \left\{\mathbf{I} - e^{-sT_s}\, \tilde{\mathbf{\Phi}}\right\}^{-1}\, \tilde{\mathbf{k}}\, \delta r_0^*(s) \qquad (3.57)$$

where

$$\delta r_0^*(s) = \frac{1}{T_s} \sum_{n=-\infty}^{\infty} \delta r_0(s + \frac{2n\pi i}{T_s}) \qquad (3.58)$$

Equation (3.57) describes the *small-signal frequency response* of a simple ideal two-switched-state dc-to-dc converter system.

3.3 Constant-Switching-Frequency PWM Converters

With use of the framework for describing ideal converters discussed above, an open-loop constant-switching-frequency pulse-width-modulated (PWM) converter is

described by $M_{2n} = M^t$ and $M_{2n+1} = M^u$, $\forall n \in \mathbf{Z}$; i.e., the transition from switched-state $2n-1$ to switched-state $2n$ is time-modulated, and the transition from switched-state $2n$ to switched-state $2n+1$ is unmodulated. Notice that for any converter to be operating at constant switching frequency, it is necessary that $M^u \in \{M_j\}$.

According to Eq. (3.57), the frequency response of an open-loop constant-switching-frequency PWM converter system with respect to the control-input r_0 is:

$$\delta \mathbf{x}(s) = \left\{ \tilde{\mathbf{H}}_0(s) + e^{-sT_0}\, \tilde{\mathbf{H}}_1(s)\, e^{\mathbf{A}_0 T_0} \right\} \left\{ \mathbf{I} - e^{-sT_s}\, \tilde{\mathbf{\Phi}} \right\}^{-1} \tilde{\mathbf{k}}\, \delta r_0^*(s) \tag{3.59}$$

where

$$\begin{aligned} \tilde{\mathbf{H}}_i(s) &= [s\,\mathbf{I} - \mathbf{A}_i]^{-1} \left[\mathbf{I} - e^{-sT_i}\, e^{\mathbf{A}_i T_i} \right] \\ \tilde{\mathbf{k}} &= (m_0^t)^{-1} \left\{ (\mathbf{A}_1 - \mathbf{A}_0)\, \mathbf{X}_0 + (\mathbf{B}_1 - \mathbf{B}_0)\, \mathbf{u} \right\} \\ \tilde{\mathbf{\Phi}} &= \tilde{\mathbf{K}}_0^t\, \tilde{\mathbf{\Phi}}_1\, \tilde{\mathbf{K}}_1^u\, \tilde{\mathbf{\Phi}}_0 \\ &= e^{\mathbf{A}_1 T_1}\, e^{\mathbf{A}_0 T_0} \end{aligned}$$

In the *high-switching-frequency limit*, i.e., $1/T_s \to \infty$, $\mathbf{X}_0 \to \mathbf{X}$, $\tilde{\mathbf{H}}_i(s) \to T_i\, \mathbf{I}$, and $\delta r_0^*(s) \to \delta r_0(s)/T_s$, Eq. (3.59) becomes:

$$\begin{aligned} \lim_{T_s \to 0} \delta \mathbf{x}(s) &= \left\{ s\,\mathbf{I} - \left(\frac{T_0}{T_s} \mathbf{A}_0 + \frac{T_1}{T_s} \mathbf{A}_1 T_1 \right) \right\}^{-1} \tilde{\mathbf{k}}\, \frac{1}{T_s} \delta r_0(s) \\ &= \{ s\,\mathbf{I} - \mathbf{A} \}^{-1} \left\{ (\mathbf{A}_1 - \mathbf{A}_0)\, \mathbf{X}_0 + (\mathbf{B}_1 - \mathbf{B}_0)\, \mathbf{u} \right\} \frac{\delta r_0(s)}{m_0^t T_s} \end{aligned} \tag{3.60}$$

where $\mathbf{A} \equiv \frac{T_0}{T_s} \mathbf{A}_0 + \frac{T_1}{T_s} \mathbf{A}_1$. The quantities D_0 and D_1 are commonly known as duty ratios. One can easily identify $\delta r_0(s)/(m_0^t T_s)$ with the $\hat{d}(s)$, $\frac{T_1}{T_s}$ with D, the duty ratio; $\frac{T_0}{T_s}$ with the D'; and $\delta \mathbf{x}(s)$ with the $\hat{\mathbf{x}}(s)$ used in the literature on the *State Space Averaging Modelling Method*[4,5,6]. By applying the notation used in the *State Space Averaging Modelling Method*, Eq. (3.60) becomes:

$$\lim_{T_s \to 0} \hat{\mathbf{x}}(s) = \{ s\,\mathbf{I} - (D'\mathbf{A}_0 + D\mathbf{A}_1) \}^{-1} \left\{ (\mathbf{A}_1 - \mathbf{A}_0)\, \mathbf{X} + (\mathbf{B}_1 - \mathbf{B}_0)\, \mathbf{u} \right\} \hat{d}(s) \tag{3.61}$$

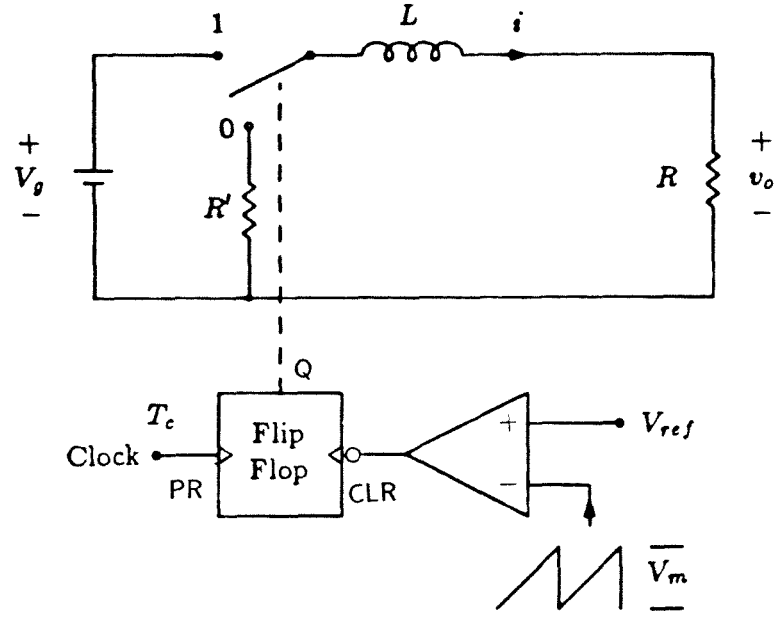

Figure 3.2: A constant-switching-frequency PWM R-L converter:
$V_g = 15$Volts, $L = 1.41$mH, $R = 56\Omega$, $R' = 0\Omega$, $T_s = T_c$.

which is exactly the prediction given by the *State Space Averaging Modelling Method*. Therefore, the frequency response prediction of the *State Space Averaging Modelling Method* for open-loop PWM converter systems is exact when the switching frequency of the converter systems approaches infinity. This result is not surprisingly new. A similar result is given in the *Equivalent Control Method* of *Sliding Mode Control* in *Variable Structure System Theory* developed by Utkin[8].

Consider the circuit shown in Fig. 3.2 as an example:

$$\begin{aligned} \mathbf{A}_0 &= -\tfrac{R+R'}{L} & \mathbf{A}_1 &= -\tfrac{R}{L} \\ \mathbf{B}_0 &= 0 & \mathbf{B}_1 &= \tfrac{1}{L} \\ \mathbf{x} &= i & \mathbf{u} &= V_g \\ D_0 &= \tfrac{T_0}{T_s} & D_1 &= \tfrac{T_1}{T_s} \\ m_0^t &= \tfrac{V_m}{T_s} & R' &= 0\Omega \end{aligned}$$

Since both $\mathbf{A}_0$ and $\mathbf{A}_1$ are invertible, the steady state $\mathbf{X}_0$ is given by:

$$\mathbf{X}_0 = \left[\mathbf{I} - e^{\mathbf{A}_1 T_1} e^{\mathbf{A}_0 T_0}\right]^{-1} \left\{\mathbf{A}_1^{-1}\left[e^{\mathbf{A}_1 T_1} - \mathbf{I}\right]\mathbf{B}_1\,\mathbf{u} + e^{\mathbf{A}_1 T_1}\mathbf{A}_0^{-1}\left[e^{\mathbf{A}_0 T_0} - \mathbf{I}\right]\mathbf{B}_0\,\mathbf{u}\right\} \quad (3.62)$$

The steady state $\mathbf{X}_1$ is given by:

$$\mathbf{X}_1 = e^{\mathbf{A}_0 T_0}\,\mathbf{X}_0 + \mathbf{A}_0^{-1}\left[e^{\mathbf{A}_0 T_0} - \mathbf{I}\right]\mathbf{B}_0\mathbf{u} \quad (3.63)$$

Therefore, the steady state I_0 is:

$$I_0 = \left[1 - e^{-\frac{RT_1 + (R+R')T_0}{L}}\right]^{-1}\left[1 - e^{-\frac{RT_1}{L}}\right]\frac{V_g}{R} \quad (3.64)$$

Then, according to Eq. (3.59), the pulse transfer function is:

$$G(s) = \tilde{H}(s)\,(1 - e^{-sT_s}\tilde{\Phi})^{-1}\,\tilde{k} \quad (3.65)$$

where:

$$\begin{aligned} \tilde{H}(s) &= \left\{\frac{1 - e^{-(s+\frac{R+R'}{L})T_0}}{s + \frac{R+R'}{L}} + \frac{1 - e^{-(s+\frac{R}{L})T_1}}{s + \frac{R}{L}}\,e^{-(s+\frac{R+R'}{L})T_0}\right\} \\ \tilde{\Phi} &= e^{-\frac{RT_1 + (R+R')T_0}{L}} \\ \tilde{k} &= \frac{T_s V_g}{L V_m}\left\{1 + \frac{R'}{R}\left[1 - e^{-\frac{RT_1 + (R+R')T_0}{L}}\right]^{-1}\left[1 - e^{-\frac{RT_1}{L}}\right]\right\} \end{aligned}$$

In this example converter circuit, the resistance $R' = 0\Omega$, and the pulse transfer function from the sampled control-input $\delta v_{ref}^*(s)$ to the output $\delta v_o(s)$, according to Eq. (3.65) is:

$$RG(s) = \frac{T_s\,R/L}{s + R/L}\,\frac{V_g}{V_m} \quad (3.66)$$

where V_m is the peak-to-peak voltage of the PWM ramp. In this degenerated case of $R' = 0\Omega$, the expression for the pulse transfer function is very simple when compared to the non-degenerated case in Eq. (3.65). This predicted pulse transfer function agrees with what would be expected after examining the circuit shown in Fig. 3.2 — the transfer function of a R-L low pass filter with time constant L/R.

The schematic of the converter circuit used in the experiment is shown in Fig. 3.3. The waveform of the steady state solution of the voltage across the load resistor $R = 56\Omega$, and the corresponding Bode plots up to three times the switching frequency of the theoretical *"transfer function"* from v_{ref} to v_o; i.e., $RG(s)/T_s$, overlaid with measurement results are shown in Fig. 3.4 through Fig. 3.6. Three switching frequencies: 100Hz, 40kHz, and 20kHz are used in these Bode plots. These switching frequencies are chosen because: at 100kHz, $\|\mathbf{A}T_s\| < 1$, the *small-ripple assumption* is valid; at 40kHz, $\|\mathbf{A}T_s\| \approx 1$, the *small-ripple assumption* begins to break down; at 20kHz, $\|\mathbf{A}T_s\| > 1$, the *small-ripple assumption* breaks down totally and the ripple is large. The discrepancies between the theoretical and the measurement results in the Bode plots at high frequencies come from the unmodelled dynamics in the pulse width modulator circuit which are unaccounted for in the ideal converter circuit model, Fig. 3.2, used in obtaining the theoretical prediction.

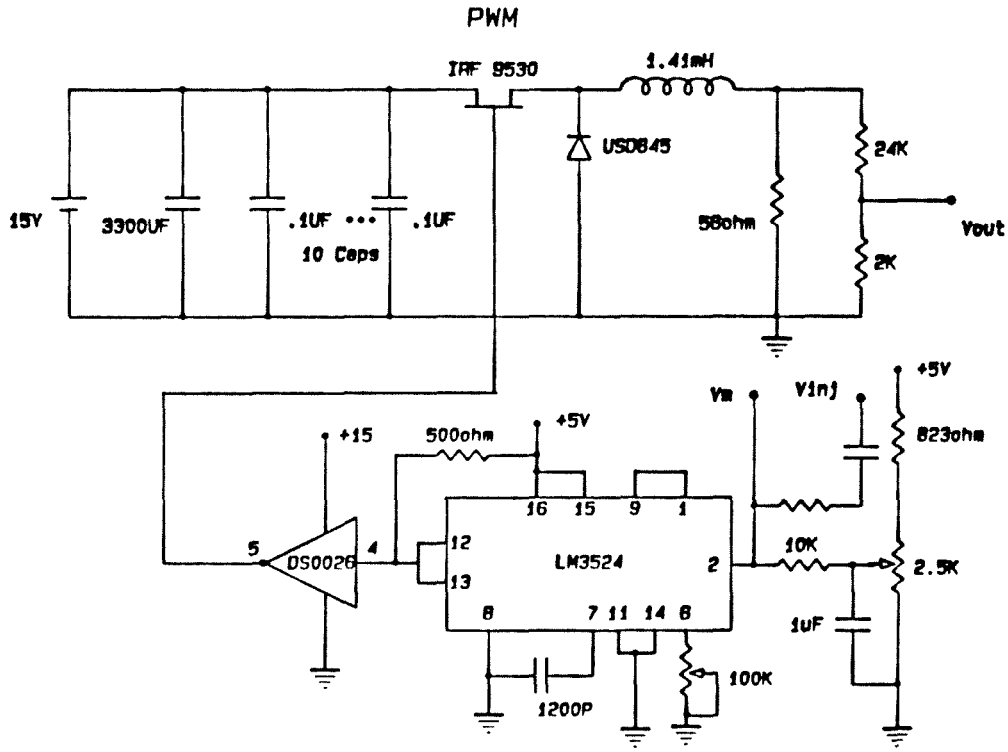

Figure 3.3: The realization of the constant-switching-frequency PWM converter circuit shown in Fig. 3.2 for use in the experiments.

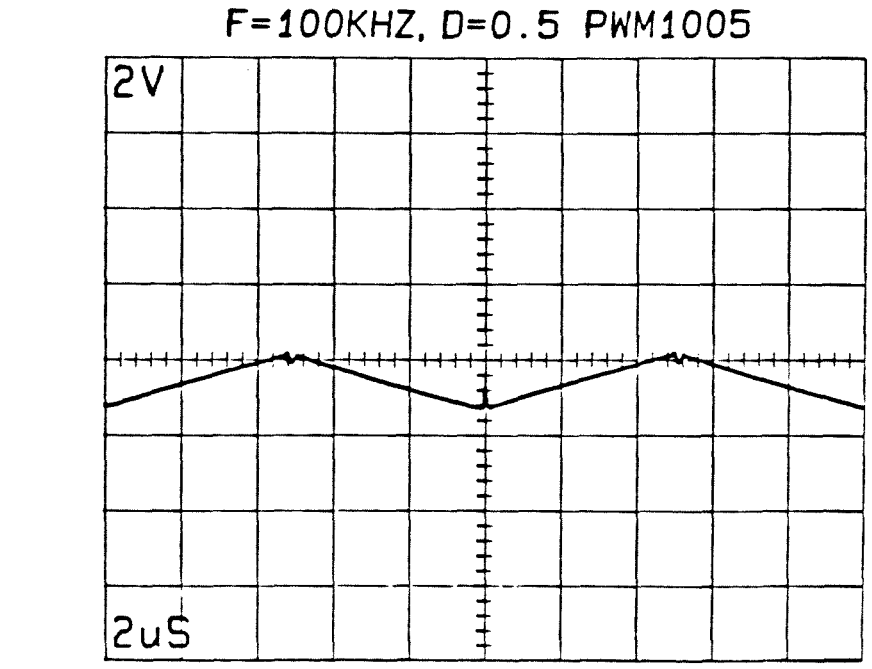

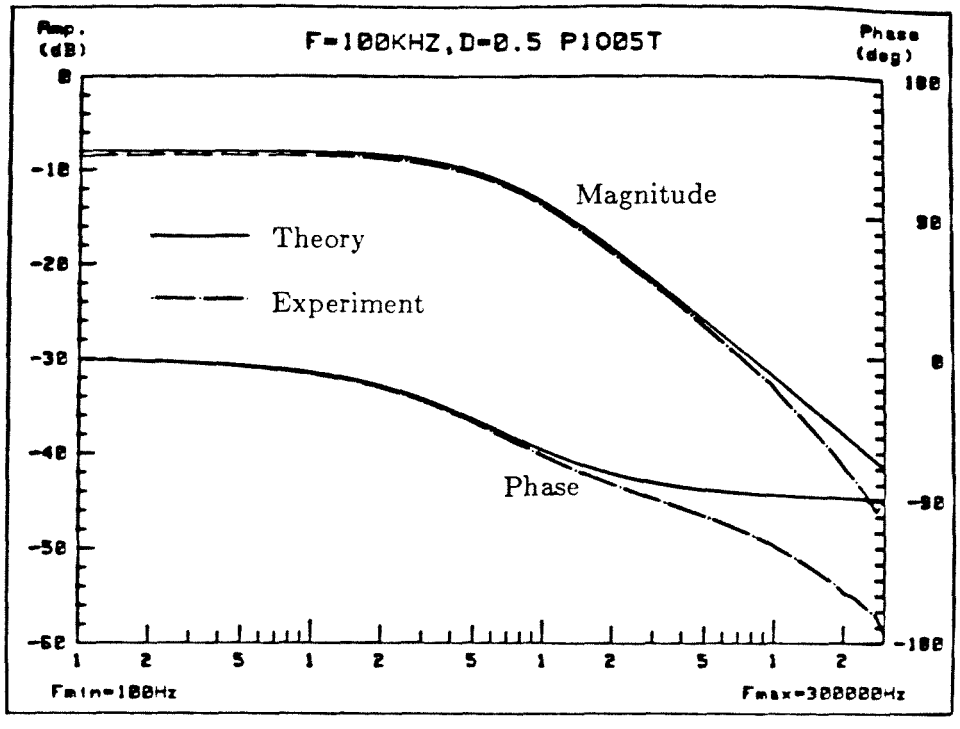

Figure 3.4: The waveform of the steady state solution of the voltage across the load resistor $R = 56\Omega$ and the corresponding Bode plots of the theoretical prediction and the experimental results of the converter circuit shown in Fig. 3.2 operating at $f_s = 1/T_s = 100kHz$, $D = T_1/T_s = .5$.

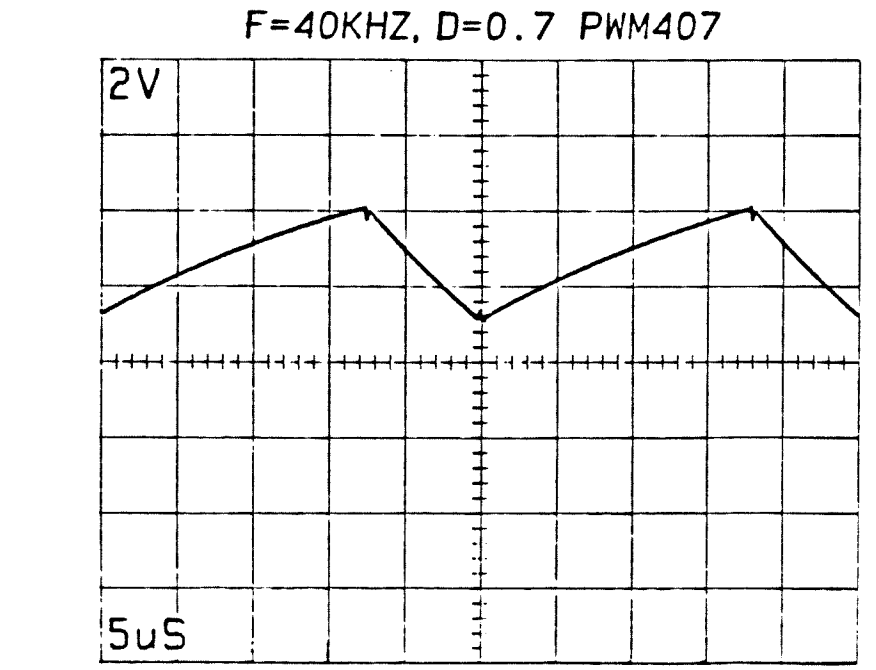

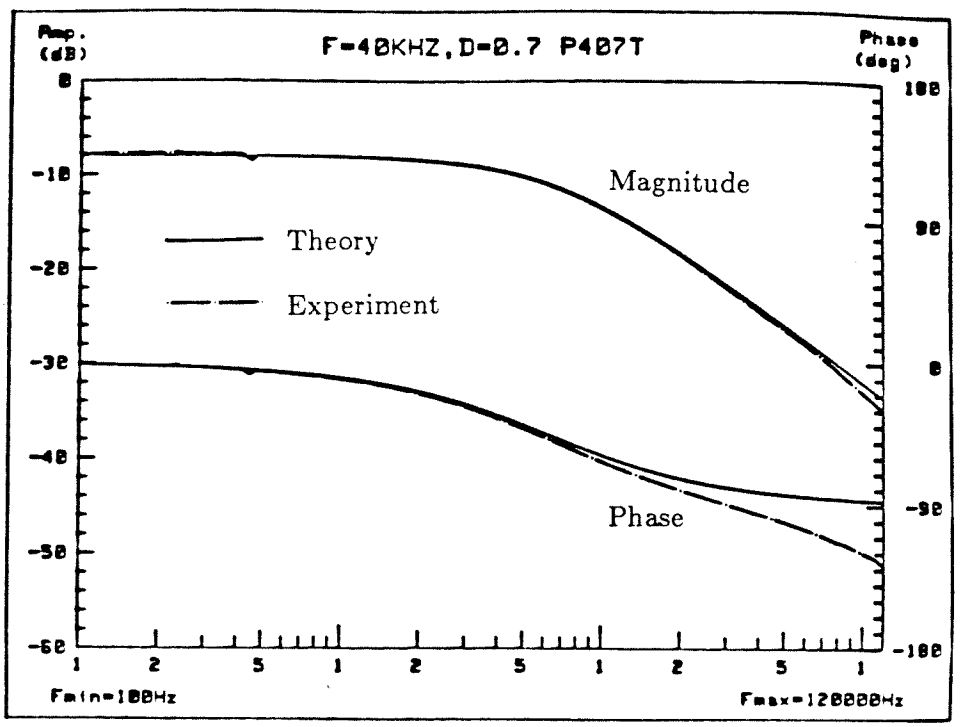

Figure 3.5: The waveform of the steady state solution of the voltage across the load resistor $R = 56\Omega$ and the corresponding Bode plots of the theoretical prediction and the experimental results of the converter circuit shown in Fig. 3.2 operating at $f_s = 1/T_s = 40kHz$, $D = T_1/T_s = .7$.

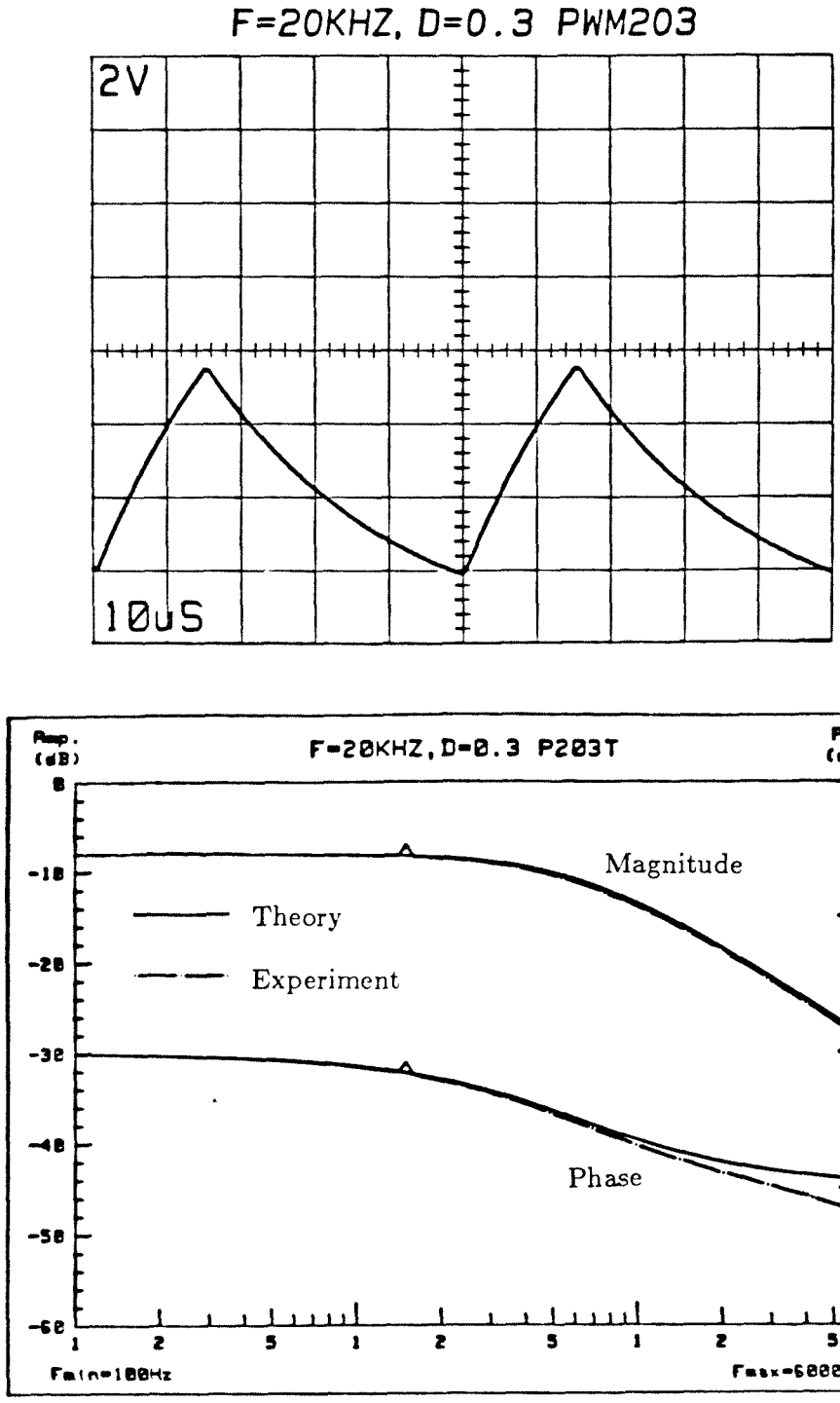

Figure 3.6: The waveform of the steady state solution of the voltage across the load resistor $R = 56\Omega$ and the corresponding Bode plots of the theoretical prediction and the experimental results of the converter circuit shown in Fig. 3.2 operating at $f_s = 1/T_s = 20kHz$, $D = T_1/T_s = .3$.

3.4 Constant-Switching-Frequency Programmed Converters

The control strategy of constant-switching-frequency programmed converters may be described by $M_{2n} = M^c$ and $M_{2n+1} = M^u$, $\forall n \in \mathbf{Z}$; i.e., i.e., the transition from switched-state $2n-1$ to switched-state $2n$ is constraint-modulated, and the transition from switched-state $2n$ to switched-state $2n+1$ is unmodulated. As in Section 2.1, it is possible for this class of converter circuit to have multiple stable steady state solutions under a given operating condition. In this section, the frequency response of only one of the solutions, the two-switched-state solution, with $T_s = T_1 + T_2 = T_c$, is treated. The non-uniqueness of the stable steady state solution under a given operating condition in an experimental converter circuit using the constant-switching-frequency programming control strategy is also discussed.

Suppose the constraint equation for determining when to switch from switched-state $2n-1$ to switched-state $2n$, $\forall\, n \in \mathbf{Z}$, is:

$$\mathbf{f}_0^T\, \mathbf{x}(\mathbf{T}_{nN_s} + \Delta t_0[n]) + m_0^c\, \Delta t_0[n] + c_0 - r_0[n] = 0 \tag{3.67}$$

The constraint equation is the mathematical model of the switching action of the comparator circuit that determines when this change of switched-state occurs in a constant-switching-frequency programmed converter circuit. This comparator circuit has the control-input $r_0(t)$ at one of its inputs, and the sum of the weighted sum of the system states $\mathbf{f}_0^T\, \mathbf{x}(t)$ and a sawtooth ramp with slope m_0^c at its other input. The linearized constraint equation, according to Eq. (3.27), is:

$$\mathbf{f}_0^T\, \delta\tilde{\mathbf{x}}_1[n-1] + \mathbf{f}_0^T\, \dot{\mathbf{X}}_0^-\, \delta t_0[n] + m_0^c\, \delta t_0[n] - \delta r_0[n] = 0 \tag{3.68}$$

where $\dot{\mathbf{X}}_0^- = \mathbf{A}_1\, \mathbf{X}_0 + \mathbf{B}_1\, \mathbf{u}$.

According to Eq. (3.57), the frequency response of the converter system with

respect to the control-input r_0 corresponding to the steady state solution $\mathbf{X}(t)$ is:

$$\delta\mathbf{x}(s) = \left\{\tilde{\mathbf{H}}_0(s) + e^{sT_0}\,\tilde{\mathbf{H}}_1(s)\,e^{\mathbf{A}_0 T_0}\right\}\,\left\{\mathbf{I} - e^{-sT_s}\,\tilde{\mathbf{\Phi}}\right\}^{-1}\,\tilde{\mathbf{k}}\,\delta r_0^*(s) \tag{3.69}$$

where

$$\begin{aligned}
\tilde{\mathbf{H}}_i(s) &= [s\,\mathbf{I} - \mathbf{A}_i]^{-1}\left[\mathbf{I} - e^{-sT_i}\,e^{\mathbf{A}_i T_i}\right] \\
\tilde{\mathbf{\Phi}} &= \tilde{\mathbf{K}}_0^c\,e^{\mathbf{A}_1 T_1}\,e^{\mathbf{A}_0 T_0} \\
\tilde{\mathbf{k}} &= m_0\,\bar{\mathbf{k}}_0 \\
\tilde{\mathbf{K}}_0^c &= \mathbf{I} - \bar{\mathbf{k}}_0\,\mathbf{p}_0^T \\
\bar{\mathbf{k}}_i &= (\mathbf{A}_1 - \mathbf{A}_0)\mathbf{X}_0 + (\mathbf{B}_1 - \mathbf{B}_0)\mathbf{u} \\
m_0 &= \left[\mathbf{f}_0^T\,(\mathbf{A}_1\,\mathbf{X}_0 + \mathbf{B}_1\,\mathbf{u}) + m_0^c\right]^{-1} \\
\mathbf{p}_0 &= m_0\,\mathbf{f}_0
\end{aligned}$$

The quantity $\mathbf{X}_0$ which is used in calculating $\tilde{\mathbf{K}}_0^c$ and $\tilde{\mathbf{k}}_0^c$ may be found by using Eq. (3.62) if $\mathbf{A}_0$ and $\mathbf{A}_1$ is invertible.

As an example, consider the converter circuit shown in Fig. 3.7, in which,

$$\begin{aligned}
\mathbf{A}_0 &= -\tfrac{R+R'}{L} & \mathbf{A}_1 &= -\tfrac{R}{L} \\
\mathbf{B}_0 &= 0 & \mathbf{B}_1 &= \tfrac{1}{L} \\
\mathbf{x} &= i & \mathbf{u} &= V_g \\
D_0 &= \tfrac{T_0}{T_s} & D_1 &= \tfrac{T_1}{T_s} \\
m_0^c &= 0 & \mathbf{f}_0 &= 1
\end{aligned} \tag{3.70}$$

The schematic of the converter circuit used in the experiment is shown Fig. 3.8. As discussed in Section 2.1, constant-switching-frequency constraint-modulated dc-to-dc converter circuits may have multiple stable steady state solutions. To illustrate this phenomenon, an experiment is performed on the circuit. In this experiment, the reference voltage V_{ref} is raised slowly from 0V to 14V, and then slowly lowered from 14V back to

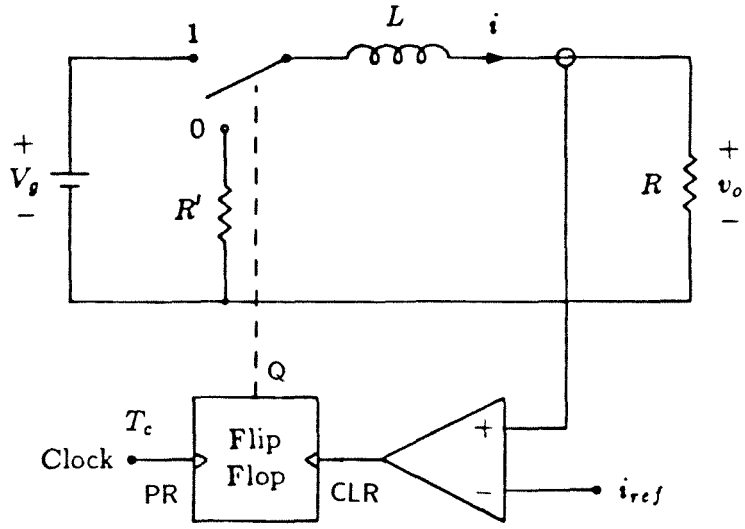

Figure 3.7: A constant-switching-frequency programmed R-L converter: $V_g = 15\text{Volts}$, $L = 1.41\text{mH}$, $R = 56\Omega$, $R' = 51.4\Omega$.

0V. Of the many type of solution observed as V_{ref} is varied, only three are discussed here. They are:

Type (a): $T_s = T_c$, $N_T = 2$, $N_s = 2$.

Type (b): $T_s = 2T_c$, $N_T = 4$, $N_s = 4$.

Type (c): $T_s = 2T_c$, $N_T = 2$, $N_s = 2$.

The reference voltages V_{ref} at which the steady state solution changes from Type (a) to Type (b) and vice versa, and from Type (b) to Type (c) and vice versa are recorded. For convenience of recording the results, define the following quantities:

V_1^r = V_{ref} at which the solution changes from Type (a) to Type (b) as V_{ref} is raised.

V_2^r = V_{ref} at which the solution changes from Type (b) to Type (c) as V_{ref} is raised.

V_2^l = V_{ref} at which the solution changes from Type (c) to Type (b) as V_{ref} is lowered.

V_1^l = V_{ref} at which the solution changes from Type (b) to Type (a) as V_{ref} is lowered.

The result of this experiment is listed in the following tables:

1. Clock frequency $f_c = 20$kHz:

	V_{ref} raised	V_{ref} lowered	
V_1^r	12.7V	12.2V	V_1^l
V_2^r	12.8V	12.7V	V_2^l

The waveform of the stable steady state solutions of the voltage across the resistor $R = 56\Omega$ for $V_{ref} = 12.4$V and $V_{ref} = 12.8$V are shown in Fig. 3.9 and Fig. 3.10 respectively.

2. Clock frequency $f_c = 40$kHz:

	V_{ref} raised	V_{ref} lowered	
V_1^r	8.6V	8.3V	V_1^l
V_2^r	9.9V	9.1V	V_2^l

The waveform of the stable steady state solutions of the voltage across the resistor $R = 56\Omega$ for $V_{ref} = 9.8$V are shown in Fig. 3.11.

3. Clock frequency $f_c = 100$kHz:

	V_{ref} raised	V_{ref} lowered	
V_1^r	6.5V	6.5V	V_1^l
V_2^r	6.6V	7.2V	V_2^l

The waveform of the stable steady state solutions of the voltage across the resistor $R = 56\Omega$ for $V_{ref} = 7.1$V are shown in Fig. 3.12.

These results indicate that it is possible to have more than one stable steady state solutions to the system under a given operating condition — V_g and V_{ref}. In addition, it is possible to measure the frequency response of the system corresponding to the different stable steady state solutions of the system under a given operating condition with a network analyzer. In general, the frequency response corresponding to the different steady state solutions of the system under the same operating condition are different.

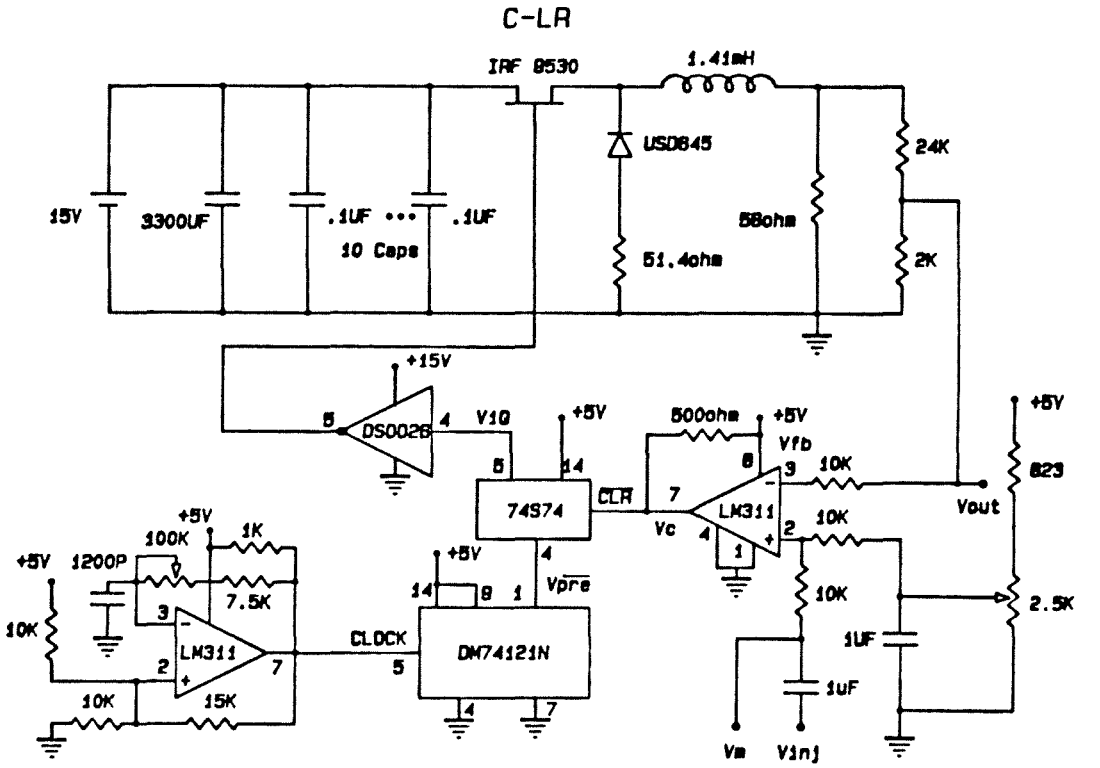

Figure 3.8: The realization of the constant-switching-frequency programmed converter circuit shown in Fig. 3.7 for use in the experiments.

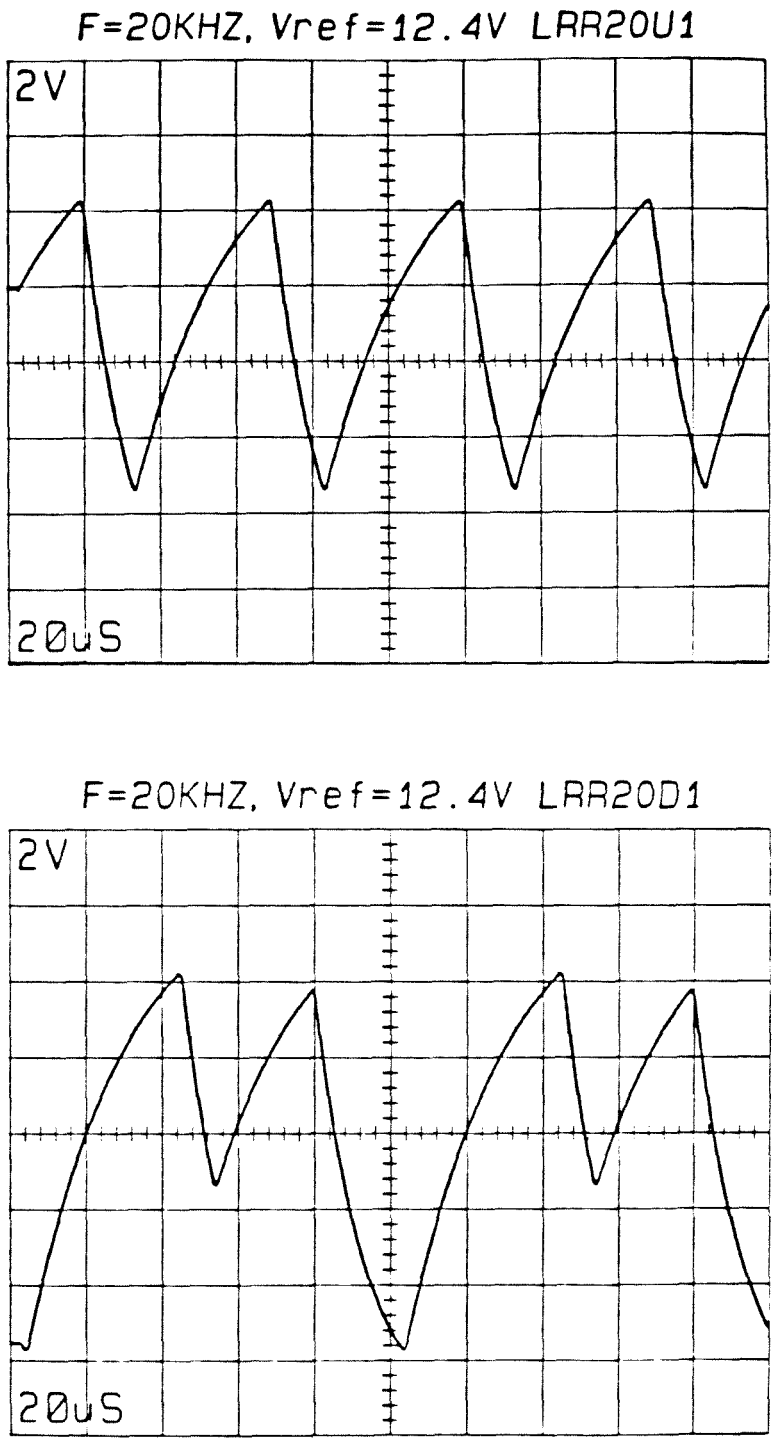

Figure 3.9: The waveform of the two steady state solutions to the voltage across the output resistor $R = 56\Omega$ of the circuit shown in Fig. 3.8 for the operating condition: $V_{ref} = 12.4\,V$, $V_g = 15\,V$, clock frequency $f_c = 20kHz$.

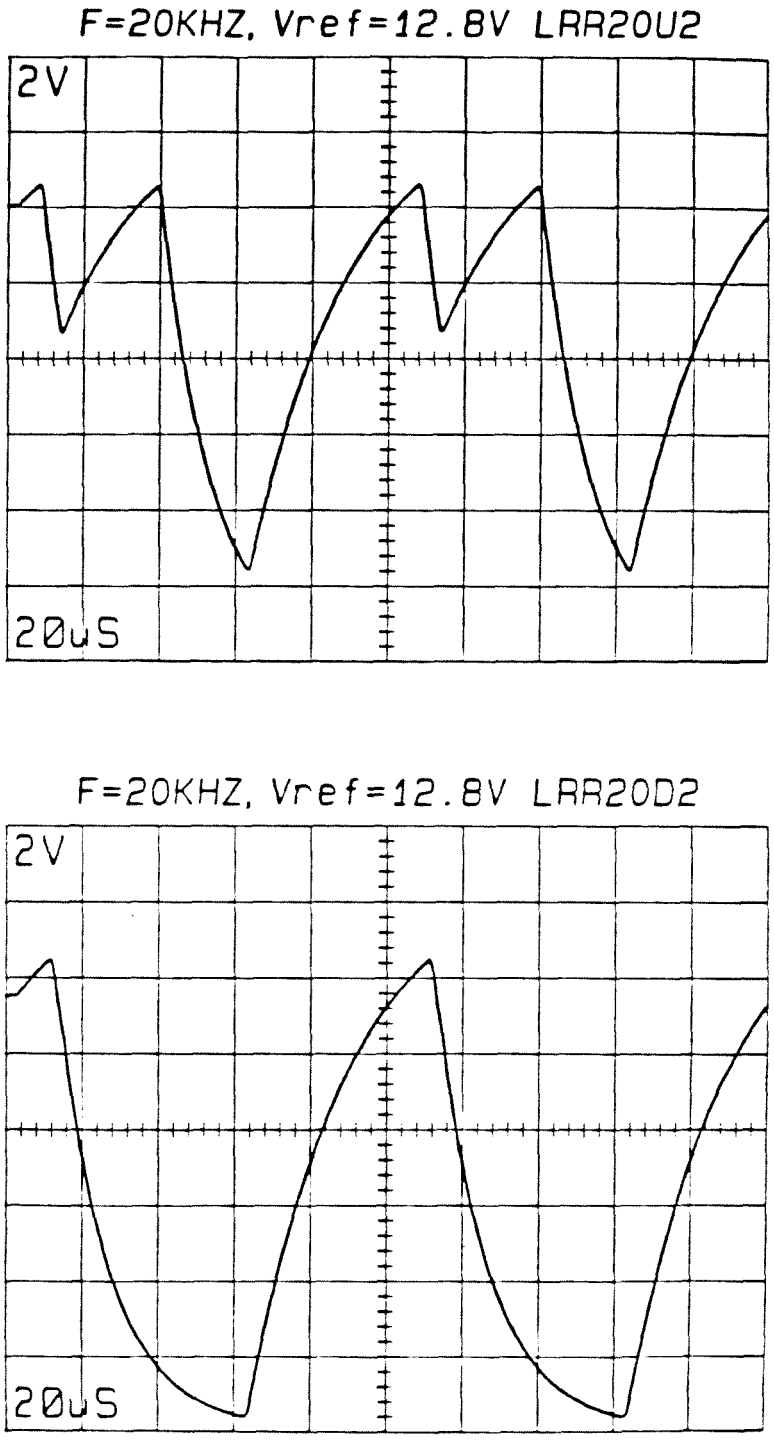

Figure 3.10: The waveform of the two steady state solutions to the voltage across the output resistor $R = 56\Omega$ of the circuit shown in Fig. 3.8 for the operating condition: $V_{ref} = 12.8\,V$, $V_g = 15\,V$, clock frequency $f_c = 20kHz$.

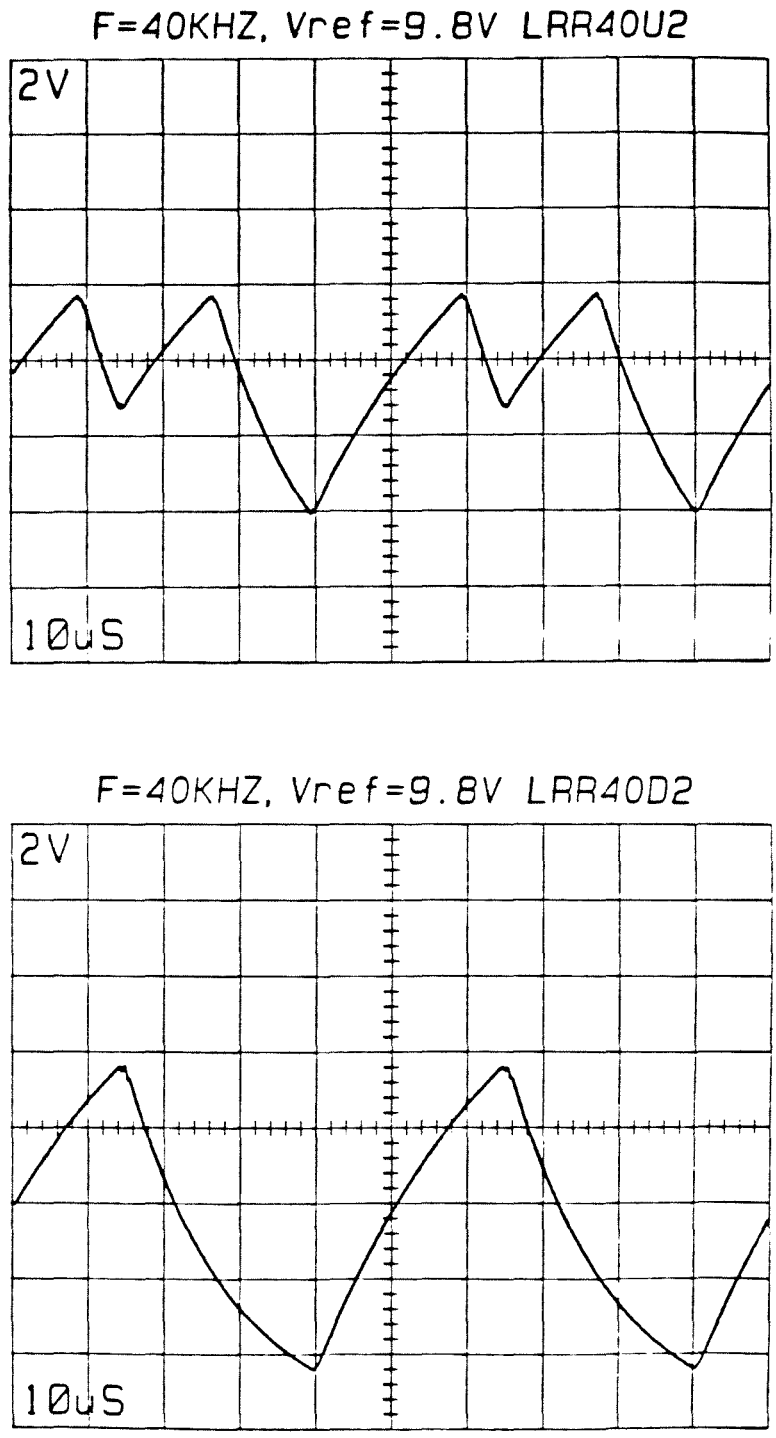

Figure 3.11: The waveform of the two steady state solutions to the voltage across the output resistor $R = 56\Omega$ of the circuit shown in Fig. 3.8 for the operating condition: $V_{ref} = 9.8\,V$, $V_g = 15\,V$, clock frequency $f_c = 40kHz$.

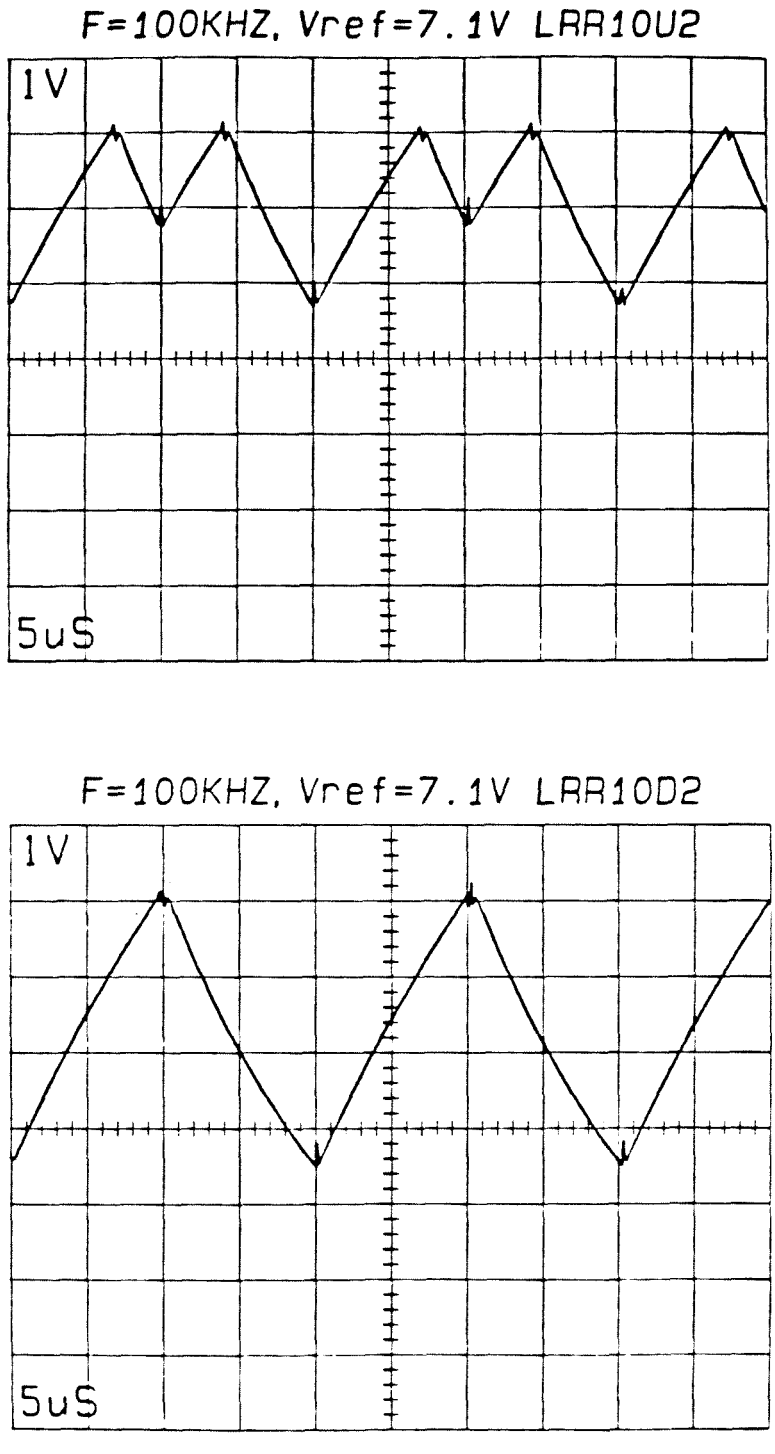

Figure 3.12: The waveform of the two steady state solutions to the voltage across the output resistor $R = 56\Omega$ of the circuit shown in Fig. 3.8 for the operating condition: $V_{ref} = 7.1\,V$, $V_g = 15\,V$, clock frequency $f_c = 100kHz$.

In the following analysis of the frequency response of the converter system, only solution Type (a): $T_s = T_c$, $N_T = 2$, $N_s = 2$, will be studied. By using Eq. (3.62), the steady state I_0 is:

$$I_0 = \left[1 - e^{-\frac{RT_1+(R+R')T_0}{L}}\right]^{-1} \left[1 - e^{-\frac{RT_1}{L}}\right] \frac{V_g}{R} \tag{3.71}$$

According to Eq. (3.69), the pulse transfer function is:

$$G(s) = \tilde{H}(s)\,(1 - e^{-sT_s}\tilde{\Phi})^{-1}\,\tilde{k} \tag{3.72}$$

where:

$$\begin{aligned}
\tilde{H}(s) &= \left\{ \frac{1 - e^{-(s+\frac{R+R'}{L})T_0}}{s + \frac{R+R'}{L}} + \frac{1 - e^{-(s+\frac{R}{L})T_1}}{s + \frac{R}{L}}\, e^{-(s+\frac{R+R'}{L})T_0} \right\} \\
\tilde{\Phi} &= e^{-\frac{RT_1+(R+R')T_0}{L}}\,(1 - \bar{k}_0\, p_0) \\
\tilde{k} &= m_0\, \bar{k}_0 \\
\bar{k}_0 &= \frac{R'}{L}\, I_0 + \frac{1}{L} V_g \\
m_0 &= \left(-\frac{R}{L}\, I_0 + \frac{1}{L} V_g\right)^{-1} \\
p_0 &= \left(-\frac{R}{L}\, I_0 + \frac{1}{L} V_g\right)^{-1}
\end{aligned}$$

The Bode plots of the theoretical *"transfer function"* $\frac{1}{T_s} G(s)$ overlaid with measurement results of this dc-to-dc converter circuit and the waveforms of the corresponding steady state solution of the voltage across the resistor $R = 56\Omega$ operating with different switching frequencies are shown in Fig. 3.13 through Fig. 3.15. The three switching frequencies chosen for the calculations and the experiments are: 20kHz, 40KHz, 100kHz. The switching frequency 20kHz is chosen because it is the *large-ripple* or the *resonant* case. The switching frequency 100kHz is chosen because it is the *small-ripple* or the *high-switching-frequency* case. The switching frequency 40kHz is chosen because $\|\mathbf{A}_i\, T_s\| \approx 1$. The discrepancies between the theoretical predictions and the measurements in the Bode plots at high frequencies are the results of the unmodelled dynamics

in the converter circuits, especially, the controller circuit. These unmodelled dynamics are mostly from distributed resistances and reactances, nonidealities in switching devices, active devices, and logic circuits; above all, the nonidealities in the comparator integrated circuits.

For this example converter circuit which uses the constant-switching-frequency constraint modulation (programming) control strategy, all of the three approximate analytical methods which are discussed in the introduction, namely, the *State Space Averaging Modelling Method*[4,5,6], the *Sampled-Data Modelling Method*[1], and the *Small Signal Analysis of Resonant Converters*[9] break down at some point. It is well known that the *State Space Averaging Model* does not work for any constant frequency programmed converters when the frequency of the signal injected for measurement is close to and higher than half the switching frequency[1]. The *Sampled-Data Modelling Method* breaks down when the time constants in the converter circuit are much shorter than the switching period — this converter circuit does not satisfy the *small-ripple assumption* if the switching frequency is lower than approximately 50kHz. The *Small Signal Analysis of Resonant Converter* can handle the large ripple in the circuit. For the injected signal at a multiple of half the switching frequency, however, its predicted transfer function of any converter system is always real; therefore, the phase is always a multiple of 180 degrees. From the experimental results on the Bode plots, it is obvious that this is clearly not the case.

The Bode plots of the frequency response of the converter circuit shown in Fig. 3.8 in this section clearly demonstrate the breakdown of the approximate analytical methods discussed in the Introduction and the validity of the prediction of the *Small-Signal Frequency Response Theory*. This is not a surprising result because the *Small-Signal Frequency Response Theory* linearizes ideal dc-to-dc converter systems exactly in

the vicinity of its steady state solution, instead of finding an approximate linear model for the system under an operating condition. The discrepancies between the theoretical prediction and experimental measurement in the Bode plots at high frequencies suggest that the circuit shown in Fig. 3.7 is not an adequate model for studying the very high-frequency behavior of the physical converter circuit used in the experiment.

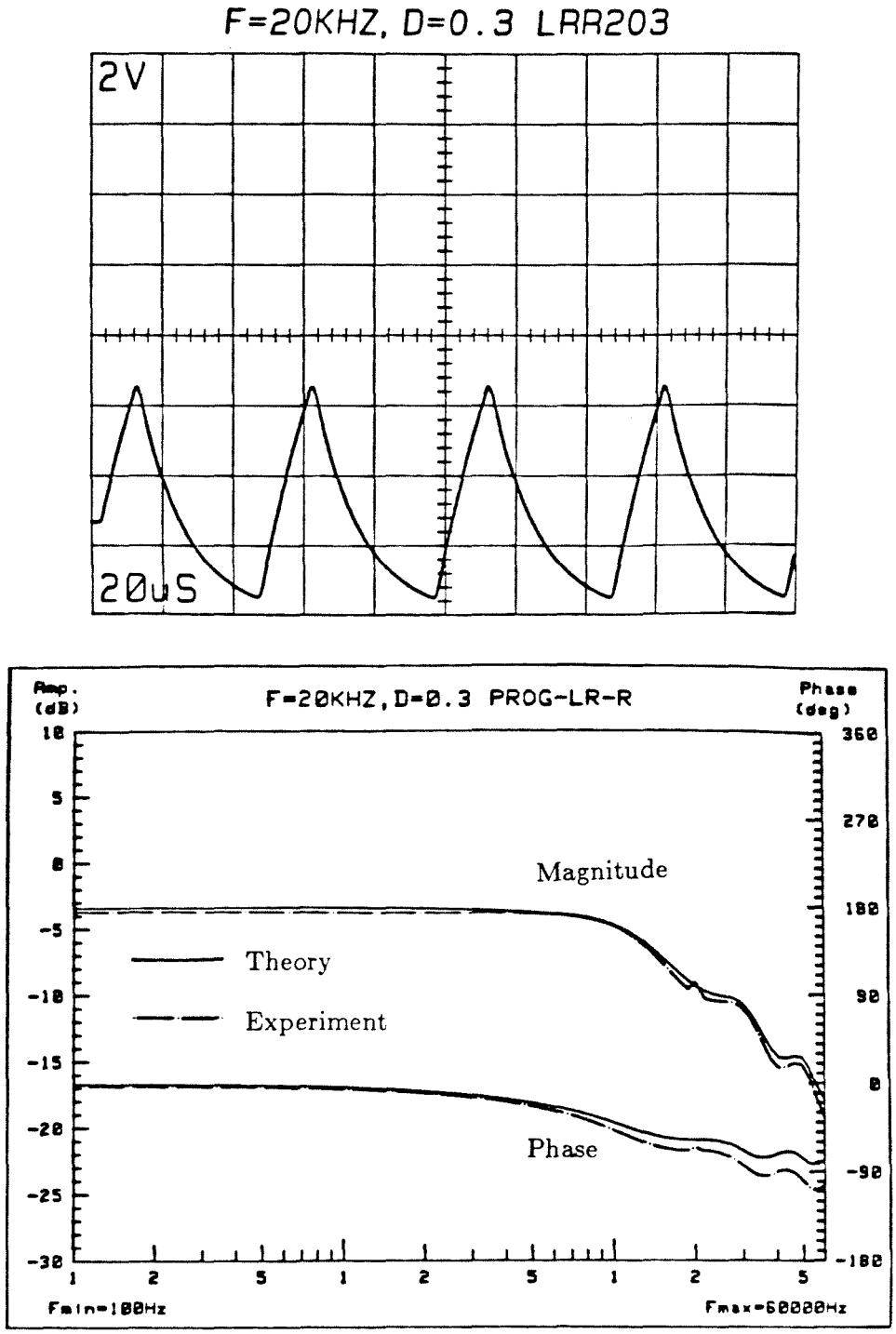

Figure 3.13: The waveform of the steady state solution of the voltage across the load resistor $R = 56\Omega$ and the corresponding Bode plots of the theoretical prediction and the experimental results of the converter circuit shown in Fig. 3.8 operating at $f_s = 1/T_s = 20kHz$, $D = T_1/T_s = .3$.

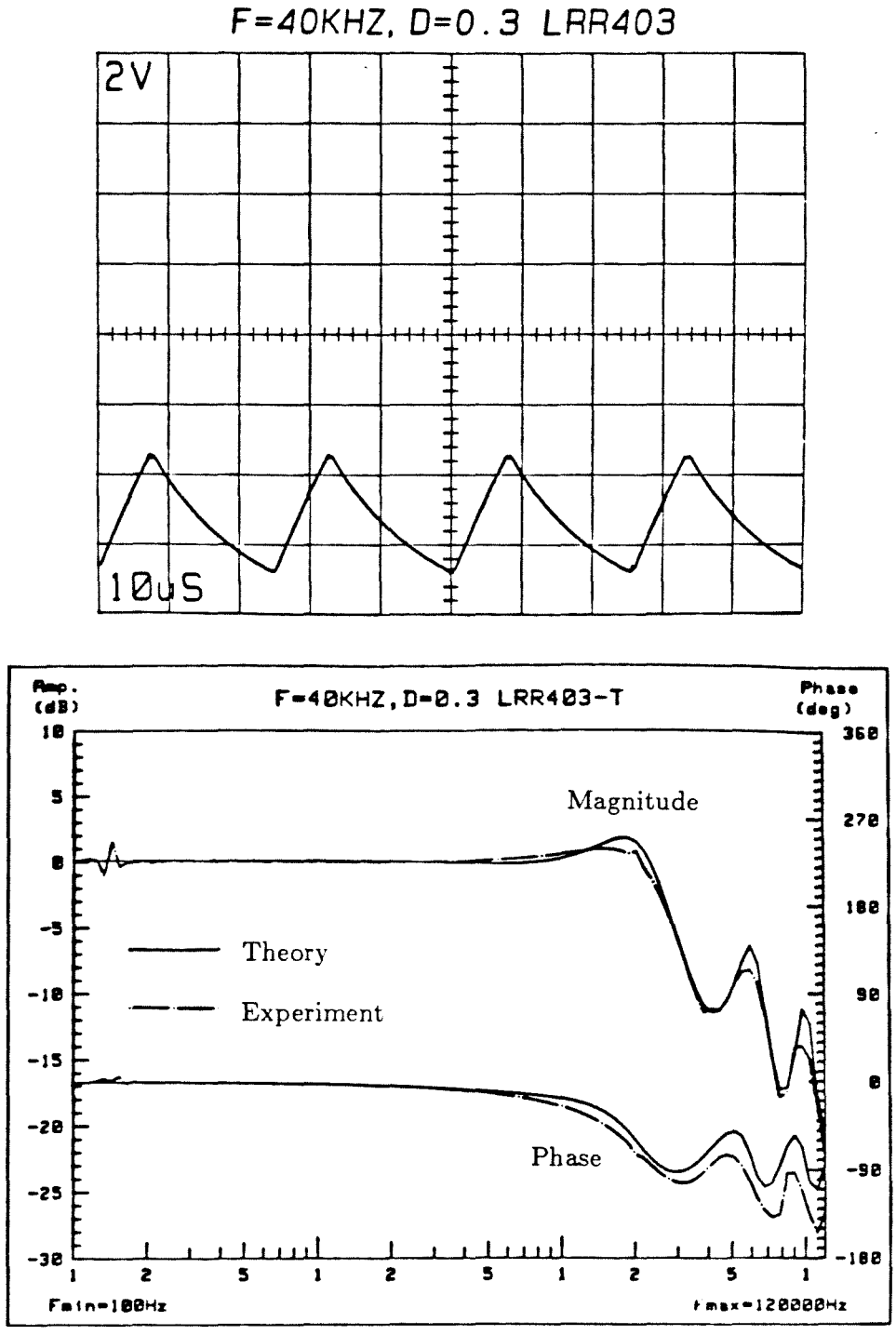

Figure 3.14: The waveform of the steady state solution of the voltage across the load resistor $R = 56\Omega$ and the corresponding Bode plots of the theoretical prediction and the experimental results of the converter circuit shown in Fig. 3.8 operating at $f_s = 1/T_s = 40kHz$, $D = T_1/T_s = .3$.

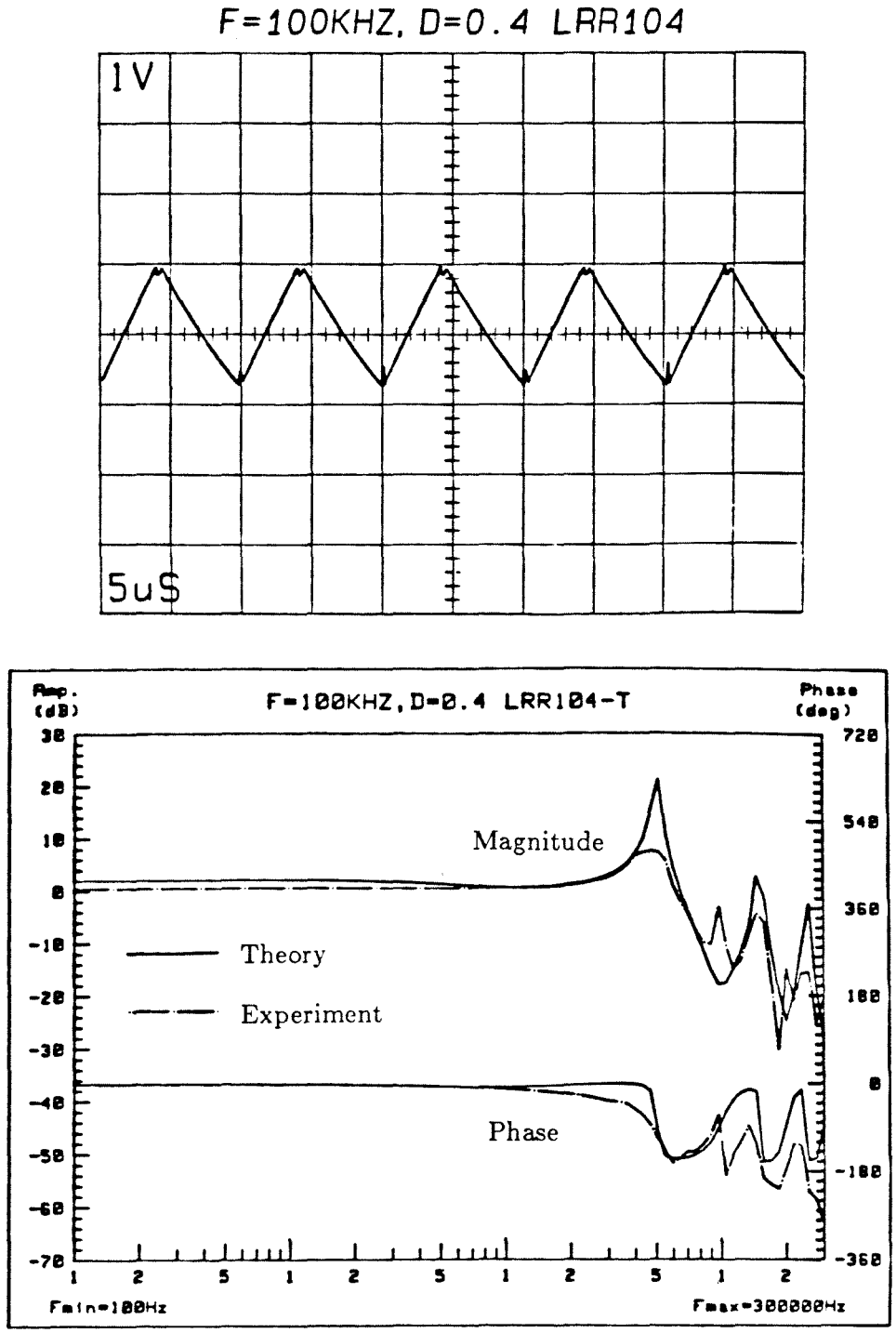

Figure 3.15: The waveform of the steady state solution of the voltage across the load resistor $R = 56\Omega$ and the corresponding Bode plots of the theoretical prediction and the experimental results of the converter circuit shown in Fig. 3.8 operating at $f_s = 1/T_s = 100kHz$, $D = T_1/T_s = .4$.

3.5 Bang-Bang Controlled Converters

The control strategy of a bang-bang controlled two-switched-state converter system may be characterized by $M_j = M^c$, $\forall j \in \mathbf{Z}$, $N_s = 2$; i.e., the converter has two switched-states and all the transition from one switched-state to another is constraint-modulated. The first step in finding the frequency response of the system is to find $\tilde{\mathbf{K}}_0^c$, $\tilde{\mathbf{K}}_1^c$, $\tilde{\mathbf{k}}_0^c$, and $\tilde{\mathbf{k}}_1^c$. These quantities are defined in Eq. (3.30) and Eq. (3.31). The $\mathbf{X}_0$ and $\mathbf{X}_1$ used in calculating these quantities may be found by using Eq. (3.62) and Eq. (3.63) provided that $\mathbf{A}_0$ and $\mathbf{A}_1$ are invertible.

The frequency response of $\delta\mathbf{x}$ with respect to δr_0, according to Eq. (3.57), is:

$$\begin{aligned}\delta\mathbf{x}(s) &= \left\{\tilde{\mathbf{H}}_0(s) + e^{-sT_0}\,\tilde{\mathbf{H}}_1(s)\,\tilde{\mathbf{K}}_1^c\,e^{\mathbf{A}_0T_0}\right\} \\ &\quad \cdot\left\{\mathbf{I} - e^{-sT_s}\,\tilde{\mathbf{K}}_0^c\,e^{\mathbf{A}_1T_1}\,\tilde{\mathbf{K}}_1^c\,e^{\mathbf{A}_0T_0}\right\}^{-1}\,\tilde{\mathbf{k}}_0^c\,\delta r_0^*(s) \qquad (3.73)\end{aligned}$$

where $\tilde{\mathbf{H}}_i(s) = [s\,\mathbf{I} - \mathbf{A}_i]^{-1}\,\{\mathbf{I} - e^{-sT_i}\,e^{\mathbf{A}_iT_i}\}$.

The frequency response of $\delta\mathbf{x}$ with respect to δr_1 may be obtained by interchanging the subscripts 0 and 1 in Eq. (3.73):

$$\begin{aligned}\delta\mathbf{x}(s) &= \left\{\tilde{\mathbf{H}}_1(s) + e^{-sT_1}\,\tilde{\mathbf{H}}_0(s)\,\tilde{\mathbf{K}}_0^c\,e^{\mathbf{A}_1T_1}\right\} \\ &\quad \cdot\left\{\mathbf{I} - e^{-sT_s}\,\tilde{\mathbf{K}}_1^c\,e^{\mathbf{A}_0T_0}\,\tilde{\mathbf{K}}_0^c\,e^{\mathbf{A}_1T_1}\right\}^{-1}\,\tilde{\mathbf{k}}_1^c\,\delta r_1^*(s) \qquad (3.74)\end{aligned}$$

Figure 3.16 is a bang-bang controlled converter circuit, in which:

$$\begin{aligned}\mathbf{A}_0 &= -\tfrac{R+R'}{L} & \mathbf{A}_1 &= -\tfrac{R}{L} \\ \mathbf{B}_0 &= 0 & \mathbf{B}_1 &= \tfrac{1}{L} \\ \mathbf{x} &= i & \mathbf{u} &= V_g \\ m_0^c &= 0 & m_1^c &= 0 \\ \mathbf{f}_0 &= 1 & \mathbf{f}_1 &= 1\end{aligned}$$

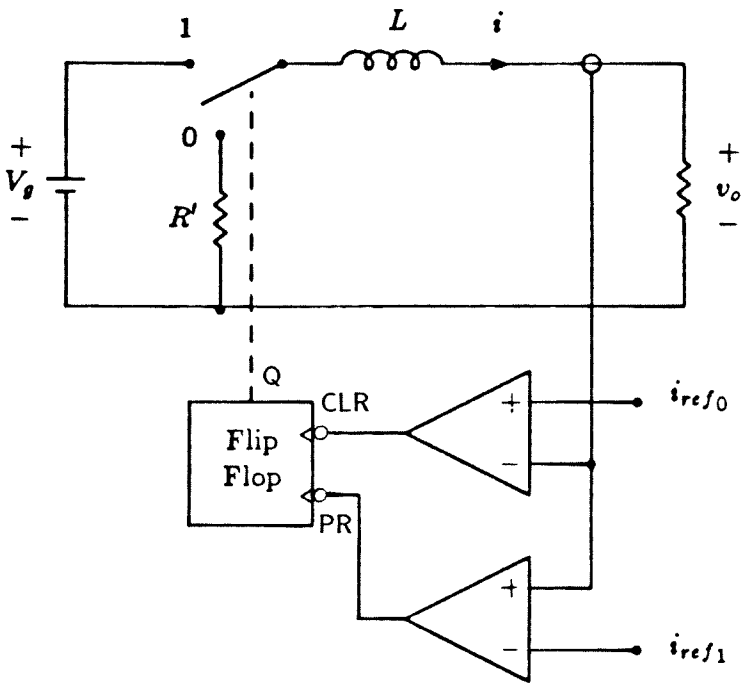

Figure 3.16: A bang-bang controlled R-L converter: $V_g = 15$Volts, $L = 1.43$mH, $R = 56\Omega$, $R' = 6.7\Omega$.

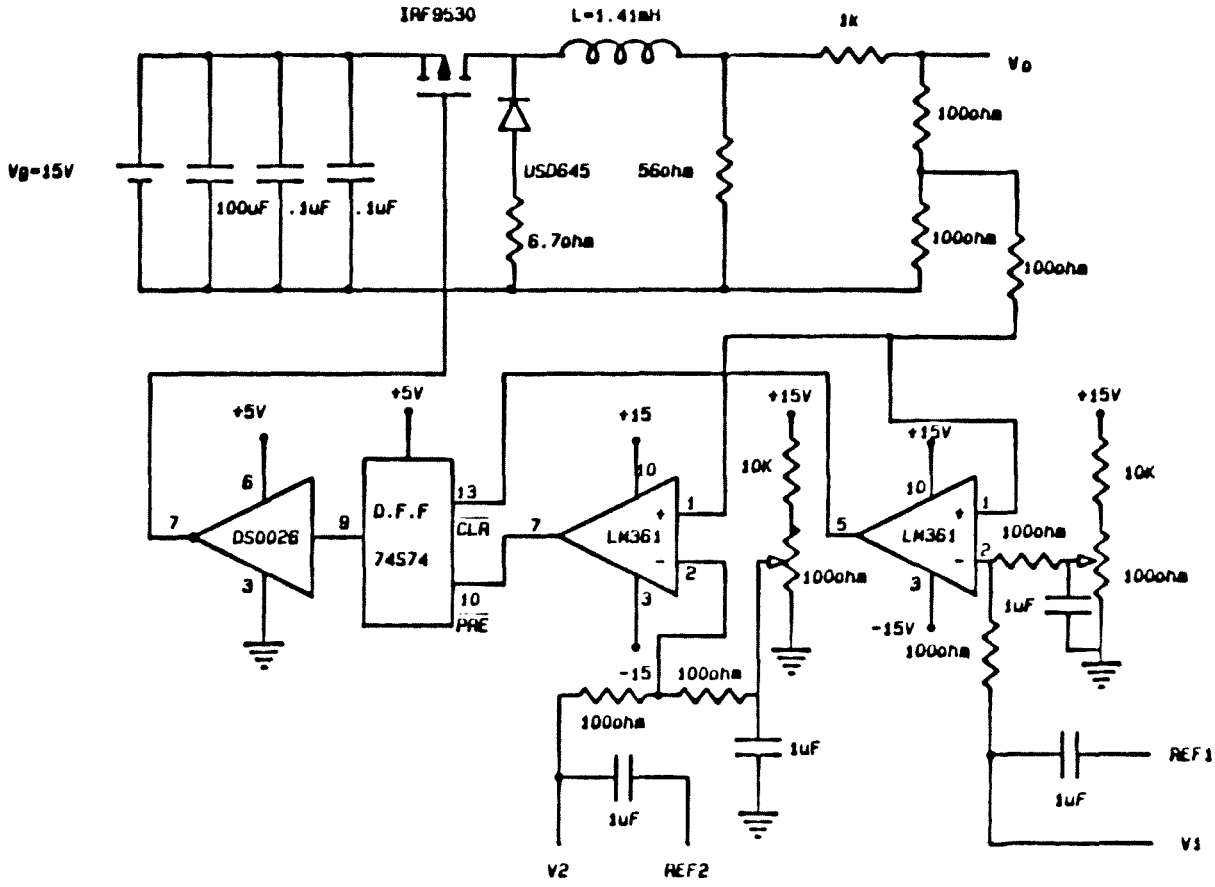

Figure 3.17: The realization of the bang-bang controlled converter circuit shown in Fig. 3.16 for use in the experiments.

With use of Eq. (3.62) and Eq. (3.63), I_0 and I_1, the steady state i at the transitions, are:

$$I_0 = \left[1 - e^{-\frac{R}{L}T_1}\, e^{-\frac{R+R'}{L}T_0}\right]^{-1} \left[1 - e^{-\frac{R}{L}T_1}\right] \frac{V_g}{R} \tag{3.75}$$

$$I_1 = e^{-\frac{R+R'}{L}T_0}\, I_0 \tag{3.76}$$

Then:

$$\tilde{\mathbf{K}}_0^c = -\frac{I_0(R+R')}{V_g - I_0 R} \tag{3.77}$$

$$\tilde{\mathbf{K}}_1^c = -\frac{V_g - I_1 R}{I_1(R+R')} \tag{3.78}$$

$$\tilde{\mathbf{k}}_0^c = \frac{V_g + I_0 R'}{V_g - I_0 R} \tag{3.79}$$

$$\tilde{\mathbf{k}}_1^c = \frac{V_g + I_1 R'}{I_1(R+R')} \tag{3.80}$$

According to Eq. (3.73), the frequency response of δi with respect to δi_{ref_0} is:

$$\delta i(s) = G_0(s)\, \delta i_{ref_0}^*(s) \tag{3.81}$$

where

$$G_0(s) = \frac{V_g + I_0 R'}{V_g - I_0 R} \left\{ \tilde{H}_0(s) - e^{-(s+\frac{R+R'}{L})T_0}\, \frac{V_g - I_1 R}{I_1(R+R')}\, \tilde{H}_1(s) \right\} \cdot \left\{ 1 - e^{-sT_s}\, e^{-\frac{R}{L}T_1}\, e^{-\frac{R+R'}{L}T_0}\, \frac{I_0}{I_1}\, \frac{V_g - I_1 R}{V_r - I_0 R} \right\}^{-1}$$

$$\tilde{H}_0(s) = \frac{1 - e^{-(s+\frac{R+R'}{L})T_0}}{s + \frac{R+R'}{L}}$$

$$\tilde{H}_1(s) = \frac{1 - e^{-(s+\frac{R}{L})T_1}}{s + \frac{R}{L}}$$

$$\delta i_{ref_0}^*(s) = \frac{1}{T_s} \sum_n \delta i_{ref_0}(s + \frac{2n\pi i}{T_s})$$

The schematic of the bang-bang controlled converter circuit used in the experiments is shown in Fig. 3.17. The Bode plots of the theoretical *"transfer function"*

for modulating i_{ref_0} only, $G_0(s)/T_s$, overlaid with the experimental results for various operating conditions and switching frequencies are shown in Figs. 3.18 through 3.20.

An interesting feature in the Bode plots is that the phase of the "transfer function" is increasing with increase in frequency up to the switching frequency for the case $D = T_1/T_s > 0.5$, and decreasing with increase in frequency for the case of $D < 0.5$. Three switching frequencies, 25kHz, 40kHz, and 100kHz are chosen in the experiments. The switching frequency 25kHz is chosen because it is the *large-ripple* or the *resonant* case. The switching frequency 100kHz is chosen because it is the *small-ripple* or the *high-switching-frequency* case. The switching frequency 40kHz is chosen because $\|\mathbf{A}_i T_s\| \approx 1$.

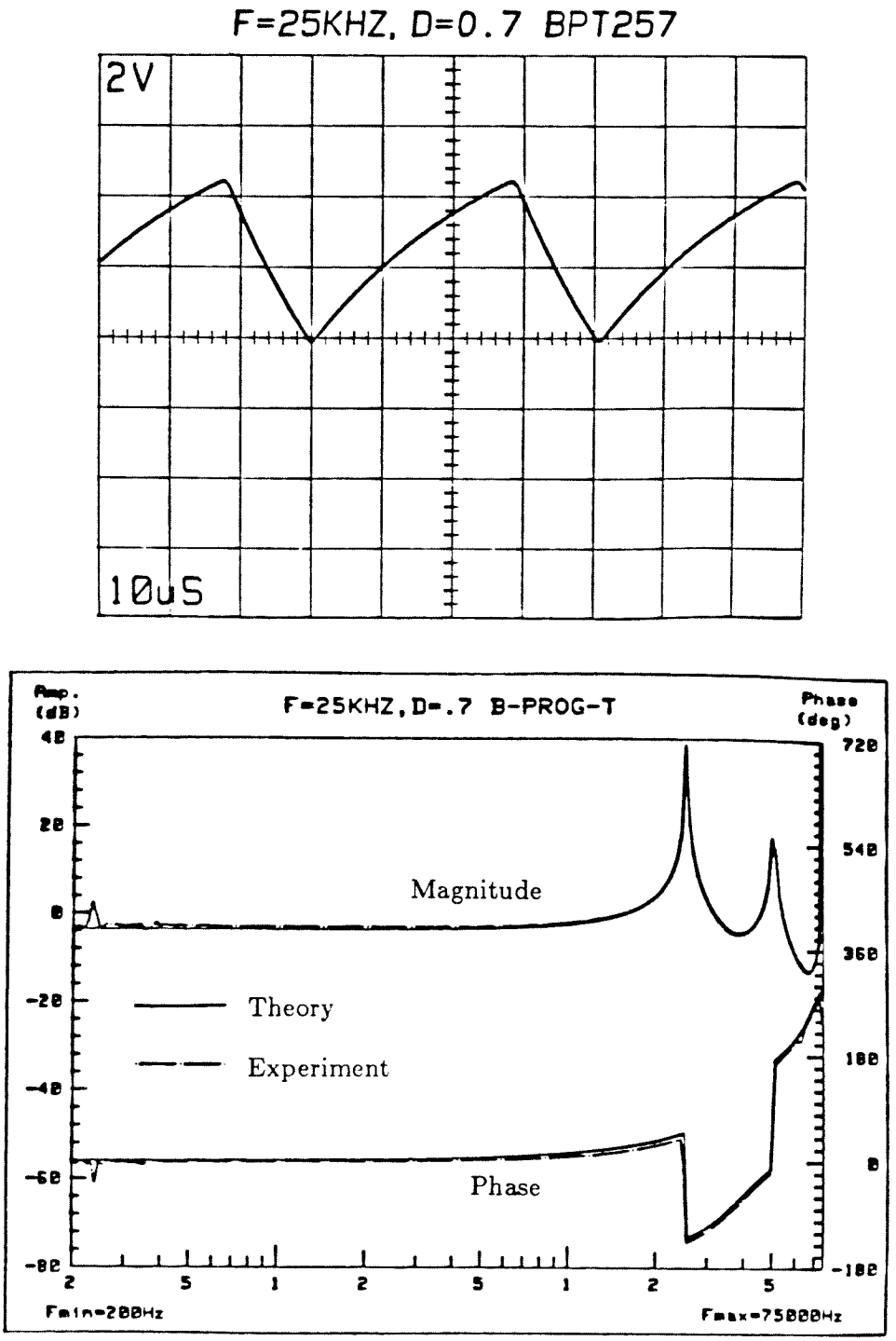

Figure 3.18: The waveform of the steady state solution of the voltage across the load resistor $R = 56\Omega$ and the corresponding Bode plots of the theoretical prediction and the experimental results of the converter circuit shown in Fig. 3.17 operating at $f_s = 1/T_s = 25kHz$, $D = T_1/T_s = .7$; only i_{ref_0} is modulated.

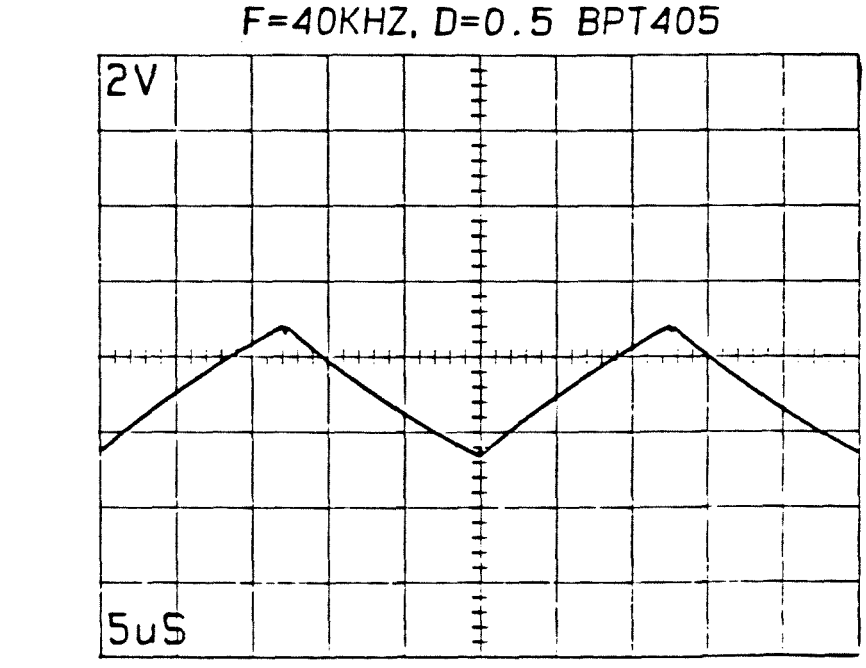

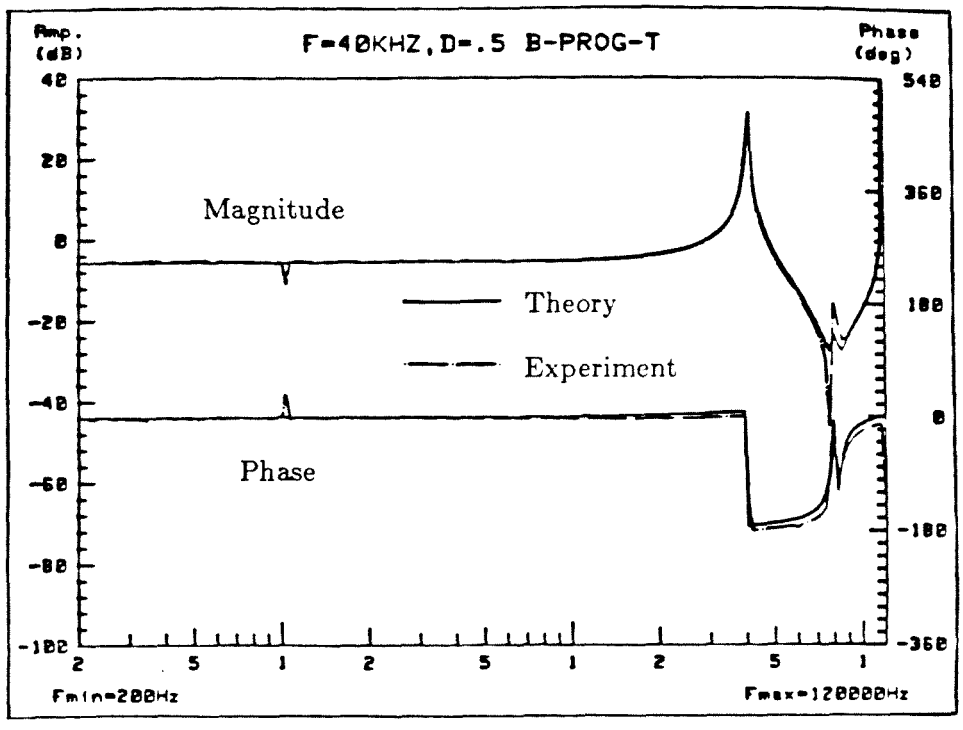

Figure 3.19: The waveform of the steady state solution of the voltage across the load resistor $R = 56\Omega$ and the corresponding Bode plots of the theoretical prediction and the experimental results of the converter circuit shown in Fig. 3.17 operating at $f_s = 1/T_s = 40kHz$, $D = T_1/T_s = .5$; only i_{ref_0} is modulated.

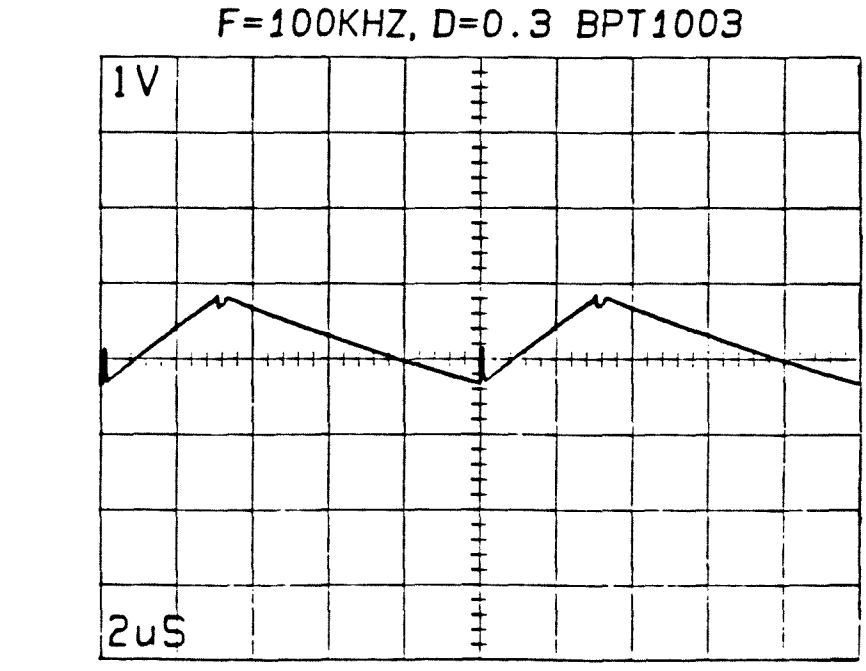

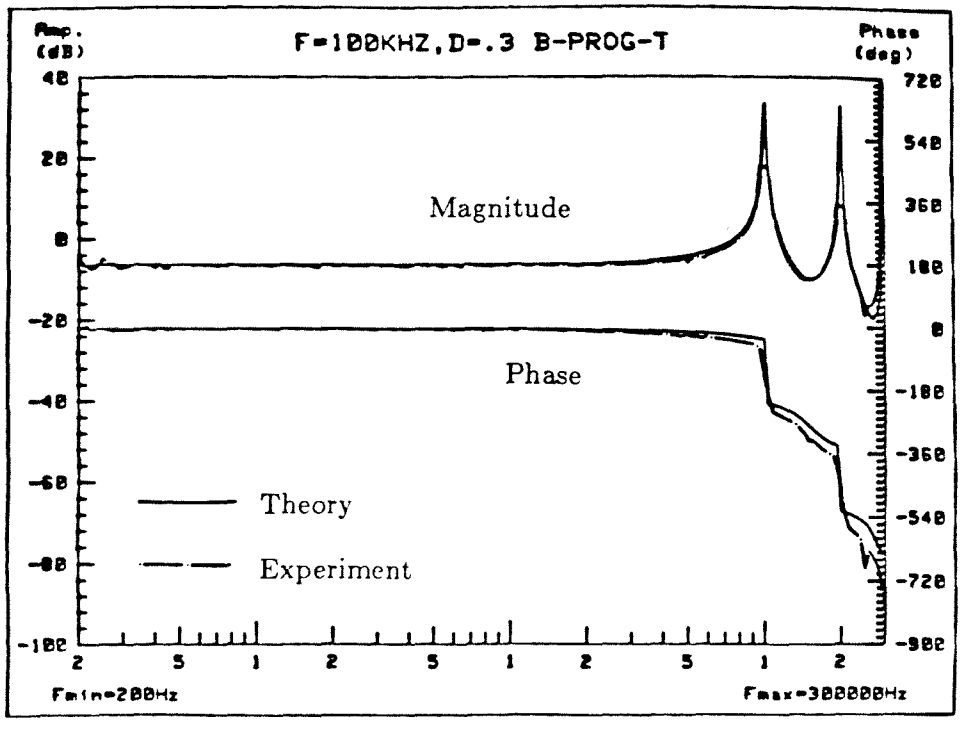

Figure 3.20: The waveform of the steady state solution of the voltage across the load resistor $R = 56\Omega$ and the corresponding Bode plots of the theoretical prediction and the experimental results of the converter circuit shown in Fig. 3.17 operating at $f_s = 1/T_s = 100kHz$, $D = T_1/T_s = .3$; only i_{ref_0} is modulated.

The frequency response of δi with respect to δi_{ref_1}, according to Eq. (3.73), is:

$$\delta i(s) = G_1(s)\, \delta i^*_{ref_1}(s) \tag{3.82}$$

where

$$\begin{aligned}
G_1(s) &= \frac{V_g - I_1 R}{I_1(R+R')} \left\{ \tilde{H}_1(s) - e^{-(s+\frac{R}{L})T_1} \frac{I_0(R+R')}{V_g - I_0 R} \tilde{H}_0(s) \right\} \\
&\qquad \cdot \left\{ 1 - e^{-sT_s} e^{-\frac{R}{L}T_1} e^{-\frac{R+R'}{L}T_0} \frac{I_0}{I_1} \frac{V_g - I_1 R}{V_r - I_0 R} \right\}^{-1} \\
\tilde{H}_0(s) &= \frac{1 - e^{-(s+\frac{R+R'}{L})T_0}}{s + \frac{R+R'}{L}} \\
\tilde{H}_1(s) &= \frac{1 - e^{-(s+\frac{R}{L})T_1}}{s + \frac{R}{L}} \\
\delta i^*_{ref_1}(s) &= \frac{1}{T_s} \sum_n \delta i_{ref_1}(s + \frac{2n\pi i}{T_s})
\end{aligned}$$

If both δi_{ref_0} and δi_{ref_1} are modulated with the same signal δi_{ref}, then the *"transfer function"* from δi_{ref} to δi is $G/T_s = [G_0(s)+G_1(s)]/T_s$. The Bode plots of the theoretical prediction overlaid with experimental measurements of this *"transfer function"*, and the waveform of the steady state solution of the voltage across the load resistor $R = 56\Omega$ to which the Bode plots correspond, are shown in Figs. 3.21 through 3.23. Again, three switching frequencies, 25kHz, 40kHz, and 100kHz are used. The theoretical predictions and the experimental results are almost indistinguishable in the Bode plots, except at relatively high frequencies.

All of the three approximate analytical methods discussed before, namely, the *State Space Averaging Modelling Method*[4,5,6], the *Sampled-Data Modelling of Switching Regulator*[1], and the *Small-Signal Analysis of Resonant Converter*[9], fail to predict the high-frequency response and the fine features of this bang-bang controlled converter, such as, the direction of the phase response as the frequency of the injected signal increases.

Only the *Small-Signal Frequency Response Theory* can predict the fine features in the frequency response. The discrepancies between the theoretical predictions and the experimental results at high frequencies are mostly from the unmodelled behavior of the circuit elements, such as the delay in the active circuit elements and non-ideal switching in switching elements.

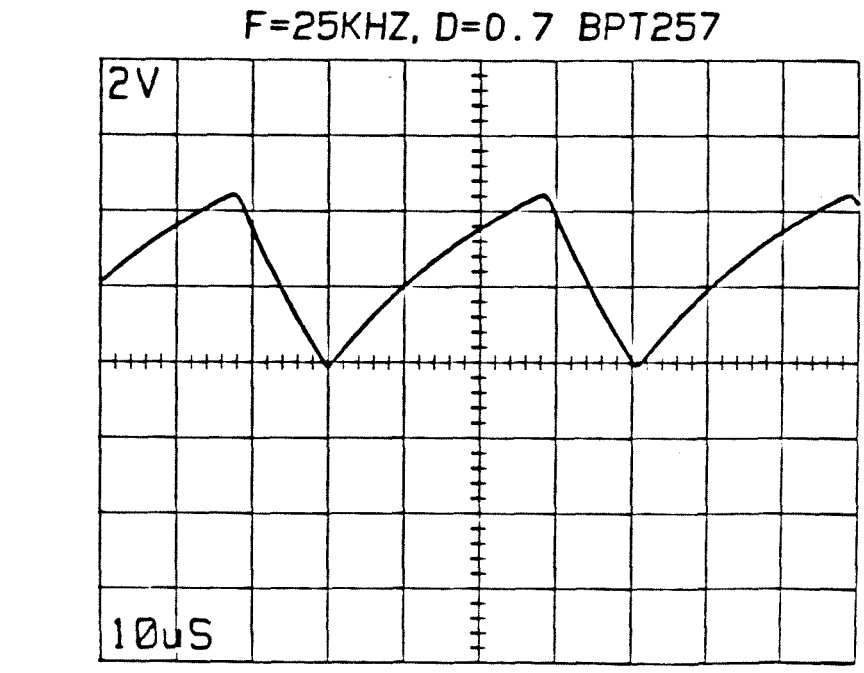

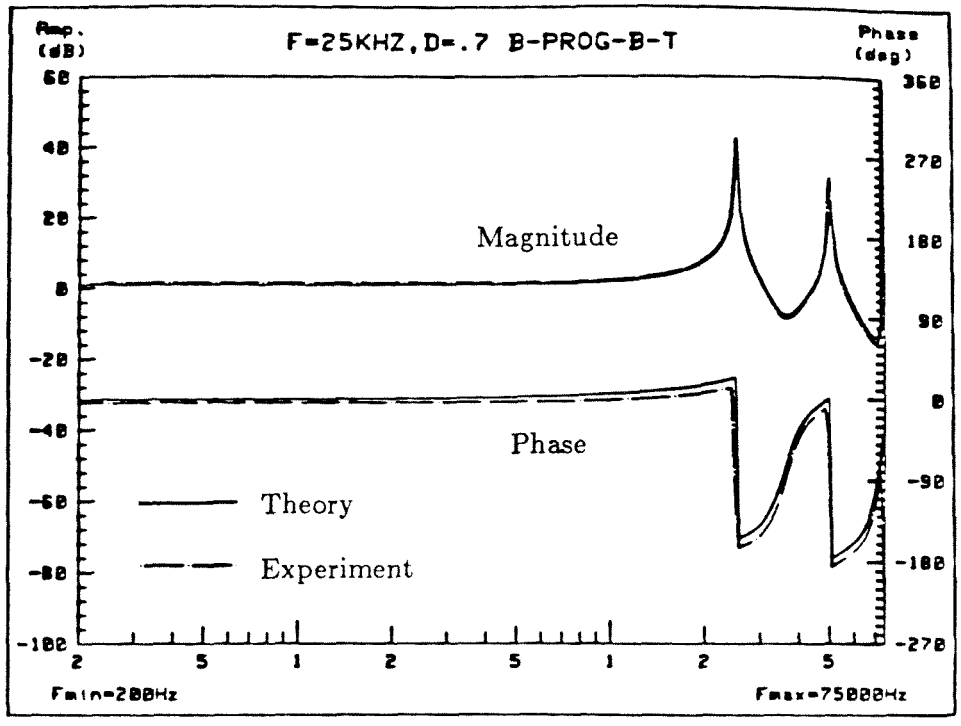

Figure 8.21: The waveform of the steady state solution of the voltage across the load resistor $R = 56\Omega$ and the corresponding Bode plots of the theoretical prediction and the experimental results of the converter circuit shown in Fig. 8.17 operating at $f_s = 1/T_s = 25kHz$, $D = T_1/T_s = .7$; both i_{ref_0} and i_{ref_1} are modulated by the same signal.

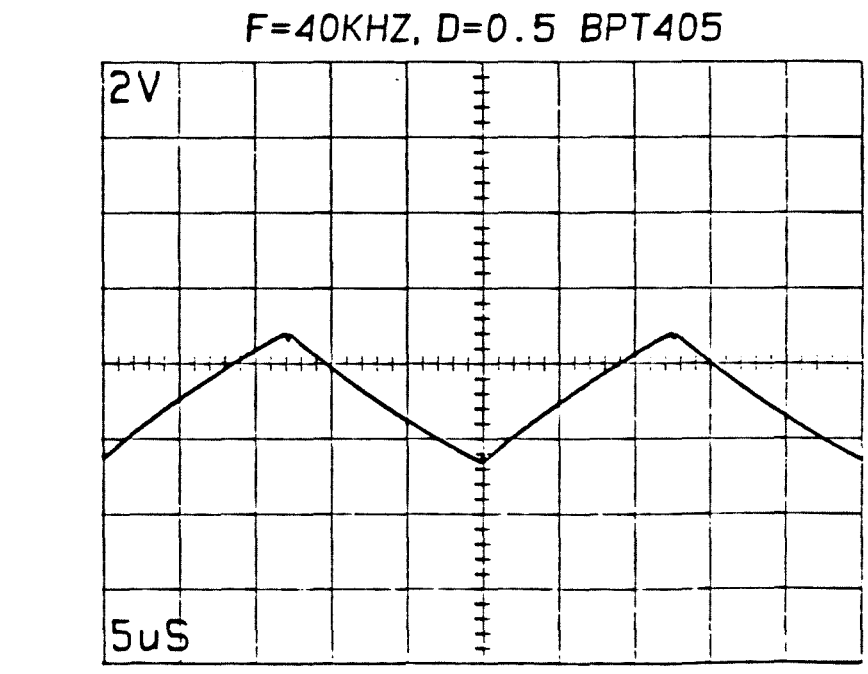

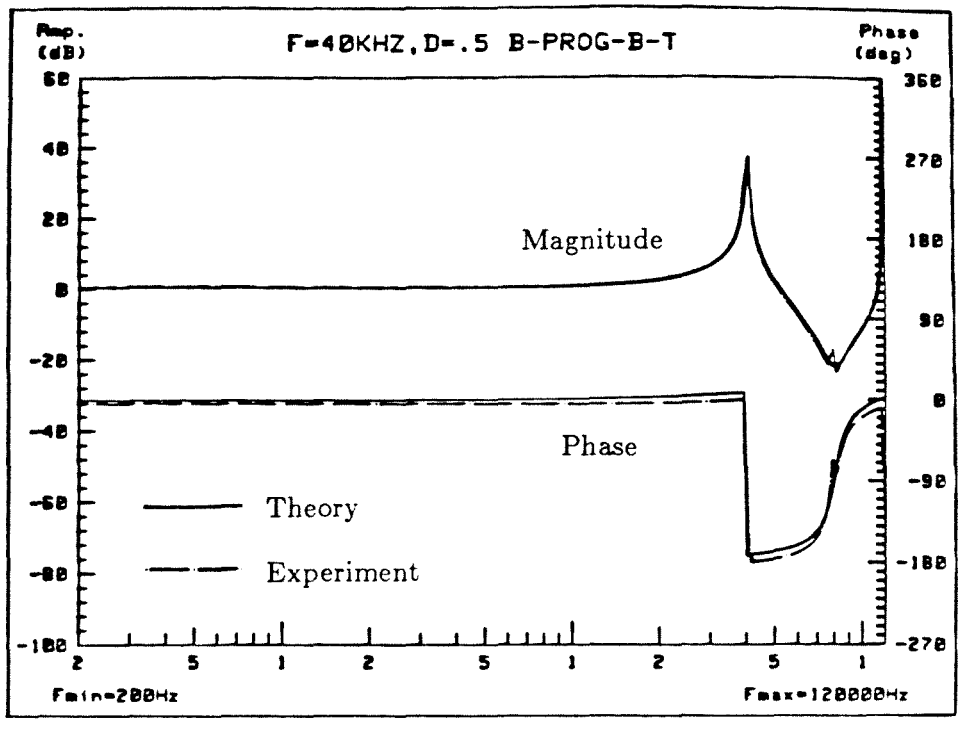

Figure 3.22: The waveform of the steady state solution of the voltage across the load resistor $R = 56\Omega$ and the corresponding Bode plots of the theoretical prediction and the experimental results of the converter circuit shown in Fig. 3.17 operating at $f_s = 1/T_s = 40kHz$, $D = T_1/T_s = .5$; both i_{ref_0} and i_{ref_1} are modulated by the same signal.

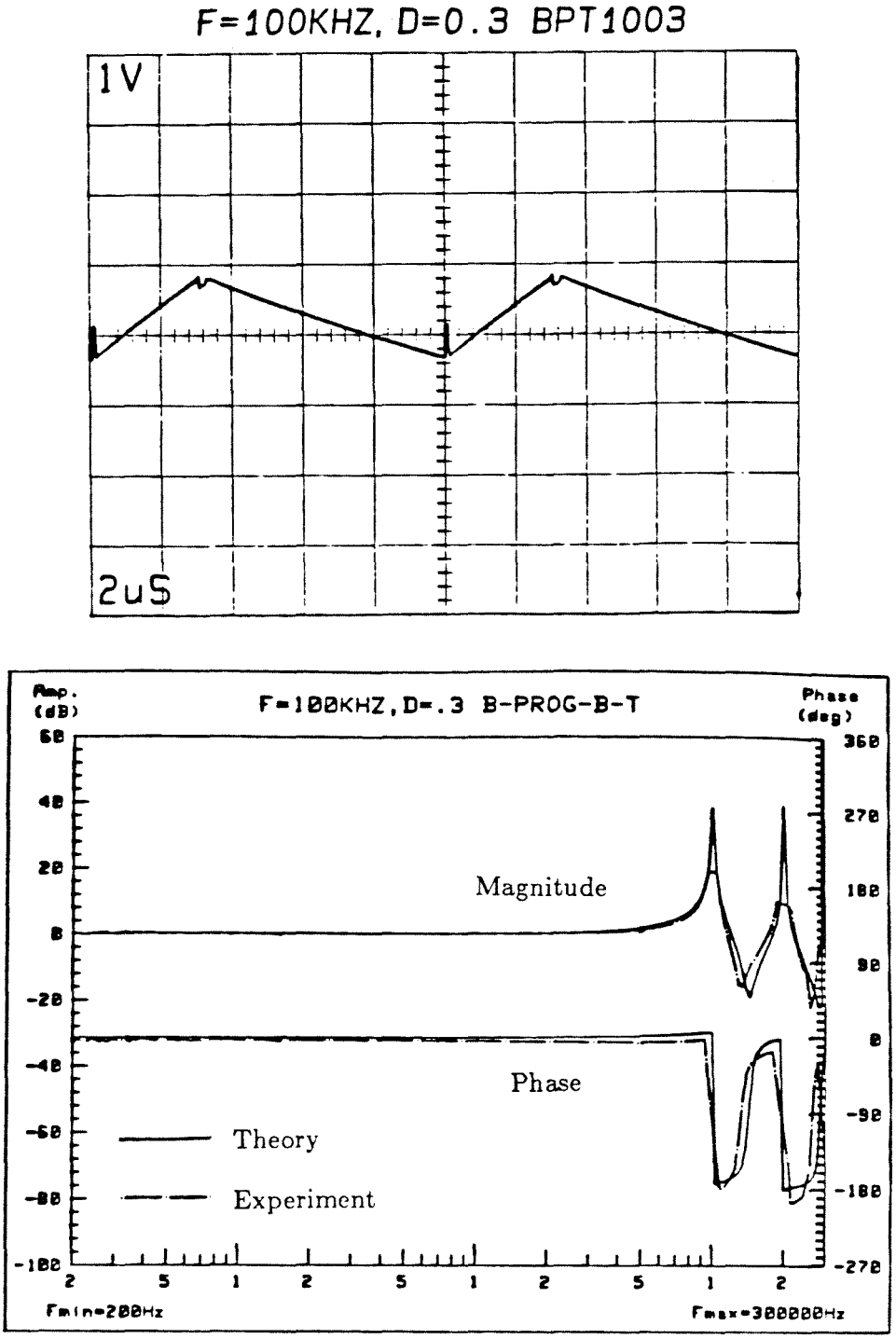

Figure 3.23: The waveform of the steady state solution of the voltage across the load resistor $R = 56\Omega$ and the corresponding Bode plots of the theoretical prediction and the experimental results of the converter circuit shown in Fig. 3.17 operating at $f_s = 1/T_s = 100kHz$, $D = T_1/T_s = .3$; both i_{ref_0} and i_{ref_1} are modulated by the same signal.

Chapter 4

The Mathematics of the Small-Signal Frequency Response Theory

In the establishment of the *Small-Signal Frequency Response Theory* for ideal dc-to-dc converter systems in Chapter 3, a few key results are taken for granted without much justification. These results are:

1. The effect of the excitation at the control-input r_0 on the spectrum of the state $\mathbf{x}$ of a converter system is the same as the effect of the excitation at the control-input r_0 on the spectrum of the perturbed state $\Delta\mathbf{x}$.

2. The small-signal asymptotic stability of a steady state solution of an ideal dc-to-dc converter system guarantees the existence of a stability region in the vicinity of that steady state solution.

3. For an analog signal $\Delta r(t)$, $\Delta r_n^*(s)$ — the spectrum of the naturally sampled $\Delta r(t)$, is the same as $\Delta r_u^*(s)$ — the spectrum of the uniformly sampled $\Delta r(t)$, with the addition of noise and harmonics.

4. The *equivalent hold* is exact in the *small-signal limit.*

In this chapter, these results are discussed in detail. The derivation and the implications of these results are discussed in Sections 4.1 through 4.4.

4.1 The Spectrum of the State of the System

Suppose that in the steady state, the state of an ideal dc-to-dc converter system $\mathbf{x}(t)$ is $\mathbf{X}(t)$. When the control-input r_0 of the system is perturbed, the state $\mathbf{x}(t)$ is no longer $\mathbf{X}(t)$, and the perturbed state $\Delta\mathbf{x}(t) \equiv \mathbf{x}(t) - \mathbf{X}(t) \neq 0$. In the *small-signal limit*, $\Delta\mathbf{x}(t) \to \delta\mathbf{x}(t)$.

The spectrum of the state $\mathbf{x}$ is the Laplace transform of $\mathbf{x}(t)$, $\mathcal{L}\{\mathbf{x}(t)\}$.

$$\mathcal{L}\{\mathbf{x}(t)\} \equiv \int_0^\infty \mathbf{x}(t)\, e^{-st}\, dt. \tag{4.1}$$

The Laplace transform operator $\mathcal{L}$ is linear; i.e.,

$$\mathcal{L}\{\mathbf{x}(t)\} = \mathcal{L}\{\mathbf{X}(t)\} + \mathcal{L}\{\Delta\mathbf{x}(t)\} \tag{4.2}$$

The steady state solution of the state of the system $\mathbf{X}(t)$ is periodic with period T_s; $1/T_s$ is the steady state switching frequency. As a result, the steady state solution of the state $\mathbf{X}(t)$ has frequency components only at multiples of the steady state switching frequency. Consequently, it does not contribute to the frequency components of $\mathbf{x}(t)$ that are not at a multiple of the steady state switching frequency. Therefore, any frequency component in the state $\mathbf{x}(t)$ that is not at a multiple of the steady state switching frequency comes from the perturbed state $\Delta\mathbf{x}(t)$. This simple result which is based on the linearity of the Laplace transform operator is trivial. Nevertheless, it has profound implications: for the study of the change in the spectrum of the state $\mathbf{x}(t)$ resulted from perturbations at the control-input of an ideal dc-to-dc converter system, it is not necessary to compute the spectrum of the state $\mathbf{x}(s)$; it is only necessary to compute the spectrum of the perturbed state $\Delta\mathbf{x}(s)$.

The difficulties in computing the steady state solutions of the state $\mathbf{X}(t)$ and the state $\mathbf{x}(t)$ of an ideal dc-to-dc converter system arise from the fact that if the system matrix $\mathbf{A}_i$ of any of the switched-state i is not invertible, then the closed-form solutions

of both $\mathbf{x}(t)$ and $\mathbf{X}(t)$ contain an integral of the form $\int_{t_0}^{t} e^{\mathbf{A}_i \tau}\, d\tau\, \mathbf{B}_i \mathbf{u}$. The integral in the expression for the state $\mathbf{x}(t)$ and the expression for the steady state solution of the state $\mathbf{X}(t)$ make the computation of the *equivalent hold* for the state $\mathbf{x}$ discussed in Section 3.2 very difficult.

Fortunately, the perturbed state $\Delta\mathbf{x}(t)$ is governed by a set of differential equations which is quite different from that which governs the state $\mathbf{x}(t)$ and the steady state solution of the state $\mathbf{X}(t)$. Except in very short time intervals about the instants of switching, the set of differential equations governing the perturbed state $\Delta\mathbf{x}(t)$ has no forcing term $\mathbf{u}$, and therefore, no integral. Furthermore, these time intervals which are close to the instant of switching can be made arbitrarily small in the *small-signal limit*. As a result, the perturbed state $\Delta\mathbf{x}(t)$ in these time intervals have arbitrary small contribution to the spectrum of $\mathbf{x}$ (see Section 4.4). In the *small-signal limit*, $\Delta\mathbf{x}(t)$ becomes $\delta\mathbf{x}(t)$ and the evolution of $\delta\mathbf{x}(t)$ in these time intervals can be described by a constant matrix that can be computed easily (see Section 3.1). The initial conditions of the perturbed state $\Delta\mathbf{x}(t)$ for the time intervals between consecutive switching are given by the samples of the perturbed state $\Delta\mathbf{x}_i[n]$.

In general, for any system, studying the effect of the excitations at the control-input r_0 on the spectrum of the state $\mathbf{x}$ of a system may be simplified to studying the effect of excitations at r_0 on the spectrum of the perturbed state $\Delta\mathbf{x}$ of the system. In the case of an ideal dc-to-dc converter system, computing the perturbed state $\Delta\mathbf{x}$ is much easier than computing the state $\mathbf{x}$.

4.2 The Small-Signal Stability of the System

The concept of the stability of an operating condition or an operating point is widely used in analog electronic circuits. This concept of stability only applies to sys-

tems which have a unique constant steady state solution corresponding to each operating condition. Obviously, this concept of stability cannot be applied to nonlinear systems in general, because nonlinear systems in general may have multiple stable steady state solutions under a given operating condition; for example, the simple ideal dc-to-dc converter discussed in Chapter 2, and the constant-switching-frequency programmed L-R converter of Section 3.4. It is, therefore, necessary to apply the concept of the stability of a solution to a nonlinear system. For a detailed discussion of the stability of a system, see Appendix A.

The small-signal or local stability of a steady state solution of an ideal dc-to-dc converter system is determined by the difference equation that describes its small-signal motion in the vicinity of its steady state solution. Nevertheless, the small-signal stability may not have any meaning for a steady state solution of nonlinear system such as the ideal dc-to-dc converter system, because, while the solution may be small-signal stable, it may also be a meta-stable solution. In the case of meta-stable, any infinitesimal perturbation to the system will result in the instability of the solution.

Fortunately, for ideal dc-to-dc converter systems, if a steady state solution is asymptotically stable, then this solution is not meta-stable. This is a result developed by Caughey and Masri[2], which is stated in the theorem below.

Theorem 1 *For the nonlinear difference equation:*

$$\Delta\mathbf{x}[n] = \mathbf{\Phi}\,\Delta\mathbf{x}[n-1] + R(\Delta\mathbf{x}[n-1]) \tag{4.3}$$

If:

1. $||\Delta\mathbf{x}[0]||$ *is sufficiently small,*
2. $\lim_{||\Delta\mathbf{x}||\to 0} \dfrac{||R(\Delta\mathbf{x})||}{||\Delta\mathbf{x}||} = 0,$
3. *The difference equation* $\Delta\mathbf{x}[n] = \mathbf{\Phi}\,\Delta\mathbf{x}[n-1]$ *is asymptotically stable; i.e.,* $\max|\lambda(\mathbf{\Phi})| < 1,$

then the nonlinear difference equation, Eq. (4.3), is also asymptotically stable.

This theorem is extremely important for the class of ideal dc-to-dc converter systems which have small-signal asymptotically stable solution; i.e., all the eigenvalues of the transition matrix Φ in the difference equation that describes the small-signal motion of the system in the vicinity of the solution have modulus less than unity. This class of converter systems includes all the constant-switching-frequency converter systems. In this class of converter systems, $R(\Delta \mathbf{x}) = O(\Delta^2)$. This theorem guarantees that if the steady state solution of this class of converter systems is small-signal stable, then the solution is not meta-stable. As a result, the small-signal frequency response corresponding to a small-signal asymptotically stable solution always has meaning.

4.3 Almost Periodic Sampling

Natural-sampling is commonly used in the control of converter systems. It is chosen over uniform-sampling because it does not require the relatively costly sample and hold circuitry, and it does not introduce delay in the control loop. Nevertheless, the analysis of a natural-sampling process is not as straightforward as that of a uniform-sampling process. This section is devoted to the analysis of the difference between the spectrum of a naturally sampled signal and the spectrum of the corresponding uniformly sampled signal.

Given an analog signal $\Delta r(t)$, the uniformly sampled $\Delta r(t)$ is:

$$\sum_n \Delta r(nT)\, \delta(t - nT) \tag{4.4}$$

where T is the sampling period. The almost-periodically-sampled $\Delta r(t)$ is:

$$\sum_n \Delta r(nT + \Delta t[n])\, \delta(t - nT - \Delta t[n]) \tag{4.5}$$

where $\{\Delta t[n]\}$ is a sequence. If $\Delta t[n]$ satisfies Eq. (4.6), the constraint equation:

$$\Delta r(nT + \Delta t[n]) = m\,\Delta t[n] \tag{4.6}$$

for $m \in \mathbf{R}$, and $\forall n \in \mathbf{Z}$, then the signal $\Delta r(t)$ is naturally sampled.

If $\{\Delta t[n]\}$ is a random sequence, it is natural to expect that the spectrum of the resulting almost-periodically-sampled $\Delta r(t)$ is the same as the spectrum of the uniformly sampled $\Delta r(t)$ except that it is corrupted by random noise. For the naturally sampled $\Delta r(t)$, however, the sequence $\{\Delta t[n]\}$ and the analog signal $\Delta r(t)$ has correlation. This correlation may add extra frequency components to the spectrum of the naturally sampled $\Delta r(t)$. Exactly how the spectrum of the naturally sampled $\Delta r(t)$ is related to the spectrum of $\Delta r(t)$, and to the spectrum of the uniformly sampled $\Delta r(t)$ is not obvious.

Let $\Delta r_u^*(s)$ denote the spectrum of the uniformly sampled $\Delta r(t)$, and $\Delta r_n^*(s)$ denote the spectrum of the naturally sampled Δr.

$$\Delta r_u^*(s) = \sum_n \Delta r(nT)\, e^{-snT} \tag{4.7}$$

$$\Delta r_n^*(s) = \sum_n \Delta r(nT + \Delta t[n])\, e^{-s(nT+\Delta t[n])} \tag{4.8}$$

On the assumption that the series in Eq. (4.7) and Eq. (4.8) converge uniformly, $\Delta r_n^*(s)$ may then be expressed in terms of $\Delta r_u^*(s)$ and other terms.

$$\begin{aligned}
\Delta r_n^*(s) &= \sum_n \Delta r(nT + \Delta t[n])\, e^{-s(nT+\Delta t[n])} \\
&= \sum_n \Delta r(nT)\, e^{-snT} \\
&\qquad + \sum_n \Delta r(nT + \Delta t[n])\, e^{-s(nT+\Delta t[n])} - \Delta r(nT)\, e^{-snT} \\
&= \Delta r_u^*(s) + \sum_n \{\Delta r(nT + \Delta t[n]) - \Delta r(nT)\}\, e^{-snT} \\
&\qquad + \sum_n \Delta r(nT + \Delta t[n])\, e^{-snT}(e^{-s\,\Delta t[n]} - 1)
\end{aligned}$$

$$= \Delta r_u^*(s) + \sum_n \left\{ \Delta\dot{r}(nT)\Delta t[n] + \frac{1}{2}\Delta\ddot{r}(nT)(\Delta t[n])^2 + O(\Delta^3) \right\} e^{-snT}$$

$$+ \sum_n \left\{ \left[\Delta r(nT) + \Delta\dot{r}(nT)\,\Delta t[n] + O(\Delta^3) \right] \right.$$

$$\left. \cdot \left[-s\,\Delta t[n] + \frac{s^2}{2}(\Delta t[n])^2 + O(\Delta^3) \right] \right\} e^{-snT}$$

Hence:

$$\Delta r_n^*(s) = \Delta r_u^*(s) + \sum_n \left\{ \Delta\dot{r}(nT)\,\Delta t[n] - s\,\Delta r(nT)\,\Delta t[n] + O(\Delta^3) \right\} e^{-snT} \tag{4.9}$$

A first approximation for $\Delta t[n]$ is:

$$\Delta t[n] = \frac{\Delta r(nT)}{m} + O(\Delta^2) \tag{4.10}$$

where m is defined in Eq. (4.6). With use of this approximation, Eq. (4.9) becomes:

$$\Delta r_n^*(s) = \Delta r_u^*(s) + \sum_n \frac{1}{m} \left\{ \Delta\dot{r}(nT)\,\Delta r(nT) - s\,[\Delta r(nT)]^2 + O(\Delta^3) \right\} e^{-snT} \tag{4.11}$$

The difference term between $\Delta r_n^*(s)$ and $\Delta r_u^*(s)$ is of $O(\Delta^2)$. These difference terms do not have a linear correlation with Δr. The effects of these terms on $r_n^*(s)$ may be described by *additional noise* or *harmonic distortion.* In the *small-signal limit,* $\Delta r \to 0$, these difference terms, of $O(\Delta^2)$, approach zero faster than Δr. Therefore, these difference terms may be neglected and a naturally sampled signal may be treated as a uniformly sampled signal in the *small-signal limit.*

4.4 The Equivalent Hold

In the derivation of the *equivalent hold* in Section 3.2, it is assumed that given the initial perturbed state $\Delta\mathbf{x}_i[n]$, the perturbed state for $\mathbf{T}_{i+nN_s} < t < \mathbf{T}_{i+1+nN_s}$ is given by:

$$\Delta\mathbf{x}^\ddagger(t) = e^{\mathbf{A}_i(t-\mathbf{T}_{i+nN_s})}\,\Delta\mathbf{x}_i[n] \tag{4.12}$$

where $\Delta\mathbf{x}^{\ddagger}(t)$ is the assumed perturbed state, and $\mathbf{T}_j$ is the time at which the system switches from switched-state $j-1$ to switched-state j in steady state. Nevertheless, the actual perturbed state $\Delta\mathbf{x}(t) = \mathbf{x}(t) - \mathbf{X}(t)$ is considerably more complicated than what is described by Eq. (4.12). For time t, $\max(\mathbf{T}_{i+nN_s}, \mathcal{T}_{i+nN_s}) < t < \min(\mathbf{T}_{i+1+nN_s}, \mathcal{T}_{i+1+nN_s})$, the differential equation that describes the actual perturbed state $\Delta\mathbf{x}(t)$ is:

$$\Delta\mathbf{x}(t) = e^{\mathbf{A}_i(t-\mathbf{T}_{i+nN_s})}\left(\Delta\mathbf{x}_i[n] + \mathrm{O}(\Delta^2)\right) \tag{4.13}$$

There are three discrepancies between the assumed perturbed state $\Delta\mathbf{x}^{\ddagger}(t)$ described by Eq. (4.12) and the actual perturbed state $\Delta\mathbf{x}(t)$ described by Eq. (4.13).

1. The initial value of the perturbed state is not exactly $\Delta x_i[n]$; it is off by $\mathrm{O}(\Delta^2)$.

2. If $\mathcal{T}_{i+nN_s} > \mathbf{T}_{i+nN_s}$, then Eq. (4.12) and Eq. (4.13) cannot describe the evolution of the perturbed state $\Delta\mathbf{x}(t)$ for $\mathbf{T}_{i+nN_s} < t < \mathcal{T}_{i+nN_s}$. Nevertheless, it is possible to prove that for $\mathbf{T}_{i+nN_s} < t < \mathcal{T}_{i+nN_s}$, $\Delta\mathbf{x}(t)$ is of $\mathrm{O}(\Delta\mathbf{x}_i[n])$.

3. Similarly, if $\mathcal{T}_{i+1+nN_s} < \mathbf{T}_{i+1+nN_s}$ then Eq. (4.12) and Eq. (4.13) cannot describe the evolution of the perturbed state $\Delta\mathbf{x}(t)$ for $\mathcal{T}_{i+1+nN_s} < t < \mathbf{T}_{i+1+nN_s}$. It is also possible to prove that for $\mathcal{T}_{i+nN_s} < t < \mathbf{T}_{i+nN_s}$, $\Delta\mathbf{x}(t)$ is of $\mathrm{O}(\Delta\mathbf{x}_{i+1}[n])$.

For the claim that the *equivalent hold* derived in Chapter 3 is exact in the *small-signal limit* to be valid, it is necessary to prove that there is negligible difference for calculating the *equivalent hold* by using the assumed perturbed state $\Delta\mathbf{x}^{\ddagger}(t)$ described in Eq. (4.12), instead of the actual perturbed state $\Delta\mathbf{x}(t)$ in the *small-signal limit*.

Consider the time period $t \in \Gamma_j$, $\Gamma_j \equiv \{t \mid \mathbf{T}_j < t < \mathbf{T}_{j+1}\}$. For the quantity $\Delta\mathbf{x}^{\ddagger}_{\Gamma_j}(s)$ to be the Laplace transform of the assumed perturbed state $\Delta\mathbf{x}^{\ddagger}(t)$, $t \in \Gamma_j$, it must satisfy the following equation:

$$\left\|\Delta\mathbf{x}^{\ddagger}(t) - \mathcal{L}^{-1}\{\Delta\mathbf{x}^{\ddagger}_{\Gamma_j}(s)\}\right\|_{\Gamma_j} \equiv \left\{\int_{t\in\Gamma_j}\left\|\Delta\mathbf{x}^{\ddagger}(t) - \mathcal{L}^{-1}\{\Delta\mathbf{x}^{\ddagger}_{\Gamma_j}(s)\}\right\|_2^2\, dt\right\}^{\frac{1}{2}}$$

$$= 0 \tag{4.14}$$

where $\| \cdot \|_2$ is the spatial Euclidean norm. The Γ_j-norm, $\| \cdot \|_{\Gamma_j}$, of a signal is a measure of its energy for time $t \in \Gamma_j$. Consider a norm similar to that defined in Eq. (4.14) for the perturbed state $\Delta\mathbf{x}(t)$ for $t \in \Gamma_j$,

$$\left\|\Delta\mathbf{x}(t) - \mathcal{L}^{-1}\{\Delta\mathbf{x}^{\ddagger}_{\Gamma_j}(s)\}\right\|_{\Gamma_j} = \left\{\int_{t\in\Gamma_j} \left\|\Delta\mathbf{x}(t) - \mathcal{L}^{-1}\{\Delta\mathbf{x}^{\ddagger}_{\Gamma_j}(s)\}\right\|_2^2 \, dt\right\}^{\frac{1}{2}} \tag{4.15}$$

Obviously, this norm is not zero because the perturbed state $\Delta\mathbf{x}(t)$ is not exactly the same as the assumed perturbed state $\Delta\mathbf{x}^{\ddagger}(t)$. The square of this norm may be expanded as follows:

$$\begin{aligned}
&\left\|\Delta\mathbf{x}(t) - \mathcal{L}^{-1}\{\Delta\mathbf{x}^{\ddagger}_{\Gamma_j}(s)\}\right\|_{\Gamma_j}^2 \\
&\quad = \int_{t\in\Gamma_j} \left\|\Delta\mathbf{x}(t) - \mathcal{L}^{-1}\{\Delta\mathbf{x}^{\ddagger}_{\Gamma_j}(s)\}\right\|_2^2 \, dt \\
&\quad = \int_{t\in\Gamma_j} \left\|\Big(\Delta\mathbf{x}(t) - \Delta\mathbf{x}^{\ddagger}(t)\Big) + \Big(\Delta\mathbf{x}^{\ddagger}(t) - \mathcal{L}^{-1}\{\Delta\mathbf{x}^{\ddagger}_{\Gamma_j}(s)\}\Big)\right\|_2^2 \, dt \\
&\quad = \int_{t\in\Gamma_j} \left\|\Delta\mathbf{x}(t) - \Delta\mathbf{x}^{\ddagger}(t)\right\|_2^2 \, dt \\
&\qquad\quad + 2\int_{t\in\Gamma_j} \Big(\Delta\mathbf{x}(t) - \Delta\mathbf{x}^{\ddagger}(t)\Big)^T \Big(\Delta\mathbf{x}^{\ddagger}(t) - \mathcal{L}^{-1}\{\Delta\mathbf{x}^{\ddagger}_{\Gamma_j}(s)\}\Big) \, dt \\
&\qquad\quad + \int_{t\in\Gamma_j} \left\|\Delta\mathbf{x}^{\ddagger}(t) - \mathcal{L}^{-1}\{\Delta\mathbf{x}^{\ddagger}_{\Gamma_j}(s)\}\right\|_2^2 \, dt
\end{aligned} \tag{4.16}$$

The only term in the expansion in Eq. (4.16) that has significant contribution is the first integral. Equation (4.14) implies that the sum of all the time intervals for which $\mathcal{L}^{-1}\{\Delta\mathbf{x}^{\ddagger}_{\Gamma_j}(s)\}$ is different from $\Delta\mathbf{x}^{\ddagger}(t)$ for $t \in \Gamma_j$ has measure zero. Since $\Delta\mathbf{x}(t) - \Delta\mathbf{x}^{\ddagger}(t)$ is continuous, well-behaved, and of order Δ, the second integral in the expansion is zero. The third integral in the expansion is zero from Eq. (4.14). Hence:

$$\left\|\Delta\mathbf{x}(t) - \mathcal{L}^{-1}\{\Delta\mathbf{x}^{\ddagger}_{\Gamma_j}(s)\}\right\|_{\Gamma_j}^2 = \int_{t\in\Gamma_j} \left\|\Delta\mathbf{x}(t) - \Delta\mathbf{x}^{\ddagger}(t)\right\|_2^2 \, dt \tag{4.17}$$

For convenience, define three nonintersecting subsets of Γ_j as follows:

$$\begin{aligned}
\Gamma_{j\alpha} &\equiv \{t \mid \mathbf{T}_j < t < \max(\mathbf{T}_j, \mathcal{T}_j)\} \\
\Gamma_{j\beta} &\equiv \{t \mid \max(\mathbf{T}_j, \mathcal{T}_j) < t < \min(\mathcal{T}_{j+1}, \mathbf{T}_{j+1})\} \\
\Gamma_{j\gamma} &\equiv \{t \mid \min(\mathcal{T}_{j+1}, \mathbf{T}_{j+1}) < t < \mathbf{T}_{j+1}\}
\end{aligned}$$

Depending on the values of $\mathcal{T}_j$ and $\mathcal{T}_{j+1}$, both $\Gamma_{j\alpha}$ and $\Gamma_{j\gamma}$ may be empty. Since the integrand is well-behaved, the integral in Eq. (4.17) may be further split up into three integrals:

$$\begin{aligned}
\left\|\Delta\mathbf{x}(t) - \mathcal{L}^{-1}\{\Delta\mathbf{x}^{\ddagger}_{\Gamma_j}(s)\}\right\|^2_{\Gamma_j} &= \int_{t\in\Gamma_{j\alpha}} \left\|\Delta\mathbf{x}(t) - \Delta\mathbf{x}^{\ddagger}(t)\right\|_2^2 \, dt \\
&\quad + \int_{t\in\Gamma_{j\beta}} \left\|\Delta\mathbf{x}(t) - \Delta\mathbf{x}^{\ddagger}(t)\right\|_2^2 \, dt \\
&\quad + \int_{t\in\Gamma_{j\gamma}} \left\|\Delta\mathbf{x}(t) - \Delta\mathbf{x}^{\ddagger}(t)\right\|_2^2 \, dt \qquad (4.18)
\end{aligned}$$

Consider the first integral in Eq. (4.18):

$$\begin{aligned}
\int_{t\in\Gamma_{j\alpha}} \left\|\Delta\mathbf{x}(t) - \Delta\mathbf{x}^{\ddagger}(t)\right\|_2^2 \, dt &\leq \max(0, \Delta t_j) \max_{t\in\Gamma_{j\alpha}} \left\|\Delta\mathbf{x}(t) - \Delta\mathbf{x}^{\ddagger}(t)\right\|_2^2 \\
&= O(\Delta^3) \qquad (4.19)
\end{aligned}$$

Similarly, for the third integral in Eq. (4.18):

$$\begin{aligned}
\int_{t\in\Gamma_{j\gamma}} \left\|\Delta\mathbf{x}(t) - \Delta\mathbf{x}^{\ddagger}(t)\right\|_2^2 \, dt &\leq \max(0, -\Delta t_{j+1}) \max_{t\in\Gamma_{j\gamma}} \left\|\Delta\mathbf{x}(t) - \Delta\mathbf{x}^{\ddagger}(t)\right\|_2^2 \\
&= O(\Delta^3) \qquad (4.20)
\end{aligned}$$

For the time period $t \in \Gamma_{j\beta}$, $\|\Delta\mathbf{x}(t) - \Delta\mathbf{x}^{\ddagger}(t)\| = O(\Delta^2)$; therefore, for the second integral in Eq. (4.18):

$$\begin{aligned}
\int_{t\in\Gamma_{j\beta}} \left\|\Delta\mathbf{x}(t) - \Delta\mathbf{x}^{\ddagger}(t)\right\|_2^2 \, dt &\leq T_j \max_{t\in\Gamma_{j\beta}} \left\|\Delta\mathbf{x}(t) - \Delta\mathbf{x}^{\ddagger}(t)\right\|_2^2 \\
&= O(\Delta^4) \qquad (4.21)
\end{aligned}$$

Hence,

$$\left\|\Delta\mathbf{x}(t) - \mathcal{L}^{-1}\{\Delta\mathbf{x}^{\ddagger}_{\Gamma_j}(s)\}\right\|^2_{\Gamma_j} = \mathrm{O}(\Delta^3) \tag{4.22}$$

Equation (4.22) indicates that the error in the energy of the perturbed state $\Delta\mathbf{x}$ for $t \in \Gamma_j$ results from using the assumed perturbed state $\Delta\mathbf{x}^{\ddagger}$ instead of the perturbed state $\Delta\mathbf{x}$, is of $\mathrm{O}(\Delta^3)$. Nevertheless, the energy of the perturbed state for $t \in \Gamma_j$ is $\|\Delta\mathbf{x}(t)\|^2_{\Gamma_j}$ which is of $\mathrm{O}(\Delta^2)$. Therefore, the ratio of the error in energy resulted from using the assumed perturbed state $\Delta\mathbf{x}^{\ddagger}$ instead of the actual perturbed state $\Delta\mathbf{x}$ for calculating the *equivalent hold*, to the energy of the perturbed state, can be made arbitrarily small in the *small-signal limit.* As a result, the *equivalent hold* is exact in the *small-signal limit.*

Chapter 5

Multiple-Switched-State Converter Systems

Systematic procedures for the construction of the difference equation that describes the small-signal motion of a simple two-switched-state ideal dc-to-dc converter system in the vicinity of its steady state solution and the frequency response corresponding to the solution are developed in Chapter 3. Nevertheless, the formulation introduced in Chapter 3 can neither be applied to converter systems that use the modified-constraint modulation in its control strategy, nor can it take into account the output equation if the output signal is discontinuous. In this chapter, this formulation is modified to overcome these problems, and extended to accommodate multiple-switched-state ideal dc-to-dc converter systems — ideal dc-to-dc converter systems with multiple-switched-state solutions.

Two steps are involved in modifying the formulation discussed in Chapter 3. First, the state of the system and the difference equation that describes the small-signal motion of that system in the vicinity of its steady state solution are augmented to carry the information for describing the modified-constraint modulation. In Section 5.1, a systematic procedure for constructing this augmented difference equation is developed. Second, the *equivalent hold* is generalized to take into account the discontinuities in the output signal. This *generalized equivalent hold* uses the augmented state to obtain information on the discontinuities of the output signal. The *generalized equivalent hold* is discussed in Section 5.2. Since all the basic concepts are already introduced in Chapters 3, along with the mathematical details in Chapter 4, the results in this chapter are

presented without detailed derivation.

5.1 The Small-Signal Motion of the Systems

The difference equation that describes the small-signal motion of the converter systems in the vicinity of their steady state solutions, introduced in Chapter 3, does not carry the necessary information for describing the modified-constraint modulation. In this section, the difference equation is augmented to carry this information. In formulating this augmented difference equation, a new approach is taken, in which all the modulation methods discussed in Chapter 3 are treated as degenerate cases of the modified-constraint modulation. This approach has the advantage of treating all of the four modulation methods uniformly. Consequently, the results can be put into a very concise form.

All of the four types of transitions, controlled by the four different modulation methods described in Section 1.2, namely, *unmodulated transitions*, *time-modulated transitions*, *constraint-modulated transitions*, and *modified-constraint-modulated transitions*, may be described by Eq. (5.1) and Eq. (5.2) below:

$$\delta t_i[n] = m_i\, \delta r_i[n] + h_i\, \delta t_{i-1}[n] - \mathbf{p}_i^T\, \delta\tilde{\mathbf{x}}_{i-1}[n] \tag{5.1}$$

$$\delta \mathbf{x}_i[n] = \delta\tilde{\mathbf{x}}_{i-1}[n] + \bar{\mathbf{k}}_i\, \delta t_i[n] \tag{5.2}$$

where $\bar{\mathbf{k}}_i = (\mathbf{A}_{i-1} - \mathbf{A}_i)\,\mathbf{X}_i + (\mathbf{B}_{i-1} - \mathbf{B}_i)\,\mathbf{u}$. Equation (5.1) describes the dependence of $\delta t_i[n]$, the derivation of the time of transition from switched-state $i-1+nN_s$ to switched-state $i+nN_s$ from its steady state value, on the current sample of the control-input $\delta r_i[n]$, the derivation of the time of the previous transition from its steady state value, and the value of the perturbed state before the transition, in the *small-signal limit*. For each type of modulated transition, there is a different set of m_i, h_i, and $\mathbf{p}_i$. The values of m_i, h_i, and $\mathbf{p}_i$ depend on the modulation method as well as the parameters used in the modulation. Equation (5.2) is the same as Eq. (3.22), which is derived in Section 3.1.2.

The values of m_i, h_i, and $\mathbf{p}_i$ are derived below for each of the four types of transitions:

1. For *unmodulated transitions*, in which $M_{i+nN_s} = M^u$ and $\delta t_i[n] \equiv 0$, $\forall n \in \mathbf{Z}$:

$$\begin{aligned} m_i &= 0 \\ h_i &= 0 \\ \mathbf{p}_i &= \mathbf{0} \end{aligned}$$

2. For the *time-modulated transitions*, in which $M_{i+nN_s} = M^t$, $\forall n \in \mathbf{Z}$, from Eq. (3.20):

$$\delta t_i[n] = (m_i^t)^{-1}\, \delta r_i[n]$$

Hence:

$$\begin{aligned} m_i &= (m_i^t)^{-1} \\ h_i &= 0 \\ \mathbf{p}_i &= \mathbf{0} \end{aligned}$$

3. For *constraint-modulated transitions*, in which $M_{i+nN_s} = M^c$, $\forall n \in \mathbf{Z}$, the *constraint equation* is:

$$\mathbf{f}_i^T\, \mathbf{x}(\tau_{i+nN_s}) + m_i^c\, \Delta t_{i+nN_s} + c_i - r_i[n] = 0$$

where N_s is the number of switched-networks, $\mathbf{f}_i$ is a vector, $r_i[n]$ is the sampled control-input sequence formed from sampling the control-input signal $r_i(t)$, c_i is a constant, and m_i^c is the slope of a sawtooth wave. The *constraint equation* is the condition under which the converter system switches from the switched-state $i + nN_s - 1$ to the switched-state $i + nN_s$. In a converter circuit, the *constraint equation* is the mathematical model of the switching action of the comparator circuit

that determines when this change of the switched-state occurs. This comparator circuit has the control-input $r_i(t)$ at one of its inputs, and the sum of a sawtooth ramp with slope m_i^c and the weighted sum of the system states $\mathbf{f}_i^T\,\mathbf{x}(t)$ at its other input. In the *small-signal limit*, the linearized constraint equation is:

$$\mathbf{f}_i^T\,\dot{\mathbf{X}}_i^-\,\delta t_i[n] + \mathbf{f}_i^T\,\delta\tilde{\mathbf{x}}_i[n] - \delta r_i[n] + m_i^c\,\delta t_i[n] = 0$$

where $\dot{\mathbf{X}}_i^- = [\mathbf{A}_{i-1}\,\mathbf{X}_i + \mathbf{B}_{i-1}\,\mathbf{u}]$. The quantity $\delta t_i[n]$ may be expressed in terms of other quantities in the linearized constraint equation:

$$\begin{aligned}\delta t_i[n] &= \left\{m_i^c + \mathbf{f}_i^T\,\dot{\mathbf{X}}_i^-\right\}^{-1}\,\left\{\delta r_i[n] - \mathbf{f}_i^T\,\delta\tilde{\mathbf{x}}_i[n]\right\} \\ &= \left\{m_i^c + \mathbf{f}_i^T\,\dot{\mathbf{X}}_i^-\right\}^{-1}\,\delta r_i[n] - \left\{m_i^c + \mathbf{f}_i^T\,\dot{\mathbf{X}}_i^-\right\}^{-1}\,\mathbf{f}_i^T\,\delta\tilde{\mathbf{x}}_i[n]\end{aligned}$$

Hence:

$$\begin{aligned}m_i &= \left\{m_i^c + \mathbf{f}_i^T\,[\mathbf{A}_{i-1}\,\mathbf{X}_i + \mathbf{B}_{i-1}\,\mathbf{u}]\right\}^{-1} \\ h_i &= 0 \\ \mathbf{p}_i &= m_i\,\mathbf{f}_i^T\end{aligned}$$

4. For *modified-constraint-modulated transitions*, in which $M_{i+nN_s} = M^m$, $\forall n \in \mathbf{Z}$, the modified-constraint equation is:

$$\mathbf{f}_i^T\,\mathbf{x}(\tau_{i+nN_s}) - r_i[n] + m_i^m\,(\Delta t_{i+nN_s} - h_i^m\,\Delta t_{i-1+nN_s}) + c_i = 0$$

where N_s is the number of switched-networks, $\mathbf{f}_i$ is a vector, $r_i[n]$ is the sampled control-input sequence formed from sampling the control-input signal $r_i(t)$, c_i is a constant, and m_i^m is the slope of the added ramp. The *modified-constraint equation* is the condition under which the converter system switches from switched-state $i+nN_s-1$ to switched-state $i+nN_s$. In a converter circuit, the *modified-constraint equation* is the mathematical model of the switching action of the comparator circuit

that determines when this change of the switched-state occurs. This comparator circuit has the control-input $r_i(t)$ at one of its inputs, and the sum of a sawtooth ramp with slope m_i^m which is delayed by $h_i^m \, \Delta t_{i-1+nN_s}$ and the weighted sum of the system states $\mathbf{f}_i^T \, \mathbf{x}(t)$ at its other input. In the *small-signal limit*, the linearized modified-constraint equation is:

$$\mathbf{f}_i^T \, \dot{\mathbf{X}}_i^- \, \delta t_i[n] + \mathbf{f}_i^T \, \delta\tilde{\mathbf{x}}_i[n] - \delta r_i[n] + m_i^m(\delta t_i[n] - h_i^m \, \delta t_{i-1}[n]) = 0$$

where $\dot{\mathbf{X}}_i^- = [\mathbf{A}_{i-1} \, \mathbf{X}_i + \mathbf{B}_{i-1} \, \mathbf{u}]$. The quantity $\delta t_i[n]$ may be expressed in terms of the other quantities in the linearized modified-constraint equation:

$$\delta t_i[n] = \left\{ m_i^m + \mathbf{f}_i^T \, \dot{\mathbf{X}}_i^- \right\}^{-1} \left\{ \delta r_i[n] - \mathbf{f}_i^T \, \delta\tilde{\mathbf{x}}_i[n] \right\} + m_i^m \, h_i^m \, \delta t_{i-1}[n]$$

Hence:

$$\begin{aligned} m_i &= \left\{ m_i^m + \mathbf{f}_i^T \, [\mathbf{A}_{i-1} \, \mathbf{X}_i + \mathbf{B}_{i-1} \, \mathbf{u}] \right\}^{-1} \\ h_i &= m_i \, m_i^m \, h_i^m \\ \mathbf{p}_i &= m_i \, \mathbf{f}_i^T \end{aligned}$$

In this framework, it is obvious that a closed-loop PWM converter system is the same as a programmed converter system with an added stabilizing ramp; the control strategy is: $M_{2n} = M^c$, $M_{2n+1} = M^u$. An open-loop PWM converter system, however, is very different from its closed-loop version; its control strategy is: $M_{2n} = M^t$, $M_{2n+1} = M^u$. Hence, the steady state solution of both closed-loop PWM converter systems and programmed converter systems may go unstable under certain conditions while the steady state solutions of open-loop PWM converter systems are always stable.

From Eq. (5.1) and Eq. (5.2), its is obvious that for those converter systems which use the *modified-constraint modulation* to control the transition from one switched-state to the other, the difference equation introduced in Chapter 3 which involves only

the sequences $\delta \mathbf{x}_i[n]$ and $\delta r_i[n]$ is not sufficient for describing the small-signal motion of the system. There is a relation between $\delta t_i[n]$ and $\delta t_{i-1}[n]$. This difference equation has to be augmented to overcome this problem. The first step in augmenting the difference equation is to augment the states of the equation from $\delta \mathbf{x}_i[n]$ to $\delta \breve{\mathbf{x}}_i[n]$, where:

$$\delta \breve{\mathbf{x}}_i[n] \equiv \begin{bmatrix} \delta \mathbf{x}_i[n] \\ \delta t_i[n] \end{bmatrix} \tag{5.3}$$

With use of Eq. (5.1) and Eq. (5.2), then:

$$\begin{aligned} \delta \breve{\mathbf{x}}_i[n] &= \begin{bmatrix} \delta \mathbf{x}_i[n] \\ \delta t_i[n] \end{bmatrix} \\ &= \begin{bmatrix} \delta \tilde{\mathbf{x}}_{i-1}[n] + \bar{\mathbf{k}}_i \left\{ m_i\, \delta r_i[n] + h_i\, \delta t_{i-1}[n] - \mathbf{p}_i^T\, \delta \tilde{\mathbf{x}}_{i-1}[n] \right\} \\ m_i\, \delta r_i[n] + h_i\, \delta t_{i-1}[n] - \mathbf{p}_i^T\, \delta \tilde{\mathbf{x}}_{i-1}[n] \end{bmatrix} \\ &= \begin{bmatrix} \mathbf{I} - \bar{\mathbf{k}}_i\, \mathbf{p}_i^T & h_i\, \bar{\mathbf{k}}_i \\ -\mathbf{p}_i^T & h_i \end{bmatrix} \begin{bmatrix} \delta \tilde{\mathbf{x}}_{i-1}[n] \\ \delta t_{i-1}[n] \end{bmatrix} + \begin{bmatrix} m_i\, \bar{\mathbf{k}}_i \\ m_i \end{bmatrix} \delta r_i[n] \end{aligned}$$

Hence,

$$\delta \breve{\mathbf{x}}_i[n] = \begin{bmatrix} \{\mathbf{I} - \bar{\mathbf{k}}_i\, \mathbf{p}_i^T\}\, e^{\mathbf{A}_{i-1} T_{i-1}} & h_i\, \bar{\mathbf{k}}_i \\ -\mathbf{p}_i^T\, e^{\mathbf{A}_{i-1} T_{i-1}} & h_i \end{bmatrix} \delta \breve{\mathbf{x}}_{i-1}[n] + \begin{bmatrix} m_i\, \bar{\mathbf{k}}_i \\ m_i \end{bmatrix} \delta r_i[n] \tag{5.4}$$

For convenience, define:

$$\mathbf{\Phi}_{i-1} = \begin{bmatrix} \{\mathbf{I} - \bar{\mathbf{k}}_i\, \mathbf{p}_i^T\}\, e^{\mathbf{A}_{i-1} T_{i-1}} & h_i\, \bar{\mathbf{k}}_i \\ -\mathbf{p}_i^T\, e^{\mathbf{A}_{i-1} T_{i-1}} & h_i \end{bmatrix} \tag{5.5}$$

$$\mathbf{k}_i = \begin{bmatrix} m_i\, \bar{\mathbf{k}}_i \\ m_i \end{bmatrix} \tag{5.6}$$

Then Eq. (5.4) may be rewritten as:

$$\delta \breve{\mathbf{x}}_i[n] = \mathbf{\Phi}_{i-1}\, \delta \breve{\mathbf{x}}_{i-1}[n] + \mathbf{k}_i\, \delta r_i[n] \tag{5.7}$$

Before the construction of the augmented difference equation that describes the small-signal motion of an ideal dc-to-dc converter system in the vicinity of its steady state solution of the state $\mathbf{X}(t)$, the following steps must be taken first:

1. The converter system and its steady state solution are described in the framework laid out in Chapter 1, that is, the sequences $\{(\mathbf{A}_i, \mathbf{B}_i, \mathbf{C}_i, \mathbf{D}_i)\}$, $\{\mathbf{T}_i\}$ and $\{M_i\}$; $0 \leq i < N_s$.

2. The values of the steady state solution of the state at $\mathbf{T}_i$, $\mathbf{X}_i$, $0 \leq i < N_s$, are calculated.

3. The modulation parameters, m_i, h_i, and $\mathbf{p}_i$, that correspond to each of the modulation methods M_i in the control strategy of the system, $0 \leq i < N_s$, are evaluated.

For constructing the difference equation, consider the case in which only M_{nN_s}'s are modulated; i.e., the system is only modulated by the control-input $r_0[n]$. The case in which M_{i+nN_s}'s, $i \neq 0$, are modulated may be taken into account later. Set $r_i[n] = 0$, $0 < i < N_s$, $\forall\, n \in \mathbf{Z}$. By repeated applications of Eq. (5.7) for N_s times, Eq. (5.8) below is obtained.

$$\delta\check{\mathbf{x}}_0[n] = \mathbf{\Phi}\, \delta\check{\mathbf{x}}_0[n-1] + \mathbf{k}\, \delta r_0[n] \tag{5.8}$$

where

$$\begin{aligned} \mathbf{\Phi} &= \mathbf{\Phi}_{N_s-1}\, \mathbf{\Phi}_{N_s-2} \cdots \mathbf{\Phi}_1\, \mathbf{\Phi}_0 \\ \mathbf{k} &= \mathbf{k}_0 \end{aligned}$$

Equation (5.8) is the augmented difference equation that describes the small-signal motion of an ideal dc-to-dc converter system in the vicinity of its multiple-switched-state steady state solution. This augmented difference equation is used in the following section for calculating the frequency response of the system.

5.2 The Frequency Response of the Systems

The state $\mathbf{x}(t)$ of a dc-to-dc converter system is always continuous. Nevertheless, if the output matrix $\mathbf{C}(t)$ or the transmission matrix $\mathbf{D}(t)$ in Eq. (1.1) is discontinuous in time, the output $\mathbf{y}(t)$ is discontinuous. The *equivalent hold* introduced in Section 3.2 for calculating the frequency response of the system is only applicable to continuous output signal. Therefore, it is necessary to generalize the *equivalent hold* to take into account the discontinuity.

The contribution of the discontinuity in the output $\mathbf{y}(t)$, to the perturbed output $\delta\mathbf{y}(t)$ in the *small-signal limit*, is the addition of a pulse train of *"width"* $|\delta t_i[n]|$ and *"height"* $\mathrm{sgn}(\delta t_i[n])\,\{(\mathbf{C}_{i-1}-\mathbf{C}_i)\mathbf{X}_i+(\mathbf{D}_{i-1}-\mathbf{D}_i)\mathbf{u}\}$. In order to study the contribution of the discontinuity in the output to the perturbed output in the frequency domain, consider the contribution of a single pulse with *"height"* $\mathrm{sgn}(\delta t_i[n])\,\mathbf{h}_i$ and *"width"* $|\delta t_i|$ to the perturbed output signal spectrum $\delta\mathbf{y}(s)$, where $\mathbf{h}_i = \{(\mathbf{C}_{i-1} - \mathbf{C}_i)\mathbf{X}_i + (\mathbf{D}_{i-1} - \mathbf{D}_i)\mathbf{u}\}$. Denote the contribution by $\delta\mathbf{y}^{\ddagger}_{i,n}(s)$:

$$\delta\mathbf{y}^{\ddagger}_{i,n}(s) = \begin{cases} \displaystyle\int_{\mathbf{T}_{i+nN_s}}^{\mathbf{T}_{i+nN_s}+\delta t_i[n]} \mathbf{h}_i\, e^{-st}\, dt, & \delta t_i[n] \geq 0 \\ \displaystyle -\int_{\mathbf{T}_{i+nN_s}+\delta t_i[n]}^{\mathbf{T}_{i+nN_s}} \mathbf{h}_i\, e^{-st}\, dt, & \delta t_i[n] \leq 0 \end{cases}$$

$$= e^{\mathbf{T}_{i+nN_s}}\, \frac{1 - e^{\delta t_i[n]}}{s}\, \mathbf{h}_i$$

Hence, in the *small-signal limit*,

$$\delta\mathbf{y}^{\ddagger}_{i,n}(s) = e^{\mathbf{T}_{i+nN_s}}\, \delta t_i[n]\, \mathbf{h}_i \tag{5.9}$$

Therefore, the contribution of the discontinuity in the output to the perturbed output $\delta\mathbf{y}(s)$ can be approximated by the contribution of a train of δ-functions of magnitude $\delta t_i[n]\,\{(\mathbf{C}_{i-1} - \mathbf{C}_i)\mathbf{X}_i + (\mathbf{D}_{i-1} - \mathbf{D}_i)\mathbf{u}\}$ in the *small-signal limit*.

Denote the contribution of $\delta \mathbf{x}_i[n]$ and $\delta t_i[n]$ to the perturbed output signal in the frequency domain by $\delta \mathbf{y}^{\star}_{i,n}(s)$. By using the results in Eq. (3.49) and Eq. (5.9),

$$\begin{aligned}
\delta \mathbf{y}^{\star}_{i,n}(s) &= \mathbf{C}_i\, \delta \mathbf{x}^{\star}_{i,n}(s) + \delta \mathbf{y}^{\ddagger}_{i,n}(s) \\
&= e^{-s\mathbf{T}_{i+nN_s}} \Big\{ \mathbf{C}_i\, [s\,\mathbf{I} - \mathbf{A}_i]^{-1}\, [\mathbf{I} - e^{sT_i}\, e^{\mathbf{A}_i T_i}]\, \delta x_i[n] \\
&\qquad + [(\mathbf{C}_{i-1} - \mathbf{C}_i)\,\mathbf{X}_i + (\mathbf{D}_{i-1} - \mathbf{D}_i)\mathbf{u}]\, \delta t_i[n] \Big\} \qquad (5.10)
\end{aligned}$$

Obviously, the information carried in the difference equation that describes the small-signal motion of the system introduced in Section 3.1 is not sufficient for calculating the spectrum of the perturbed output signal $\delta \mathbf{y}$ because it does not carry the information on $\delta t_i[n]$. It is necessary to use the augmented difference equation developed in Section 5.1, Eq. (5.8), with the augmented state $\delta \check{\mathbf{x}}_i[n]$ to find $\delta \mathbf{y}$. In this case, Eq. (5.10) may be rewritten as:

$$\delta \mathbf{y}^{\star}_{i,n}(s) = e^{-s\mathbf{T}_{i+nN_s}}\, \mathbf{H}_i(s)\, \delta \check{\mathbf{x}}_i[n] \qquad (5.11)$$

where

$$\mathbf{H}_i(s) = \Big[\; \mathbf{C}_i\, [s\,\mathbf{I} - \mathbf{A}_i]^{-1}\, [\mathbf{I} - e^{sT_i}\, e^{\mathbf{A}_i T_i}], \quad (\mathbf{C}_{i-1} - \mathbf{C}_i)\,\mathbf{X}_i + (\mathbf{D}_{i-1} - \mathbf{D}_i)\,\mathbf{u} \;\Big]$$

With use of the *augmented difference equation* that describes the small-signal motion of the system in the vicinity of its steady state solution in Section 5.1 and Eq. (5.11), the control-input-to-output frequency response of a multiple-switched-state ideal dc-to-dc can be found. The procedure for finding the frequency response is similar to that laid out in Section 3.2. In this section, only the frequency response of the system to the perturbed control-input δr_0 is considered. The frequency response of the system to other control-inputs may be taken into consideration by superposition.

The first step in finding the frequency response is to establish the relation between $\delta r_0(s)$ — the spectrum of the perturbed control-input δr_0, and $\delta r^{\star}_0(s)$ — the

spectrum of the uniformly sampled or naturally sampled perturbed control-input. The relation for the uniformly sampled case was first established by Shannon — the Sampling Theorem[7]. This relation is proved to be valid even for the naturally sampled case and the almost periodically sampled case in the *small-signal limit* in Section 4.3. This relation is restated below:

$$\delta r_0^*(s) = \frac{1}{T_s} \sum_n \delta r_0(s + i\, n\, \omega_s) \tag{5.12}$$

where $i = \sqrt{-1}$, T_s is the steady state switching period of the system, and $\omega_s = 2\pi/T_s$ is the steady state radian switching frequency.

The next step in finding the frequency response is to relate $\delta \check{\mathbf{x}}_0^*(s)$ — the Laplace transform of the train of δ-functions with period T_s and magnitude $\{\delta \check{\mathbf{x}}_0[n]\}$, to $\delta r_0^*(s)$. This relation is established by applying the z-transform[3] to Eq. (5.8), the augmented difference equation that described the small-signal motion of the system in the vicinity of its steady state solution, followed by the substitution of z with e^{sT_s}; then, $\delta r_0(z) \rightarrow \delta r_0^*(s)$ and $\delta \check{\mathbf{x}}_0(z) \rightarrow \delta \check{\mathbf{x}}_0^*(s)$.

$$\delta \check{\mathbf{x}}_0[n] = \mathbf{\Phi}\, \delta \check{\mathbf{x}}_0[n-1] + \mathbf{k}\, \delta r_0[n] \tag{5.13}$$

$$\sum_n \delta \check{\mathbf{x}}_0[n]\, z^{-n} = \mathbf{\Phi} \sum_n \delta \check{\mathbf{x}}_0[n-1]\, z^{-n} + \mathbf{k} \sum_n \delta r_0[n] z^{-n} \tag{5.14}$$

$$\mathcal{Z}\{\delta \check{\mathbf{x}}_0[n]\} = \mathbf{\Phi}\, \mathcal{Z}\{\delta \check{\mathbf{x}}_0[n-1]\} + \mathbf{k}\, \mathcal{Z}\{\delta r_0[n]\} \tag{5.15}$$

$$\delta \check{\mathbf{x}}_0(z) = z^{-1}\, \mathbf{\Phi}\, \delta \check{\mathbf{x}}_0(z) + \mathbf{k}\, \delta r_0(z) \tag{5.16}$$

$$\delta \check{\mathbf{x}}_0(z) = \left[\mathbf{I} - z^{-1}\, \mathbf{\Phi}\right]^{-1} \mathbf{k}\, \delta r_0(z) \tag{5.17}$$

$$\delta \check{\mathbf{x}}_0^*(s) = \left[\mathbf{I} - s^{-sT_s}\, \mathbf{\Phi}\right]^{-1} \mathbf{k}\, \delta r_0^*(s) \tag{5.18}$$

Finally, $\delta \mathbf{y}(s)$, the spectrum of the perturbed output signal in the *small-signal limit*, may be computed as follows:

$$\delta \mathbf{y}(s) = \int_{-\infty}^{\infty} \delta \mathbf{y}(t)\, e{-}st\, dt$$

$$= \sum_{n} \sum_{i=0}^{N_s-1} \int_{\mathbf{T}_i[n]}^{\mathbf{T}_{i+1}[n]} \delta\mathbf{y}(t)\, e{-}st\, dt$$
$$= \sum_{n} \sum_{i=0}^{N_s-1} \delta\mathbf{y}^*_{i,n}(s)$$

With use of Eq. (5.8) and Eq. (5.11),

$$\begin{aligned}
\delta\mathbf{y}(s) &= \sum_{n} \sum_{i=0}^{N_s-1} e^{-s\mathbf{T}_i[n]}\, \mathbf{H}_i(s)\, \delta\check{\mathbf{x}}_i[n] \\
&= \sum_{n} \sum_{i=0}^{N_s-1} e^{-s\mathbf{T}_i[n]}\, \mathbf{H}_i(s)\, \mathbf{\Phi}_{i-1} \cdots \mathbf{\Phi}_0\, \delta\check{\mathbf{x}}_0[n] \\
&= \sum_{i=0}^{N_s-1} e^{-s\,(T_{i-1}+\cdots+T_0)}\, \mathbf{H}_i(s)\, \mathbf{\Phi}_{i-1} \cdots \mathbf{\Phi}_0 \sum_{n} e^{-s\mathbf{T}_0[n]}\, \delta\check{\mathbf{x}}_0[n] \\
&= \sum_{i=0}^{N_s-1} e^{-s\,(T_{i-1}+\cdots+T_0)}\, \mathbf{H}_i(s)\, \mathbf{\Phi}_{i-1} \cdots \mathbf{\Phi}_0 \sum_{n} e^{-snT_s}\, \delta\check{\mathbf{x}}_0[n] \\
&= \sum_{i=0}^{N_s-1} e^{-s\,(T_{i-1}+\cdots+T_0)}\, \mathbf{H}_i(s)\, \mathbf{\Phi}_{i-1} \cdots \mathbf{\Phi}_0\, \delta\check{\mathbf{x}}^*_0(s)
\end{aligned}$$

where

$$\begin{aligned}
(T_{-1} + \cdots + T_0) &\equiv 0 \\
\mathbf{\Phi}_{-1} \cdots \mathbf{\Phi}_0 &\equiv \mathbf{I}
\end{aligned}$$

Hence,

$$\delta\mathbf{y}(s) = \mathbf{H}^0(s)\, \delta\check{\mathbf{x}}^*_0(s) \tag{5.19}$$

where,

$$\mathbf{H}(s) = \sum_{i=0}^{N_s-1} e^{-s\,(T_{i-1}+\cdots+T_0)}\, \mathbf{H}_i(s)\, \mathbf{\Phi}_{i-1} \cdots \mathbf{\Phi}_0 \tag{5.20}$$

The quantity $\mathbf{H}(s)$ is the *generalized equivalent hold* of the stable steady state solution of the ideal dc-to-dc converter system under study for the control-input r_0.

By using the results in Eq. (5.12), Eq. (5.18), and Eq. (5.19),

$$\delta\mathbf{y}(s) = \mathbf{H}(s)\, \left[\mathbf{I} - e^{-sT_s}\, \mathbf{\Phi}\right]^{-1}\, \mathbf{k}\, \delta r^*_0(s) \tag{5.21}$$

Equation (5.21) describes the control-input-to-output frequency response of an ideal multiple-switched-state dc-to-dc converter system in the vicinity of its steady state solution with respect to the perturbed control-input δr_0 in the *small-signal limit.*

As proved in Chapter 4, this result is exact in the *small-signal limit.* Similar to the control-input-to-output frequency response of the class of ideal simple two-switched-state dc-to-dc converter systems discussed in Chapter 3, the control-input-to-output frequency response of a generic ideal multiple-switched-state dc-to-dc converter system resembles the frequency response of a classical single-rate sampled-data system; with the steady state switching period T_s of the converter system as the sampling period of the classical sampled-data system, the augmented difference equation that describes the small-signal motion of the converter system in the vicinity of its steady state solution, Eq. (5.8), as the discrete time system embedded in the classical sampled-data system, and the *generalized equivalent hold* $\mathbf{H}(s)$ of the converter system as the hold in the classical sampled-data system.

It is obvious that the exact small-signal control-input-to-output frequency response of an ideal dc-to-dc converter system in the vicinity of its steady state solution given by Eq. (5.21) is complicated. Nevertheless, Eq. (5.21) can be easily evaluated at different frequencies by using a computer to obtain useful plots for controller design, such as the Bode plot and the Nyquist plot. Furthermore, analytical approximations of Eq. (5.21) can be found in some special cases; for example, the open-loop constant-switching-frequency PWM converter system in the *high-switching-frequency limit* discussed in Section 3.3. Analytical approximations of the frequency response of a converter system are important for the understanding of the general small-signal behavior of different classes of dc-to-dc converter converter systems, and the design of the basic converter circuits and the feedback controllers.

Conclusion

The *Small-Signal Frequency Response Theory* is a mathematical theory for the linearization of an ideal dc-to-dc converter system in the vicinity of its steady state solution. The theory provides an exact solution to the *frequency response problem* of dc-to-dc converter systems. This theory overcomes the problems encountered when other approximate analytical methods, namely, the *State Space Averaging Modelling Method*[4,5,6], the *Sampled-Data Modelling of Switching Regulator*[1], and the *Small-Signal Analysis of Resonant Converters*[9], are employed. These problems include: not applicable to many classes of converter system, and not accurate at high frequencies. The theory assumes that the periodic steady state solution of the ideal dc-to-dc converter system under study is known. Given a stable steady state solution of the system, the theory will give the control-input-to-output frequency response of the system corresponding to the solution. In contrast to the approximate analytical methods, the results given by the theory is valid at all frequencies provided that the system model used in the calculation of frequency response is valid at all frequencies. The theory is applicable to any linearizable dc-to-dc converter system. The frequency response of a dc-to-dc converter system given by the theory resembles the frequency response of a classical single-rate sampled-data system with a very complicated hold.

In a generic ideal dc-to-dc converter circuit, there may be multiple stable steady state solutions under a single operating condition. In general, the frequency response corresponding to one of the stable steady state solutions is different from the

frequency response corresponding to other stable steady state solutions; even though the stable steady state solutions may correspond to a single operating condition of the converter circuit.

The procedure for finding the frequency response of simple two-switched-state ideal dc-to-dc converter systems with continuous output in the vicinity of its stable steady state solution is laid out in Chapter 3. For any converter system not covered in Chapter 3 but defined in Chapter 1, a procedure for finding its frequency response in the vicinity of its stable steady state solution is laid out in Chapter 5.

The first step in the procedure for finding the frequency response of a dc-to-dc converter system is to find the difference equation that describes the small-signal motion of the system in the vicinity of its steady state solution. The procedure for the construction of the difference equation that describes the small-signal motion of simple two-switched-state ideal dc-to-dc converter systems is described in Section 3.1. In Sections 3.3 through 3.5, the difference equations, in closed-form, of some representative and popular dc-to-dc converter systems, namely, the two-switched-state constant-switching-frequency PWM converter system, the two-switched-state constant-switching-frequency programmed converter system, and the two-switched-state bang-bang controlled converter system, are derived. For the ideal dc-to-dc converter systems defined in Chapter 1, a systematic procedure for constructing the augmented difference equation that describes the small-signal motion of the systems in the vicinity of their steady state solutions is developed in Section 5.1.

The second step in the procedure for finding the frequency response of a dc-to-dc converter system is to find the *equivalent hold* that relates the sequences in the difference equation and in the analog output signal. In Section 3.2, the *equivalent hold* is derived for simple two-switched-state ideal dc-to-dc converter systems without consider-

ation of the output equation. This *equivalent hold* only works for converter systems with continuous output signals, because it cannot take into account the possible discontinuity in the output signals. In Section 5.2, the *generalized equivalent hold*, which is used with the augmented difference equation described in Section 5.1, is introduced to overcome this problem. This *generalized equivalent hold* is applicable to all the ideal dc-to-dc converter systems described in Chapter 1.

In Sections 3.3 through 3.5, three example converter circuits are studied. All three converters circuit have the same circuit topology, the R-L topology, but use different control strategies: constant-switching-frequency PWM, constant-switching-frequency programming, and bang-bang control. When the Bode plots of the predictions given by the *Small-Signal Frequency Response Theory* are compared to the corresponding experimental measurements, it is found that the theory consistently gives good predictions even up to many times the switching frequency, while, in many cases, the approximate analytical methods obviously break down. In the case of the example bang-bang controlled converter system in Section 3.5, the theory even predicts the fine features of the frequency response of the converter system.

In introducing the *Small-Signal Frequency Response Theory* through a simple example in Chapter 2, it is found that the operating condition of a dc-to-dc converter circuit cannot fully specify the steady state solution of the converter. A similar observation is made in the experiments on the real life current-programmed converter circuit in Section 3.4. What is commonly referred to by the power electronics community as the instability of a dc-to-dc converter system under a certain operating condition is actually the instability of a particular steady state solution corresponding to that operating condition, while other stable steady state solutions corresponding to the same operating point are unacceptable. A method for specifying an ideal dc-to-dc converter system and

its steady state solution is proposed in Section 1.1.

In the development of a general procedure for the construction of the difference equation that describes the small-signal motion of a dc-to-dc converter system, it is found that there is no difference between the mathematical description for PWM converters in closed-loop operation and current-programmed converters. This fact is consistent with the experimental observation in the programmed converter system that, if the slope of the added stabilization ramp is varied, its frequency response varies from that of a typical current programmed converter to that of a typical closed-loop PWM converter. In contrast, in many approximate analytical methods, closed-loop PWM converter systems are treated as open-loop PWM converter systems with analog feedback, while programmed converter systems are treated using the modulator model approach[1,4,5].

From the formulation of the *Small-Signal Frequency Response Theory* described in Chapter 5, it is obvious that the theory is a powerful tool that has many applications. The most important application of the theory is in the computer-aided-design of dc-to-dc converter systems based on frequency domain controller design methods. There is no analysis method available besides the *Small-Signal Frequency Response Theory* that has a systematic procedure for calculating the frequency response of all the linearizable ideal dc-to-dc converter systems in the vicinity of their stable steady state solutions, except the costly and time-consuming numerical simulation. The limits and the nonuniformities in handling different classes of ideal dc-to-dc converter systems in the approximate analytical methods make these methods unsuitable for building a general purpose computer-aided-design system for dc-to-dc converter system design. The *Small-Signal Frequency Response Theory*, on the other hand, though not suitable for hand calculation except for very simple converter systems, is uniform in handling all classes of converter systems. This fortunate property of the theory makes the theory ideal for

building a general purpose computer-aided-design system. Furthermore, the analytical result of the theory is exact in the *small-signal limit.* The error in the approximate analytical methods from approximating the output signal of a converter system with the *average of the signal* is eliminated.

The *Small-Signal Frequency Response Theory* does not differentiate between small-ripple (PWM) converter systems and large-ripple (resonant) converter systems in its formulation. Therefore, the theory can be applied to analyze real life converter circuits that are commonly used but cannot not be satisfactorily analyzed with the approximate analytical methods, such as PWM converter systems with snubber protection circuits — a hybrid of small-ripple and large-ripple converters.

In the area of *Modelling and Analysis* of dc-to-dc converter systems in *Power Electronics*, the term *modelling* almost exclusively means *finding an approximate linear system model for an ideal dc-to-dc converter system and approximating the response of the system with the response of the approximate model.* The modelling of a physical converter circuit using an ideal lumped circuit model is often overlooked, except in numerical simulation, because other then the use of a difference equation, there was no method for analyzing the response of an ideal dc-to-dc converter system exactly, even in the *small-signal limit.* Unfortunately, the predictions using the difference equation or time domain approach cannot be compared to experimental data directly, because the experimental measurements involve aperiodic sampling and evaluation of small differences of large numbers. The *Small-Signal Frequency Response Theory* changes this situation. The theory is an exact analytical method for the analysis of the frequency response of dc-to-dc converter systems in the vicinity of its steady state solution. In other words, the theory is an exact solution of the *frequency response problem* of dc-to-dc converter systems. Furthermore, the prediction of the theory can be compared directly to the experimental

measurements from network analyzers. The *Small-Signal Frequency Response Theory* combines the best of the time domain approach and the frequency domain approach for analyzing the small-signal behavior of dc-to-dc converter system: the exactness of the time domain approach and the measurability of the frequency domain approach. It is now possible to study whether a certain ideal lumped circuit model, and therefore, a certain ideal dc-to-dc converter system model, is advisable for a certain physical dc-to-dc converter circuit.

Appendices

Appendix A

The Stability of a System

Stability is always a subject of interest in the study of systems. For a linear time-invariant system, the stability of the system is determined by the eigenvalues of the constant system matrix. For a generic nonlinear system, the concept of eigenvalue is not applicable.

For a class of nonlinear systems which has relatively mild nonlinearity, the concept of *the stability of an operating point* is widely used. Many analog electronic circuits belong to this class of nonlinear systems. There are two major characteristics in this class of systems. First, for each operating point of the system, the system can be linearized. In other words, the linearized system can be parametrized by the operating point. Second, corresponding to each operating point of the system, there is a unique constant steady state solution. The steady state solution of the system is usually used to characterize the operating point of the system. The *stability of an operating point* of a system is defined below:

> Suppose that the solution to a system with perturbation only before time t_o is $\mathbf{x}(t)$; and the steady state solution of the system is the constant vector $\mathbf{X}$. The system is small-signal or locally stable if and only if $\exists$ a $\delta > 0$ such that $\forall\ \|\mathbf{x}(t_o) - \mathbf{X}\| < \delta$,
>
> $$\lim_{t \to \infty} \|\mathbf{x}(t) - \mathbf{X}\| \leq M$$
>
> where M is a non-negative constant, $\|\ \cdot\ \|_p$ is any spatial p-norm, $p \geq 1$.

If $M = 0$, then the system is asymptotically stable. If δ can be any positive constant, then the system is globally stable. The steady state solution $\mathbf{X}$ may be interpreted as the operating point of the system.

For nonlinear systems in general, the concept of the stability of an operating point is not appropriate because nonlinear systems may have multiple solutions which are not constant in time. An example of such a system, a current-programmed buck converter, is given in Section 2.1. Therefore, it is necessary to use a different concept, the concept of the *stability of a solution of a system*, to define the stability of a general nonlinear system. The stability of a solution to a system is defined below:

Suppose $\mathbf{X}(t)$ is a solution to a system without perturbation, and $\mathbf{x}(t)$ is the perturbed solution to the system with perturbation only before time t_o. The solution $\mathbf{X}(t)$ is small-signal or locally stable, if and only if $\exists$ a $\delta > 0$, such that $\forall \ \|\mathbf{x}(t_o) - \mathbf{X}(t_o)\|_p < \delta$,

$$\lim_{t \to \infty} \|\mathbf{x}(t) - \mathbf{X}(t)\|_p \leq M$$

where M is a non-negative constant and $\| \cdot \|_p$ is any spatial p-norm, $p \geq 1$. If $M = 0$, then the solution to the system is asymptotically stable. If δ can be any positive constant, then the solution to the system $\mathbf{X}(t)$ is globally stable.

For systems which have a state space representation, i.e., the system may be described by a differential equation of the form $\dot{\mathbf{x}} = \mathbf{f}(\mathbf{x}, t)$, $\mathbf{x}(t)$ is the state of the system, and $\mathbf{X}(t)$ is the steady state solution of the state of the system.

Appendix B

The Concept of Average

Average is a concept for removing the change in a quantity with time. When the concept is applied to a system, it is used to remove the change in the motion of a system with time. In most approximate analytical frequency domain analysis methods for ideal dc-to-dc converter systems, the concept of *average* is extended to relate its sampled perturbed state, given the difference equation that describes the small-signal motion of the system, to its analog output signal. From another perspective, the concept of *average* is used in the approximate analytical analysis methods to separate the slow motion from the fast motion of the system. Different concepts of *average* are used in different approximate analytical analysis methods. The differences in the different concepts of *average* used in the approximate analytical analysis methods indicate that *average* is not a precise, but a fuzzy concept for the motion of a system. A few different concepts of *average* are examined below. In this discussion, ideal dc-to-dc converter systems are assumed to be in state space representation. The forcing term $\mathbf{u}$ is neglected in the present study.

In the *State Space Averaging Modelling Method* of Middlebrook and Ćuk[6], the process of taking the *average* is called *averaging*. This *averaging* process is taken at the equation level; in which an *averaged system matrix* $\mathbf{A}$ is formed from a weighted sum of the system matrices $\mathbf{A}_i$'s of the switched-networks of the dc-to-dc converter under analysis. The first step of this *averaging* process is the *straight line approximation*: $e^{\mathbf{A}_i T}$ in the difference equation that describes the motion of the system is replaced by

$\mathbf{I} + \mathbf{A}_i T$. This approximation greatly simplifies the expression in the difference equation that describes the small signal motion of the system. The second step is to approximate the difference equation by a differential equation through replacing the first order difference in the approximate difference equation from the first step by the product of the corresponding derivative and the switching period, together with approximating the steady state solution of the state $\mathbf{X}(t)$ by the *time-average* of the steady state solution $\mathbf{X}$. This differential equation describes the averaged system. Another interpretation of the results is that: since the steady state solution of the state $\mathbf{X}(t)$ changes very little with time (the small-ripple assumption), $\mathbf{AX}$, a weighted vector sum of the $\mathbf{A}_i\mathbf{X}$'s, is the *averaged time derivative* of the state $\mathbf{x}$ in over a switching period. The major assumptions of the *State Space Averaging Modelling Method* are that: the switching period is much shorter than any of the time constants in the system, and the frequency of the modulation signal is low compared to the switching frequency. The final result of the *State Space Averaging Method* is a differential equation that describes the *averaged motion* of the system. The result is exact in the *small-signal high-switching-frequency* limit for open-loop constant-switching-frequency PWM converter system. However, it cannot predict the high-frequency response of constant-switching-frequency current-programmed converter systems accurately; because the linear time-invariant model breaks down when it is applied to high-bandwidth feedback control loop design[1].

The development of the *Sampled-Data Modelling Method* of Brown[1] is motivated by the inadequacy of the *State Space Averaging Method* in predicting the high-frequency response of current-programmed converter systems. The step for computing the *averaged system* in the *Sampled-Data Modelling Method* is essentially the same as that used in the *State Space Averaging Method*. Brown suggests that the inadequacies of the *State Space Averaging Method* come from the elimination of the sampling process.

Brown puts the sampling processing into the *State Space Averaging Modelling Method* to form the *Sample-Data Modelling Method*. The addition of the sampling process has two effects: First, the *averaged differential equation* used in the *State Space Averaging Method* performs the function of the *equivalent hold* discussed in Sections 2.3 and 3.2. Second, the *averaged differential equation* with the sampled control-input, in essence, contains a discrete time system which is an approximation of the difference equation that describes the small-signal motion of the converter system discussed Sections 2.2 and 3.1. With this sampling process, the changes in the difference equation that describes the small-signal motion of the basic converter system that come from the application of feedback can be made correctly by using sampled-data system theory.

In resonant converter systems, some of the system time constants and the steady state switching period are of the same order of magnitude. Furthermore, the magnitude of the change of the state with time is large when compared the the magnitude of the state. Hence, the small-ripple assumption is not valid. As a result, the linear combination of the state matrices of the switched-networks cannot approximate the system motion. A different concept of *average* is developed for analyzing this class of converter systems by Vorpérian[9] in the *Small-Signal Analysis of Resonant Converters*. In the *Small-Signal Analysis of Resonant Converters*, the *average* is taken at the output signal level. The perturbed output waveform is *averaged* over each switching period. The frequency response of the system is postulated to be the z-transform of the difference equation that describes the relation between the control-input sequence and the sequence form by the *time-average* of the output signal over each switching cycle with $z = e^{sT_s}$, where T_s is the switching period. Unfortunately, the process of taking the *time-average* destroys the high-frequency signal content of the output signal. Furthermore, the sequence that is formed by the *time-average* of the output signal over a switching cycle

does not have a *hold* to relate it to the analog output signal. The absence of the *hold* in the model introduces even more errors to its prediction of the frequency response of the system at high frequencies — of the order of the switching frequency. An interesting property of the results of this method is that at multiples of half the switching frequency, the predicted transfer function is always real. As a result, the phase of the predicted transfer function is always a multiple of 180 degrees at multiple of half the switching frequency. This property is a direct result of the application of the z-transform to the difference equation that describes the relation between the time-average of the perturbed system state and the perturbed control-input, with $z = e^{sT_s}$. Obviously, counter examples of this method can be constructed easily. Nevertheless, this method gives good prediction at low frequencies; i.e., low when compared to the switching frequency.

A more mathematically tractable concept of *average* is used in the *Sliding Mode Control* of *Variable Structure System Theory*[8]. It defines the *average motion* as follows:

Consider the function $\mathbf{x}(t)$; $\bar{\mathbf{x}}(t)$ is the *average motion* of $\mathbf{x}(t)$ if

$$||\mathbf{x}(t) - \bar{\mathbf{x}}(t)||_p < M$$

for some positive constant M, where $||\cdot||_p$ is any spatial p-norm, $p \geq 1$.

Obviously, for a given M, at least one $\bar{\mathbf{x}}(t)$ can be found. Furthermore, the *average motion* $\bar{\mathbf{x}}(t)$ for each M is not unique if there is no other constraint. This non-uniqueness is a manifestation of the fuzziness of the concept of *average*. Even in the methods mentioned above, the concepts of *average* have similar fuzziness. In the *Small-Signal Analysis of Resonant Converters*, the starting point of a switching period is not unique. It is obvious that a different result will be obtained with a different starting point of the switching period, although the numerical results for the different choices may be close to each other. In the *State Space Averaging Modelling Method* and the *Sample-Data Modelling Method*,

the postulated weights which are used for combining the matrices $\mathbf{A}_i$, $\mathbf{B}_i$, $\mathbf{C}_i$, and $\mathbf{D}_i$ to form the averaged matrices $\mathbf{A}$, $\mathbf{B}$, $\mathbf{C}$, and $\mathbf{D}$, become increasingly bad as the switching frequency is lowered. In addition, the information on the order of the appearance of the switched-networks is lost after the *averaging* process. In the *Equivalent Control* of *Sliding Mode Control*[8], this non-uniqueness is removed by the extra condition that the *average motion* $\bar{\mathbf{x}}(t)$ is the limiting case, in which the imperfection disappears; i.e., the switching period approaches zero. The formal term used in the *Sliding Mode Control* for this limiting process is called the *passage of limit.*

Although in the *Sliding Mode Control* the concept of *average* is not only tractable mathematically, but also gives a unique *average motion*, the concept cannot be applied to resonant converter systems which use the resonance in the converter circuits to transfer power. If the switching frequency is raised, the converter systems do not function as desired. One can conclude from these facts that the concept of *average* is good, but not adequate for the precise description of the behavior of ideal dc-to-dc converter systems in the frequency domain.

To further illustrate the fuzziness of the concept of *average* when the concept is applied to extract the slow motion from a signal with a mixture of fast and slow motions, consider $f(t)$, a function of time, where,

$$f(t) = 10\,\alpha \sin \frac{200\pi t}{\alpha} + \sin 2\pi t$$

The following are some possible definitions of *average*:

1. *The average over an infinite period of time*: This is the universally acceptable definition of average that has no ambiguity. By using this definition:

$$\text{The } \textit{average} \text{ of } f(t) = 0$$

The *average* in this case is the dc component of the function in Fourier Analysis,

which is mathematically tractable. The definition, however, cannot extract the *slow* or *average* motion from the function $f(t)$ as desired.

2. *The average over consecutive time intervals of length* T: Consider the case in which $\alpha = 1$. This definition leads to a sequence that represents the average over consecutive time intervals of length T. This definition has the essence of the concept of *average* used in the *Small-Signal Analysis of Resonant Converters.*

   (a) If $T = 1$, the period of the low-frequency component of $f(t)$, the result is a constant sequence, a sequence of 0's.

   (b) If $T = 1/100$, the period of the high-frequency component of $f(t)$, the sequence is $\{\sin(2\pi n/100) + \epsilon_n\}$, where $|\epsilon_n| < 2\pi/100$. The exact value of ϵ_n depends on the starting time of the time intervals used to calculate the *average.*

   (c) If $T < 1/100$, then the elements in the sequence representing the average is bounded by ± 10.

   In general, different choices of the length of the time intervals used for calculating the sequence that represents the averages and the starting time of the time intervals has drastic effect on the sequence. This property of the definition is very undesirable.

3. *An average of* $f(t)$, $\bar{f}(t)$, *defined by* $| f(t) - \bar{f}(t) | \leq M$, $\forall t$: For each choice of M, there is a different set of $\bar{f}(t)$. Consider the case in which $\alpha = 1$:

   (a) For $M = 11$, 0, $\sin 2\pi t$, and $10 \sin \frac{200\pi t}{\alpha}$ are in the set of $\bar{f}(t)$.

   (b) For $M = 10$, 0, $\sin 2\pi t$, and $10 \sin \frac{200\pi t}{\alpha}$ are in the set of $\bar{f}(t)$ but not 0.

   (c) For $M < 10$, $10 \sin \frac{200\pi t}{\alpha}$ is in the set of $\bar{f}(t)$ but 0 and $\sin 2\pi t$ are not.

In the *Sliding Mode Control* in *Variable Structure System Theory*, the unique *average* is the one which $\alpha \rightarrow 0$, that is, $\bar{f}(t) = \sin 2\pi t$.

4. *The concept of average similar to that in the State Space Averaging Method and the Sampled-Data Modelling Method*: The sequence of averages is formed from sampling $f(t)$ at a fixed time interval $T = \frac{\alpha}{100}$. The sequence is $\{\beta + \sin 2\pi nT\}$, where β depends on the time at with $f(t)$ is sampled and bounded by ± 10. This sequence is not a continuous function of time. The continuous *average* in this concept of average is postulated to be $\sin 2\pi nT$ with $n = t/T$, i.e., $\sin 2\pi t$ (β postulated to be zero to eliminate the *dc component*).

In general, for any given two different concepts of *average*, an arbitrary number of $f(t)$'s can be constructed easily so that the *averages* given by the concepts are very different.

With the fuzziness of the concept of *average* for dc-to-dc converter systems in mind, it is natural to wonder why it is necessary to find the *averaged motion* of the system. In the study of the frequency response of an ideal dc-to-dc converter system, the only purpose of finding the *averaged motion* of the system is to use the frequency response of the *average motion* to external excitation to approximate the frequency response of the system. Thus, a new question arises: Can the frequency response of an ideal dc-to-dc converter system be computed directly by using the Fourier Analysis? This question is the starting point of the *Small-Signal Frequency Response Theory* for ideal dc-to-dc converter systems.

As a final remark, the extraction of any frequency component from a signal in the frequency domain is in essence an averaging process in the time domain. The concept of *average* used, however, is very different from all those discussed above. The extraction of a frequency component from a signal is equivalent to the passing of the signal through an ideal band pass filter. The effect of the ideal band pass filter in the time domain is

the convolution of the signal and the impulse response of the band pass filter, though the impulse response of the filter is not causal. The convolution integral is in essence a moving weighted average. The weight used in the convolution integral is the impulse response of the band pass filter.

Bibliography

[1] Arthur R. Brown and R. D. Middlebrook, "Sampled-Data Modeling of Switching Converters," IEEE Power Electronics Specialists Conference, 1981 Record, pp. 349–369 (IEEE Publication 81CH1652-7).

[2] T. K. Caughey and S. F. Masri, "On the Stability of the Impact Damper," Journal of Applied Mechanics, Vol. 33, No. 3, September 1966, pp. 586–592

[3] Gene F. Franklin and J. David Powell, *Digital Control of Dynamic Systems,* Addison-Wesley, Reading, MA., 1981.

[4] Shi-Ping Hsu, Arthur Brown, Loman Rensink, and R. D. Middlebrook, "Modelling and Analysis of Switching Dc-to-Dc Converters in Constant- Frequency Current-Programmed Mode," IEEE Power Electronics Specialists Conference, 1979 Record, pp. 284–301 (IEEE Publication 79CH1461-3 AES).

[5] R. D. Middlebrook, "Topics in Multi-Loop Regulators and Current-Mode Programming," IEEE Power Electronics Specialists Conference, 1985 Record, pp. 716–732 (IEEE Publication 85CH2117-0).

[6] R. D. Middlebrook and Slobodan Ćuk, "A General Unified Approach to Modelling Switching-Converter Power Stages," IEEE Power Electronics Specialists Conference, 1976 Record, pp. 18–34 (IEEE Publication 76CH1084-3 AES); also International Journal of Electronics, Vol. 42, No. 6, pp. 521–550, June 1977.

[7] C. E. Shannon, "A Mathematical Theory of Communication," The Bell System Technical Journal, Vol. 27, No. 3, pp. 379–433, July 1948; also The Bell System Technical Journal, Vol. 27, No. 4, pp. 623–656, October 1948.

[8] V. I. Utkin, 'Equation of the Slipping Regime in Discontinuous System I, II," Automation and Remote Control, Vol. 32, No. 12, pp. 1897–1907, December 1971; also Automation and Remote Control, Vol. 33, No. 2, pp. 211–219, February 1972.

[9] Vatché Vorpérian and Slobodan Ćuk, "Small-Signal Analysis of the Series Resonant Converter," IEEE Power Electronics Specialists Conference, 1983 Record, pp. 269–282 (IEEE Publication 83CH1877-0).